DOT/FAA/AR-95/90

Office of Aviation Research
Washington, D.C. 20591

Spin Synchronous X-Ray Sinography (SXS) for Nondestructive Imaging of Turbine Engines Under Load

19960524 065

March 1996

Final Report

This document is available to the U.S. public through the National Technical Information Service, Springfield, Virginia 22161.

U.S. Department of Transportation
Federal Aviation Administration

DTIC QUALITY INSPECTED 1

NOTICE

This document is disseminated under the sponsorship of the U.S. Department of Transportation in the interest of information exchange. The United States Government assumes no liability for the contents or use thereof. The United States Government does not endorse products or manufacturers. Trade or manufacturer's names appear herein solely because they are considered essential to the objective of this report.

LICENSE RIGHTS LEGEND
Contract No. DTRS-57_92-C-00012
Contractor or Subcontractor: Foster-Miller, Inc.

Except as the Contracting Officer determines necessary or desirable to protect or enforce the rights of the Government under other paragraphs of this clause, and except as the Secretary or his/her designee determines necessary in the public interest, the Government agrees, to the extent authorized by 35 U.S.C. 205, not to disclose any subject invention for a period of four years from the contractor's disclosure thereof to the Contracting Officer under paragraph (c)(1) of this clause, provided, however, that nothing in this paragraph (1) shall in any way limit or reduce the Government's rights under any other paragraph in this clause.

Technical Report Documentation Page

1. Report No.	2. Government Accession No.	3. Recipient's Catalog No.
DOT/FAA/AR-95/90		

4. Title and Subtitle	5. Report Date
SPIN SYNCHRONOUS X-RAY SINOGRAPHY (SXS) FOR NONDESTRUCTIVE IMAGING OF TURBINE ENGINES UNDER LOAD	March 1996
	6. Performing Organization Code
7. Author(s)	8. Performing Organization Report No.
T. Kirchner, P. Burstein, J. Youngberg	
9. Performing Organization Name and Address	10. Work Unit No. (TRAIS)
Foster-Miller, Inc. 350 Second Avenue Waltham, MA 02154-1196	11. Contract or Grant No. DTRS-57-92-C-00012
12. Sponsoring Agency Name and Address	13. Type of Report and Period Covered
U.S. Department of Transportation Federal Aviation Administration Office of Aviation Research Washington, DC 20491	Final Report October 1994-October 1995
	14. Sponsoring Agency Code AAR-432

15. Supplementary Notes

FAA COTR: Bruce Fenton. AAR-432

16. Abstract

This report presents results from an FAA-sponsored program for early detection of subcritical flaws in turbine engines before catastrophic failure occurs. The combination of theoretical studies and experimental evidence indicates that the Synchronous X-ray Sinography (SXS) system is suitable for finding these flaws. The SXS allows high resolution imaging inspection of the interior of the rotating engine, especially turbine disks and associated components, without engine teardowns. Since these tests can be conducted at much more frequent intervals than tests that require dismantling the engine, rational requirements for finding incipient failures are not nearly as stringent as those imposed during an inspection opportunity during a dismantling. Since the trend in modern engines is towards longer intervals between teardowns, engine teardown specifically targeted for inspection of disks and other internal parts can be potentially avoided if SXS technology is employed.

The heart of this Small Business Innovation Research (SBIR) Phase II program is a feasibility demonstration of the SXS approach. The second stage turbine section of a Lycoming T53 turboshaft engine was spun at 1800 rpm and a freeze-frame cross-sectional image was produced from that data. The SXS approach, which is based on variations of computed tomography (CT), demonstrated a spatial resolution consistent with the detection of a 0.008-in.-thick crack. With a state-of-the-art data acquisition system, much finer contrast and spatial resolution should be possible. It is projected that this system could allow detection of cracks of size 0.001 in. or smaller. As part of the SXS program the first-stage fan disk of the GE F101 engine was computer modeled to show the effect of engine speed on crack distortion (opening). A 0.3 in. long by 0.15 in. deep crack was shown to open to 0.0015 in. under load, an opening that would be detectable by SXS. This means that such a SXS may have detected the disk crack (0.0024 in. open) in the GE CF6-6 engine more than a year before the fatal Sioux City DC10 crash.

An SXS system constructed for research purposes could define the relationship between turbine anomalies seen on the bench in a dismantled engine and in the operating engine. SXS could also study regions of the engine that are far from the surface and that are otherwise unobservable under load. Clearances, deformations, and all manner of other displacements we believe can be measured to an accuracy finer than 0.001 in., in some cases, as fine as 0.001 in.

The SXS design was updated to include the lessons of the feasibility demonstration and the subsequent data analysis. This SXS demonstration work has also led to another related approach, synchronous multiplanar tomography (SMT), which promises to speed the data acquisition time over the current SXS project by acquiring data for many splices simultaneously and to reduce system cost by utilizing existing real-time radiography imaging systems.

17. Key Words	18. Distribution Statement
Turbine Engine NDE, X-Ray Computed Tomography	This document is available to the public through the National Technical Information Service, Springfield, Virginia 22161

19. Security Classif. (of this report)	20. Security Classif. (of this page)	21. No. of Pages	22. Price
Unclassified	Unclassified	97	

Form DOT F1700.7 (8-72) Reproduction of completed page authorized

TABLE OF CONTENTS

		Page
EXECUTIVE SUMMARY		vii
1.	BACKGROUND AND SYSTEM CONCEPT	1-1
1.1	Background	1-1
1.2	SXS Concept and System Description	1-2
2.	CRITICAL CRACK SIZE: ANALYTIC DETERMINATIONS OF CRACK SIZE IN ROTATING DISKS	2-1
2.1	Survey of Engine Manufacturers and Users	2-1
2.2	Analytic Methods of Determination of Crack Opening	2-1
2.3	The Predicted Opening of Disk Cracks Under Operation	2-2
3.	DEMONSTRATION	3-1
4.	POST DATA ACQUISITION ANALYSIS	4-1
4.1	Images and Detectability; Spatial Resolution, Contrast, Entropy, and Artifacts	4-1
4.2	Improvements in Imaging Quality	4-2
4.3	Expected Diagnostic Improvements	4-3
5.	UPDATED SXS DESIGN	5-1
5.1	SXS System Features	5-2
5.2	The Radiation Source	5-2
5.3	The Detectors and Analog Chain	5-2
5.4	Digitization	5-2
5.5	Digital Electronics for Processing	5-3
5.6	Operator's Console	5-3
5.7	Fixture for Holding Engine and Gantry for Slice Position Selection	5-3
5.8	Facility	5-3
5.9	Radiation Safety for Personnel and Aircraft Hardware during Inspection	5-3
6.	DATA REDUCTION AND ANALYSIS	6-1
6.1	Off-Axis Data	6-1
6.2	Noise: Nonrotating, Corotating, and Nonsynchronized Rotating Chaff	6-1
7.	FEASIBILITY OF ROUTINE ENGINE INSPECTION WITH SXS; PROCEDURE FOR ENGINE INSPECTION	7-1

7.1 Procedures for Engine Inspection (Off-Wing Inspection System) Before/ After Data Acquisition 7-1
7.2 Synchronization Requirements between Engine Phase Angle and Strobing of X-Ray Source 7-1
7.3 Data Acquisition 7-2
7.4 Total Inspection Time; Total Engine Cycle Time 7-2

8. MARKET FOR SXS 8-1

8.1 Research Tool 8-1

8.1.1 Cost 8-1
8.1.2 Cost Benefit 8-1

8.2 Commercial Inspection Tool 8-2

8.2.1 Cost 8-2
8.2.2 Cost Benefit 8-2

8.3 Sensitivity Analysis and Cost Benefit 8-3

9. CONCLUSIONS 9-1

APPENDIXES

A — ENGINE SURVEY AND SELECTED RESPONSES

B — GE F101 STAGE FAN DISK CRACKING ANALYSIS

LIST OF ILLUSTRATIONS

Figure		Page
1-1	SXS System Conceptual Design	1-2
1-2	SXS Block Diagram	1-2
1-3	Plan for Off-Axis Scan	1-4
1-4	Detector Strip	1-5
1-5	Appearance of Point Flaw in Detector as Engine Rotates	1-6
2-1	Finite Element Models of Root-Disk Structures	2-3
2-2	Details of a Deformed Surface Crack	2-4
2-3	Deformation of a Corner Crack (Solid Plot)	2-4
3-1	Turbine Section of T53 Turbojet Engine Shown on Stand with its Electrical Drive System on Right and Shaft Position Encoder on Left	3-1
3-2	Supplementary Disk With Calibrated Racks as Mounted on T53 Second Stage Turbine Disk	3-2
3-3	This Reconstruction of the Phantom Disk Clearly Shows the Oil Ports in The Turbine Axle, the Gap Between the Axle and the Phantom Disk, and the 0.008-Inch Gap Between the Phantom's Three Mounting Bolts and Their Respective Holes. Other Concentric Circular Features, as well as the Gradual Radial Gradient, Can Be Removed as Shown in Figure 3-4.	3-3
3-4	Selective Filtering of Circular Features Enables Other Features to Be More Easily Observed. To See Why the Phantom Gaps are Not Detectable in This Processed Reconstruction, Imagine Transplanting a 60-Degree Portion of the Nominal Bolt Ring Signal into the Higher Ambient Noise Region Just Beyond the Oil-Port Radius.	3-4
5-1	SXS Test Cell Configuration	5-1

LIST OF TABLES

Table		Page
2-1	Crack Opening Under Load	2-5

EXECUTIVE SUMMARY

This report presents results from an FAA-sponsored program for early detection of subcritical flaws in turbine engines before catastrophic failure occurs. The combination of theoretical studies and experimental evidence indicates that the Synchronous X-ray Sinography (SXS) system is suitable for finding these flaws. The SXS approach will potentially provide high resolution imaging inspection of the interior of the rotating engine, especially turbine disks and associated components, without engine teardowns. Since these tests can be conducted at much more frequent intervals than tests that require dismantling the engine, rational requirements for finding incipient failures are not nearly as stringent as those imposed during an inspection opportunity during a dismantling. Since the trend in modern engines is towards longer intervals between teardowns, engine teardown specifically targeted for inspection of disks and other internal parts has the potential of being completely avoided if SXS technology is employed.

The heart of this Small Business Innovation Research (SBIR) Phase II program was a feasibility demonstration of the SXS approach. The second-stage turbine section of a Lycoming T53 turboshaft engine was spun at 1800 rpm and a freeze-frame cross-sectional image was produced from that data. The SXS approach, which is based on variations of computed tomography (CT), demonstrated a spatial resolution consistent with the detection of a 0.008-in.-thick crack. With a state-of-the-art data acquisition system, much finer contrast and spatial resolution should be possible. It is projected that this system could allow detection of cracks of size 0.001 in. or smaller. As part of the SXS program the first-stage fan disk of the GE F101 engine was computer modeled to show the effect of engine speed on crack distortion (opening). A 0.3 in. long by 0.15 in. deep crack was shown to open to 0.0015 in. under load, an opening that would be detectable by SXS with a state-of-the-art data acquisition system. This means that such an SXS system may have detected the disk crack (0.0024 in. open) in the GE CF6-6 engine more than a year before the fatal Sioux City DC10 crash.

An SXS system constructed for research purposes could define the relationship between turbine anomalies seen on the bench in a dismantled engine and in the operating engine. SXS could also study regions of the engine that are far from the surface and that are otherwise unobservable under load. It is believed that clearances, deformations, and all manner of other displacements can be measured to an accuracy finer than 0.001 in., in some cases, as fine as 0.0001 in.

A commercial SXS system could provide cost-effective inspection of turbine engines. The current worldwide number of airplanes in commercial turbine fleets is 11,000. The cost of teardowns for a single commercial jet engine varies between $500 thousand and $800 thousand. If we choose $500 thousand as an average, and assume an average of 0.5 teardowns per year per airplane (once every 6 to 8 years for each multi-engine airplane), the annual cost of this procedure is about $2 billion to $3 billion. With a projected development cost of $15 million (including the first unit) and follow-on costs of approximately $7 million per system, the installation of 15 systems at a depot-level inspection would require a capital outlay of about $100 million. If we assume annual operating costs (not including amortization) of $2 million per system, SXS could become cost-effective if it provided confidence levels that would stretch the interval between teardowns by only a few percent. If SXS inspections increased the confidence

confidence level so that interval could be lengthened by 10 percent, the SXS NDT systems capital cost and services up to that point would be paid for in 6 months or so.

SXS can be used to provide a map of the interior of each individual turbine engine. Approximately 50 cross-sectional images would be made per engine, with a total average cycle time of 1 to 2 hours per engine. Thus, a single SXS facility might service as many as 4 to 12 planes per day, depending upon number of engines and configuration. Assuming an average of six planes per day allows all 4600 planes currently in the U.S. fleet to be inspected once every two years if a single facility is involved. Four such systems would allow screening every six months.

The SXS design was updated to include the lessons of the feasibility demonstration and the subsequent data analysis. This SXS demonstration work has also led to another related approach, synchronous multiplanar tomography (SMT), which promises to speed the data acquisition time over current SXS projections and reduce system cost.

1. BACKGROUND AND SYSTEM CONCEPT.

1.1 BACKGROUND.

Although today's turbine engines are reliable and continue to support a very safe air transportation system, uncontained failures of high-energy rotating components can seriously threaten aircraft safety by damaging critical aircraft systems in flight. FAA rules and guidelines require that blade failures be contained within the engine case; disk failures must be addressed by designing the aircraft to protect critical systems from high energy fragments. Both fixed-wing aircraft and helicopters can be vulnerable to this type of engine failure.

There are two fundamental observations that guide the technological and operational approach to detecting the anomalies that are the incipient phases of these failures:

- Engines are very complex, and the source of the failures is likely to be in components or assemblies that are completely inaccessible from the outside.

- An extremely likely failure mode involves fatigue cracks that propagate radially along an axial plane; often the cracks are closed when the engine is cool and still. A desirable approach allows examination of the engine under normal thermal and speed conditions.

From a naive perspective, computed tomography (CT) appears to fulfill most of the requirements for flaw detection and mensuration for anomalies hidden deep within the engine. The truly seductive aspect of CT is that it provides a visual image of a virtual cross-sectional plane of the test specimen. There is a one-to-one correspondence between each picture element seen in the image and the corresponding volume element in the real object. Conventional CT, unfortunately, has three requirements that make its use extremely difficult to accomplish on engines:

1. A test specimen, only parts of which are moving rapidly, is not a rigid unchanging scene, which conventional CT requires.

2. Every volume element in the test specimen line of reconstruction must be examined from all directions even if it is desired to inspect only the region near the center. This effectively precludes examination of all but the smallest of engines.

3. Conventional CT utilizes X-ray absorption data acquired in a plane perpendicular to the spin axis. In a large turbine, this path may require X-ray penetration of several feet of metal—too large an attenuation to result in a useful measurement.

However, CT-derivative techniques can be utilized with existing hardware; clever algorithms with sets of data smaller than those required by conventional CT allow most of the strengths of CT, yet avoid the difficulties posed by CT in producing an image. The implementation of this approach is spin-synchronous to the engine and allows an anomaly to trace a unique sinusoidal pattern in successive inspection positions of the engine.

1.2 SXS CONCEPT AND SYSTEM DESCRIPTION.

The conceptual SXS system design is shown geometrically in figure 1-1; a block diagram is given in figure 1-2.

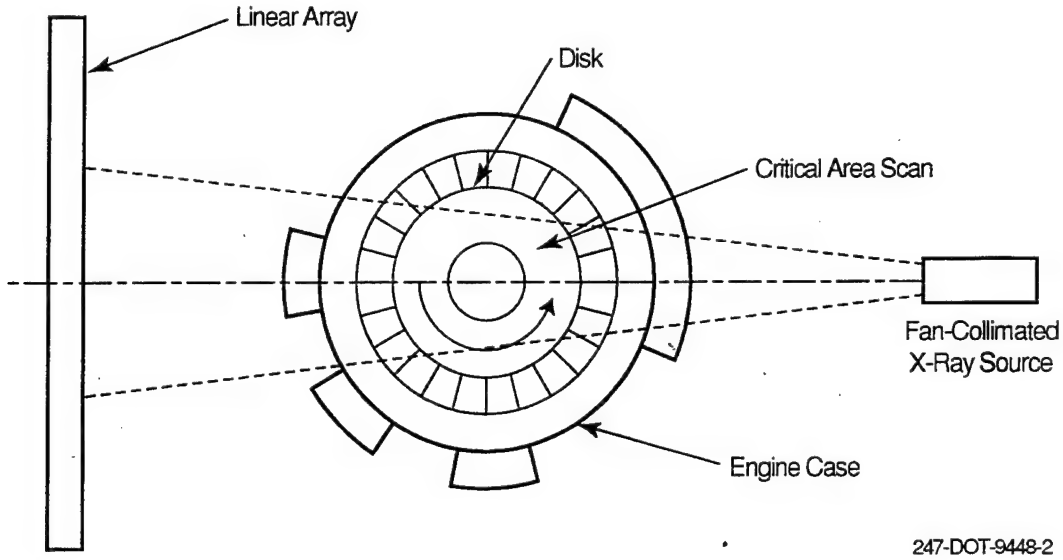

FIGURE 1-1. SXS SYSTEM CONCEPTUAL DESIGN

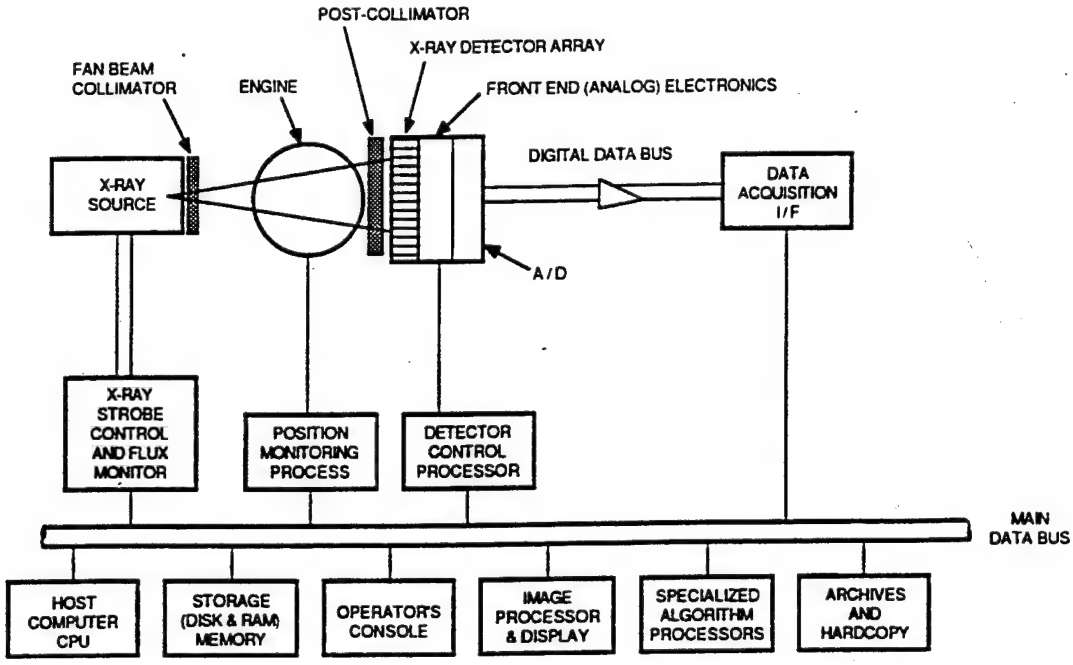

FIGURE 1-2. SXS BLOCK DIAGRAM

The X-ray source is an electron linear accelerator (linac) having an energy of 9 MeV with an output of 3000 Roentgens/min at a distance of 1 m from the focal spot. This source was chosen based on the X-ray opacity of the background, typically 4 to 8 in. of steel in turbine engines up to the largest diameters. (Data obtained in planes that are not perpendicular to the axis are shown in figure 1-3. Perpendicularity to the engine axis might require penetration of as much as 20 to 30 in. of steel in the form of rotors, blades, and containment housings. The requirements for an X-ray source to penetrate that thickness of steel are severe.) The 9 MeV system was chosen for two reasons:

1. X-ray generators of lesser photon energies cannot penetrate through larger engines, which are increasingly opaque as the photon energy decreases.

2. Commercial 9 MeV generators typically have high dose rates, e.g., 3000 to 5000 R/m/m, which allows a given statistical precision of signal/noise ratios to be determined much more quickly than a smaller dose would allow. Thus, a shorter inspection time is possible.

The detection system is a linear array of cadmium-tungstate crystals that convert incident X-rays into visible light. Attached to the crystals are silicon photodiodes that convert the light to an electric charge that proceeds to an amplifier and thence, to a digitizer. The remainder of the signal chain is handled digitally and is discussed below.

The X-ray source presents a short-pulsed (3 μsec) beam that is collimated to a fan shape, and the beam passes through the plane of interest in the engine. The beam is variously absorbed, scattered,* and transmitted as a function of the X-ray attenuation characteristics of the various parts. From the X-ray absorption perspective, all that matters is the element constituency and the amount of material between source and detector for any measurement. Typical engines have steel, nickel, and titanium as their main metallic constituents, in addition to alumina in structures. (The "superalloys" of steel and nickel have fractional amounts of other materials — negligible on the scale of these experiments and the projections we make from them.)

The absorptions of nickel, cobalt, and copper are virtually identical to that of steel on a density basis at these X-ray energies. Thus, utilizing steel's absorption characteristics is a standard radiographic practice. Other metals, e.g., titanium and aluminum, are less absorbing generally than steel and its neighbors on the periodic table. For this reason, the radiographic appearance of anomalies in components that are mostly composed of light metals like titanium will be somewhat reduced. Similar remarks hold for organic or nonmetallic components. However, virtually all current engines utilize steel and steel-based or steel-similar (from an X-ray perspective) materials for all of the components and assemblies for which SXS would be used.

* Scattering does occur, but in a line-configuration with a precollimator to limit the entrance X-ray beam to a fan rather than a cone, the fractional contribution of scattered X-rays to the total amount detected is very small.

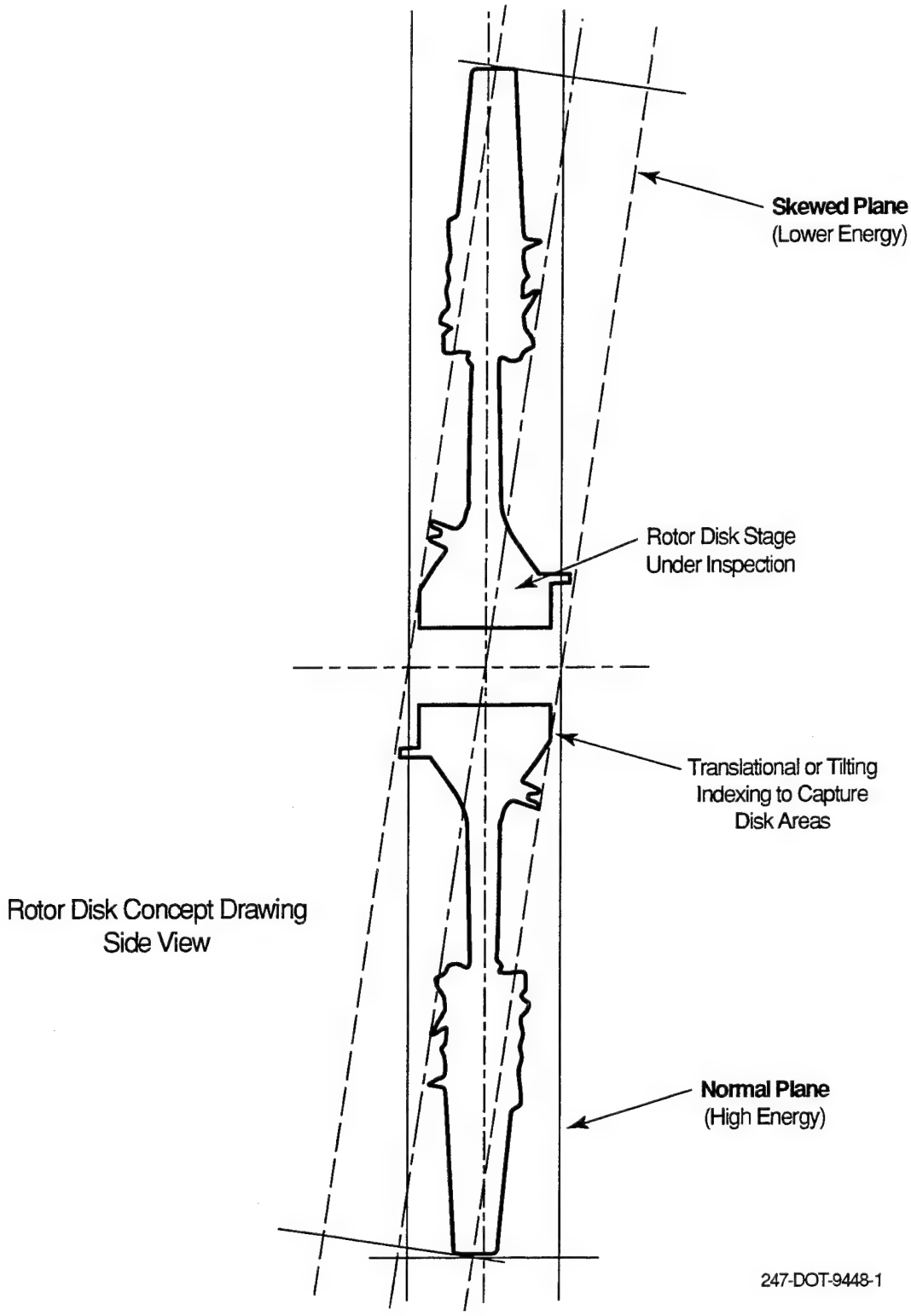

FIGURE 1-3. PLAN FOR OFF-AXIS SCAN

The output beam on the detector side of the engine presents a one-dimensional shadowgraph image of the engine at the time of the X-ray pulse. The detector is composed of a strip of contiguous detection elements, each detector being approximately 0.5 mm wide, 15 mm long, and 6 mm thick, as shown in figure 1-4. This arrangement gives good X-ray stopping power, reasonable light collection efficiency, and good spatial resolution of the interior of the test specimen. The array length in our demonstration system is approximately 8 in. and is composed of 512 elements. (A production system has 1000 to 2000 elements.) The configuration shown in figure 1-1 positions the 1000 element production system array symmetrically about the engine axis - there is just as much array above as below the motor centerline. This yields coverage of 250 mm (10 in.) in radius. The detector array can also be positioned on one side of the centerline, a configuration yielding about 500 mm (20 in.) coverage in radius.

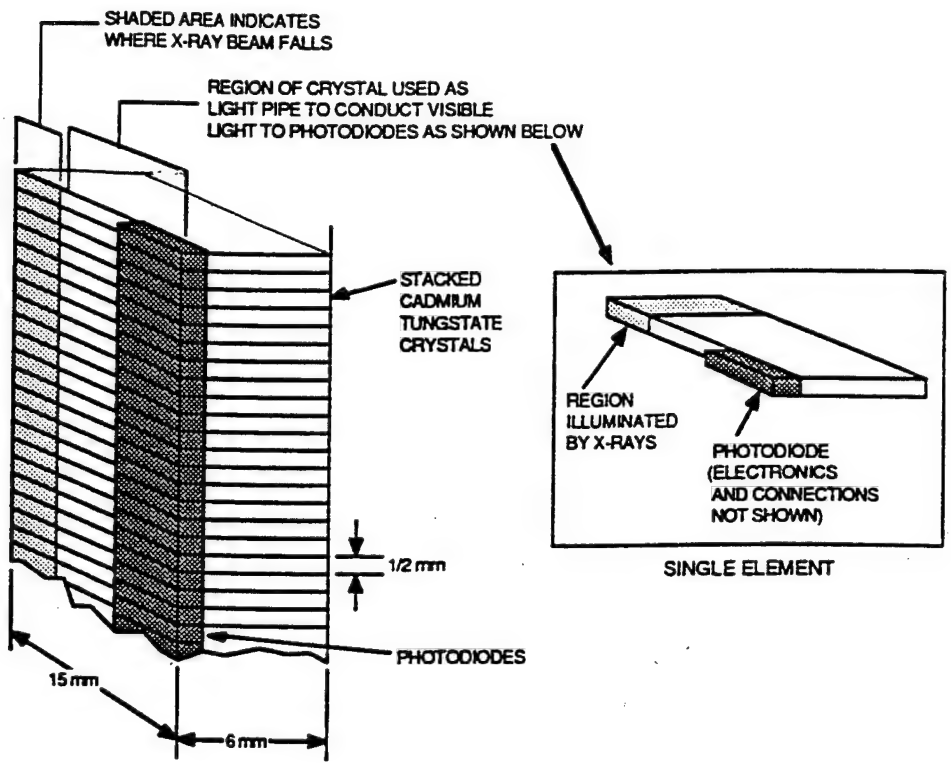

FIGURE 1-4. DETECTOR STRIP

Given this configuration, it must be asked what the appearance of a suspect (flawed) region will be in a single one-dimensional image of the plane: for this discussion it will be assumed a single point flaw, as shown in figure 1-5. As the engine is rotated, the X-ray shadow of the point flaw on the array is as shown in figure 1-5. If the outputs of the array are plotted in time, the flaw traces out the pattern of a sine curve. The amplitude shows how far out in radius the feature is located, and a correlation with rotational position locates the feature in angle on the

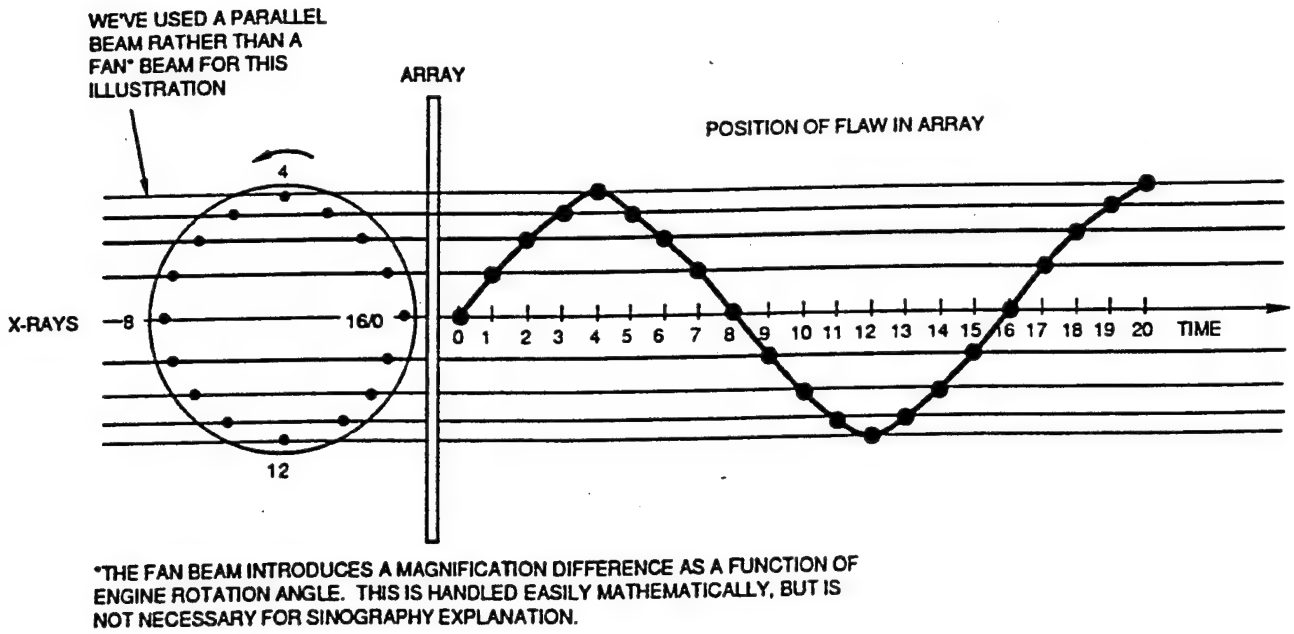

FIGURE 1-5. APPEARANCE OF POINT FLAW IN DETECTOR AS ENGINE ROTATES

test specimen.* The sinogram is a tool of conventional CT in diagnosing the health of the CT system. However, its output can be used directly, without the necessity for conventional CT image reconstructions.

While it is assumed a point flaw for discussion of the concept, any real flaw can be viewed as the superposition of a series of point flaws, and the resulting sinogram can be used to analyze the differences in expected flaws. Even though the detector resolution elements are about 1/2 mm in size, the system can detect flaws much finer than that size. However, these flaws cannot be located to an accuracy smaller than the spatial resolution, nor can detailed structure smaller than the spatial resolution be seen. Thus, a tiny high density inclusion could have the same appearance as a larger lower density inclusion (assuming that both are below the spatial resolution limits of the system). The important point, however, is that the tiny anomaly can be detected. Cracks have an unmistakable signature, and they can almost always be seen meandering through a linear, continuous set of picture elements ("pixels"), irrespective of the pixel size. The visual analog is seeing a flagpole at a long distance; even though the width of the flagpole may be below the spatial resolution threshold of the observer, he can still see the pole although he cannot isolate its position or measure its width to an accuracy comparable to that width.

Fatigue cracks are the most difficult flaws for X-ray based inspection systems to find. The reason is that X-ray measurements are based on finding the difference in transmission between

* Figure 1-5 is drawn for a parallel X-ray beam to simplify the concept of the "sinogram" for explanatory purposes; a fan beam produces a slight distortion of the sine curve as a result of the varying magnification of the flaw position as a function of rotational angle. This is easily compensated inthe algorithm as handled in the computaional analysis.

closed and open paths. Fatigue cracks are normally closed in rotating members when the engine is stopped and cool. This is the reason that the use of conventional CT has not gained wide acceptance in engine maintenance and repair, as it has in other areas of manufacturing technology.

Our concept utilizes the fact that the X-ray linac puts out a short (3 μsec length) burst of X-rays and that it can be triggered. That is, data acquisition can be stroboscopically controlled, much as a stroboscope can be used to make objects on a rapidly spinning lathe appear to stop. Engine speeds of 30 thousand to 60 thousand rpm are well matched to the pulse rate of the linacs (typically 180 to 1,000 pulses/sec). When the rotating member reaches its proper angular position, the X-ray source is triggered and a brief flash of X-rays illuminates the turbine. The process is repeated at each of the different angular positions where data are required. In this way, an entire sinogram can be built in several seconds. It must be integrated over a number of such cycles to obtain data of sufficient statistical quality to reveal the features of interest.

One of the major problems associated with data acquisition is that the image pattern will be very complex due to the extraneous material in the field of view. This extraneous material presents clutter in the sinogram, a complex overlay image that is difficult to interpret visually. However, the pattern will be stable, predictable, and most important, it is periodic. The sinographic data must be analyzed for these periodicities, and the data filtered for two types:

1. Stationary data (i.e., zero frequency) which indicates no motion and is hence part of the support structure.

2. Corotating structure, which appears at the same frequency as the material of interest but has a different amplitude owing to its different radial position with respect to the turbine axis. The result is data representing structure that is confined to a small annular band in the turbine. A crack or other such anomaly will produce a single signal with a period of one revolution but not exactly coincident with the rotational position of any other known 1-revolution period (e.g., a keyway). After this initial data conditioning, the position and extent of the flaw can be found with a proprietary algorithm that analyzes and filters the sinogram data. Finally, a CT image is reconstructed.

2. CRITICAL CRACK SIZE: ANALYTIC DETERMINATIONS OF CRACK SIZE IN ROTATING DISKS.

In this section, the critical crack sizes that would have to be found by SXS in order to confidently employ the system are discussed. There are two important findings:

1. Under inspection by SXS, with the turbine engine spinning, the distribution of forces on the disk actually opens the cracks a few thousandths of an inch. Both considerations push critical criteria for detection of cracks to wider cracks, and hence, an easier detection.

2. The standards normally given for on-bench rejection of a disk that has been inspected during engine teardown assume crack size to be two-dimensional, and hence, assume a standard length-to-depth ratio. Since only the surface of a component is available for inspection during engine teardown, inspection criteria tend to be based only on length. As a corollary, since these kinds of inspections are so rare on any particular engine, any anomaly is a cause for rejection. Under more frequent and periodic inspections, rejection criteria—which are based on very conservative length/depth criteria—would not have to be so stringent.

2.1 SURVEY OF ENGINE MANUFACTURERS AND USERS.

Early in the SXS program, 22 manufacturers and users of turbine engines were surveyed to determine the critical size at which tiny cracks, voids, anomalies, etc., needed to be seen in the course of an inspection. (The questionnaire and the more informative responses are shown in appendix A.) The responses indicated that critical sizes for cracks were typically on the order of 0.05 in. long by 0.005 in. deep. These were much smaller cracks than those which had been estimated in our preliminary studies. The discrepancy had to do with the manner in which the respondents considered the question. Responses were given for typical detection criteria when the engine was torn down and the turbine disk was examined on the bench. Under current inspection practice, the 0.05- by 0.005-in. crack criterion is correct, because the disk is examined so infrequently that we must strive to catch the smallest cracks before they grow. Otherwise, the next inspection might not occur until after the crack had opened to the point where (possibly catastrophic) failure could occur.

If more frequent inspections were possible, tiny cracks need not have been detected at such an early—and tiny—stage. Indeed, analysis of the data from the Sioux City crash shows that the turbine disk had a crack that began and extended through many thousands of flights before the catastrophic failure occurred. Had that engine been inspected regularly with an SXS system, calculations show that the crack could have been detectable more than a year before the crash occurred.

2.2 ANALYTIC METHODS OF DETERMINATION OF CRACK OPENING.

A disk cracking analysis was performed by Stress Technology, Inc., (STI) under subcontract to Foster-Miller. A simple computer model to the GE F101 fan was constructed as the necessary data were readily available to STI. A finite element model was used to calculate steady stresses

and displacements in the disk under centrifugal load. These results were then used as inputs to a crack propagation model to predict the crack mouth displacements for 10 surface cracks and 10 corner cracks of varying sizes. In addition, for each crack, the curve of the estimated stress intensity factor versus the normalized distance along the crack front was found. The complete report is given in appendix B.

2.3 THE PREDICTED OPENING OF DISK CRACKS UNDER OPERATION.

Rotational forces and heat are the two most obvious factors in changing the size of cracks in disks under operating conditions. In our expert opinion and confirmed by STI, the increases in crack size due to heat are negligible compared to those due to spinning forces. The overall disk model is shown in figure 2-1. The crack positions within the disk are shown in figure 2-2 and figure 2-3.

The crack mouth openings under load were calculated for kissing-wall cracks as shown in table 2-1.* The important conclusion is that even cracks that are closed under non-operating conditions will open under load. These calculations include only those forces due to spinning. Any pressure differentials from one side of the turbine disk to the other will only serve to increase the crack width. With SXS technology, then, we expect to be able to see those cracks that are longer than 0.3 in. and deeper than 0.15 in. under in situ rotational conditions; this is true even when the crack would be closed under the zero-load condition on the bench.

* For this analysis we did not consider residual stresses on the surface of the disk that could be built in at manufacture. These stresses could diminish crack opening under load.

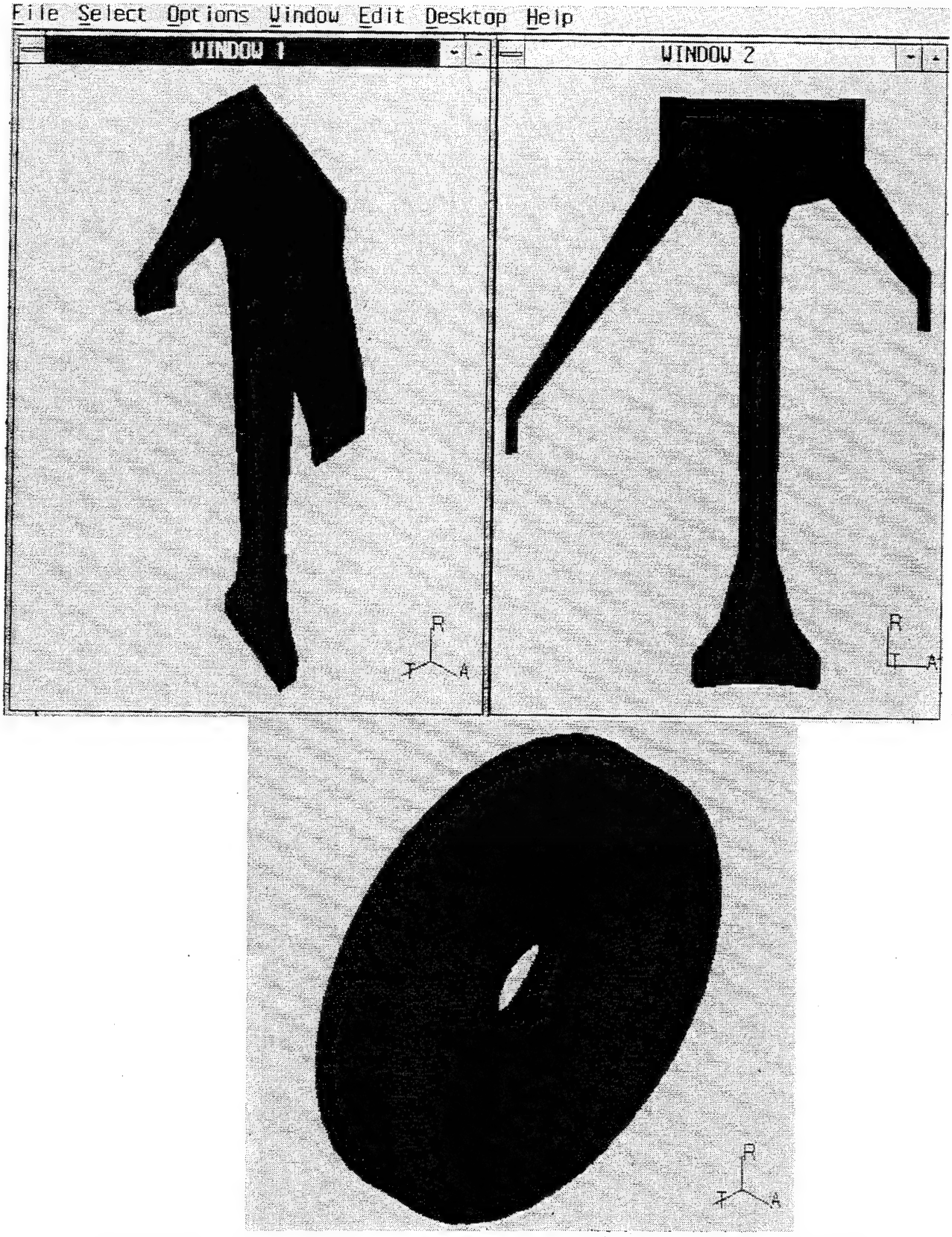

FIGURE 2-1. FINITE ELEMENT MODELS OF ROOT-DISK STRUCTURES

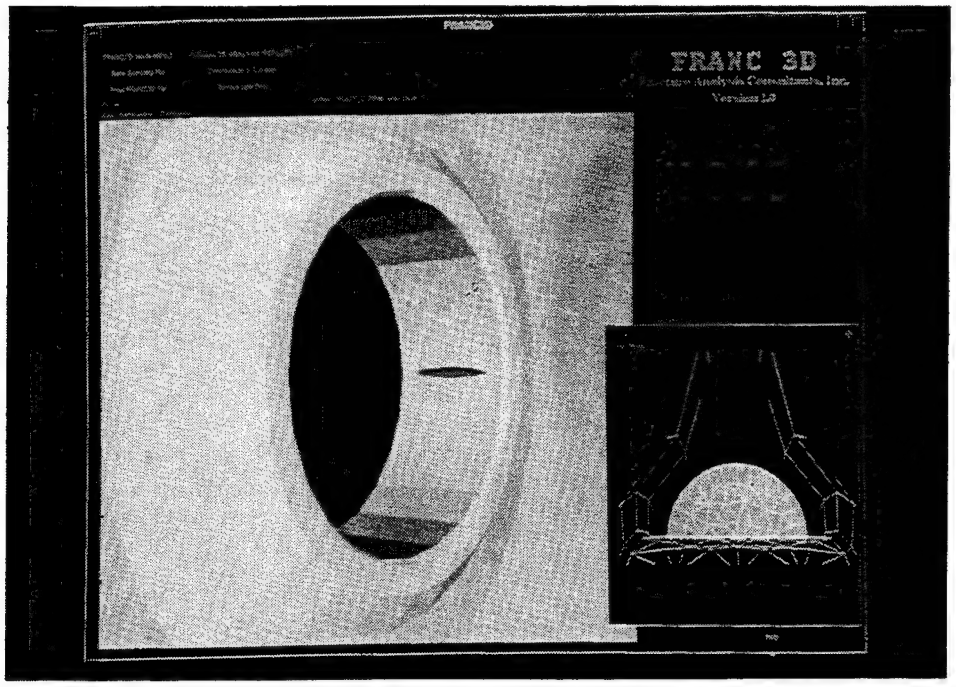

FIGURE 2-2. DETAILS OF A DEFORMED SURFACE CRACK

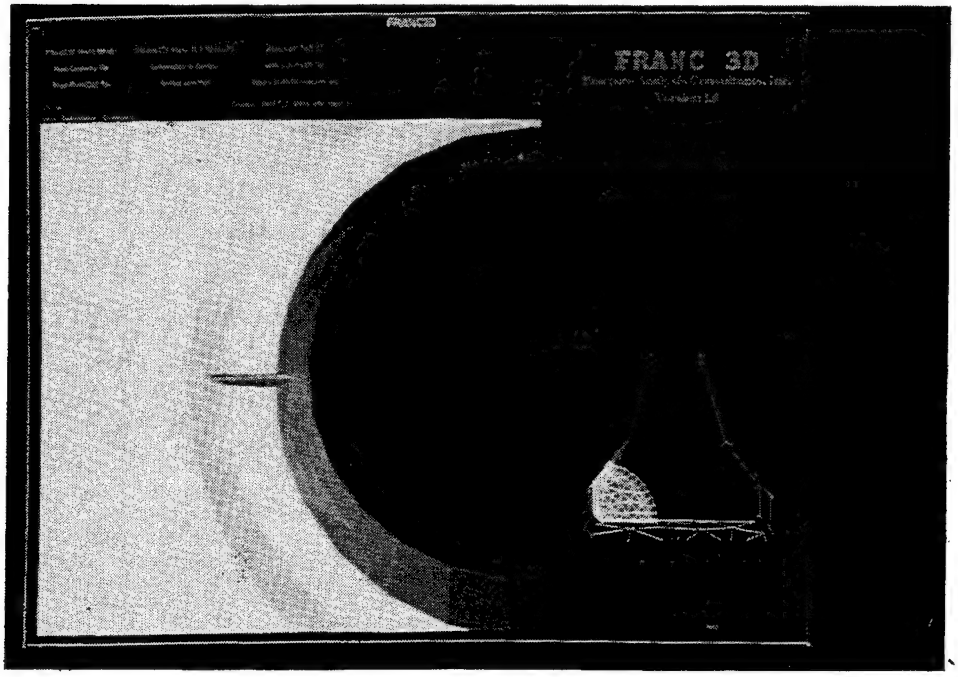

FIGURE 2-3. DEFORMATION OF A CORNER CRACK (SOLID PLOT)

TABLE 2-1. CRACK OPENING UNDER LOAD (ALL DIMENSIONS ARE IN INCHES)

Crack Length	Crack Depth	Crack Opening	
		A (corner)	B (surface)
0.01	0.005	0.00005	0.00005
0.05	0.025	0.00027	0.00026
0.1	0.05	0.00054	0.00053
0.17	0.085	0.00094	0.00088
0.3	0.15	0.0017	0.0015
0.5	0.25	0.0028	0.0024
0.8	0.4	0.0046	0.0038
1.0	0.5	0.0062	0.0047
1.3	0.65	0.0087	0.0064
1.5	0.75	0.011	0.0078

3. DEMONSTRATION.

A demonstration was conducted on the turbine section of an actual Lycoming turboshaft engine, a T53-L-II provided by the FAA. The turbine section was spun externally by an electric motor for this test in a confined X-ray bay. The T53 turbine section is shown in figure 3-1. In addition, a supplementary disk, with built-in defects as shown in figure 3-2 was manufactured and mounted on the turbine disk. The defects consisted of a series of radial cracks, approximately 1/8 in. in length and of widths ranging from 0.0005 to 0.01 in., located in two annular bands and having approximate diameters of 3 and 7 in. This experiment focused on the 3-in.-diameter band of radial cracks.

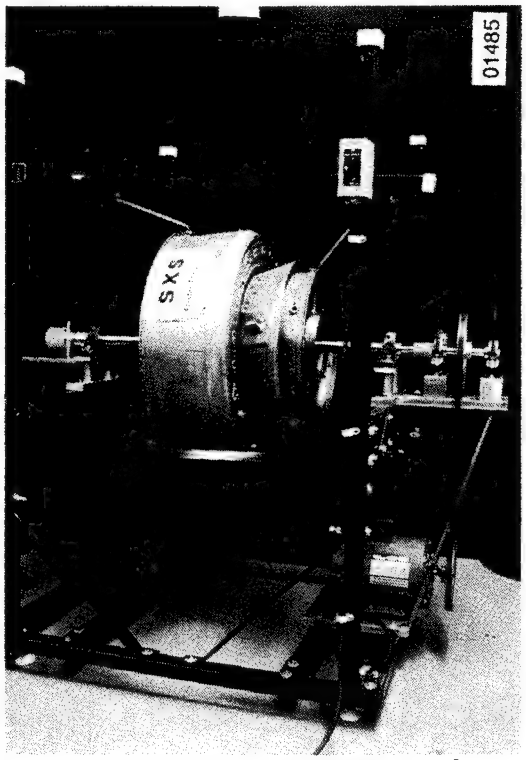

FIGURE 3-1. TURBINE SECTION OF T53 TURBOJET ENGINE SHOWN ON STAND WITH ITS ELECTRICAL DRIVE SYSTEM ON RIGHT AND SHAFT POSITION ENCODER ON LEFT

The equipment was set up at Thiokol Corporation's Elkton, Maryland, X-Ray Test facility, which contains a Varian Linatron 9 MeV electron linac-based triggered X-ray source, which emits 3000 Rads/min at 1 m in the 1 to 9 MeV X-ray band in 3 to 5 μsec wide bursts. The configuration was as shown in figure 1-1, with the source on one side of the turbine and the X-ray detectors on the opposite side. In addition to this equipment, a rotary position encoder on the shaft of the turbine was used to ascertain rotational position of the turbine disk; rotational position was used to trigger the X-ray source in a controlled stroboscopic mode. In this way, all the views necessary to reconstruct the image are provided. Data acquisition for each slice

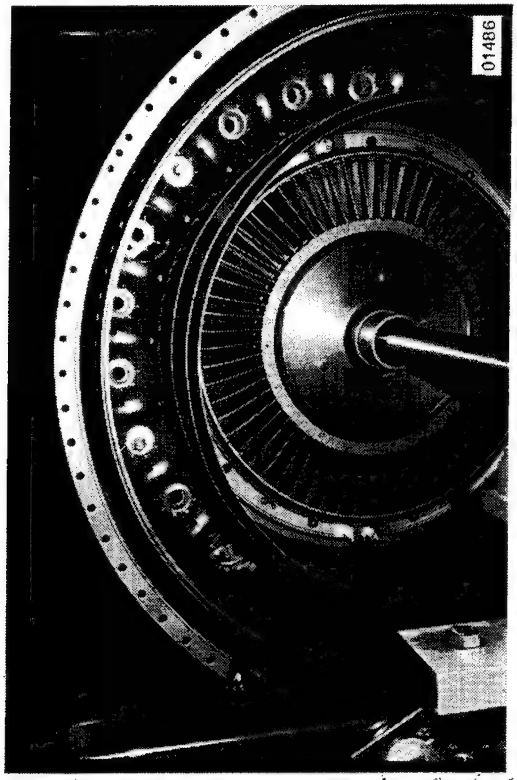

FIGURE 3-2. SUPPLEMENTARY DISK WITH CALIBRATED RACKS AS MOUNTED ON T53 SECOND STAGE TURBINE DISK

required approximately one minute. Most of these slices were acquired in a plane angled at 84 to 88 degrees rather than the conventional CT angle of 90 degrees with respect to the spin axis to eliminate the unacceptable attenuation through the entire disk that would result from a perpendicular data acquisition angle. A reconstructed image of the interior section of the phantom disk is shown in figure 3-3. Very clearly seen are the three bolts at the outer periphery of the image. Towards the center the annular band containing the defects is seen.

The reconstructed annulus of figure 3-3 extends through radii from 0.75 to 2.5 in. Imaged in this annulus are the tapering outer radius of the turbine axle (1.15 in.) and the inner radius of the phantom disk (1.31 in.). Within the turbine axle are shown two diametrically located slanting oil ports (the 0.012 in. dimension is in the tangential direction on figure 3-4). The radial extent is much larger. Near the outermost radius of the reconstructed annulus, spaced 120 degrees apart, are imaged the three bolts which were used to secure the phantom disc to the turbine. In fact, it is the space between each bolt and its hole that is imaged here. This gap, nominally 0.010 in., produced a 20 percent modulation with a full width half maximum (FWHM) of about 0.04 in., corresponding roughly to a image-derived gap width of 0.008 in. In other words, the equivalent

FIGURE 3-3. THIS RECONSTRUCTION OF THE PHANTOM DISK CLEARLY SHOWS THE OIL PORTS IN THE TURBINE AXLE, THE GAP BETWEEN THE AXLE AND THE PHANTOM DISK, AND THE 0.008-INCH GAP BETWEEN THE PHANTOM'S THREE MOUNTING BOLTS AND THEIR RESPECTIVE HOLES. OTHER CONCENTRIC CIRCULAR FEATURES, AS WELL AS THE GRADUAL RADIAL GRADIENT, CAN BE REMOVED AS SHOWN IN FIGURE 3-4.

width* of the missing materials as measured in a density profile across the screw and hole corresponds to an average gap of 0.008 in. The actual clearance between the screw whole and the bolt is smaller than 0.008 in. The average gap in terms of X-ray throughput is the sum of the bolt to hole clearance plus the missing material between the major and minor diameter of the threads. CT and CT-derivative techniques are often used to make such quantitative estimates of gaps, clearances, and the like.

* The equivalent width technique is based on the fact that any feature has a specific X-ray contrast that results in a change in the gross absorption from the case where that feature is not present. If the form of the feature is known, e.g., a gap, then the feature can be fit to a model incorporating that specific form. In this case, the form is known to be a smooth clearance hole with a bolt through it. The amount of material missing from that gap corresponds to a model fit of 0.008 in. average. No attempt was made to confirm this measurement physically, as the actual gap size, the thread size, and degree of bite would have to be measured.

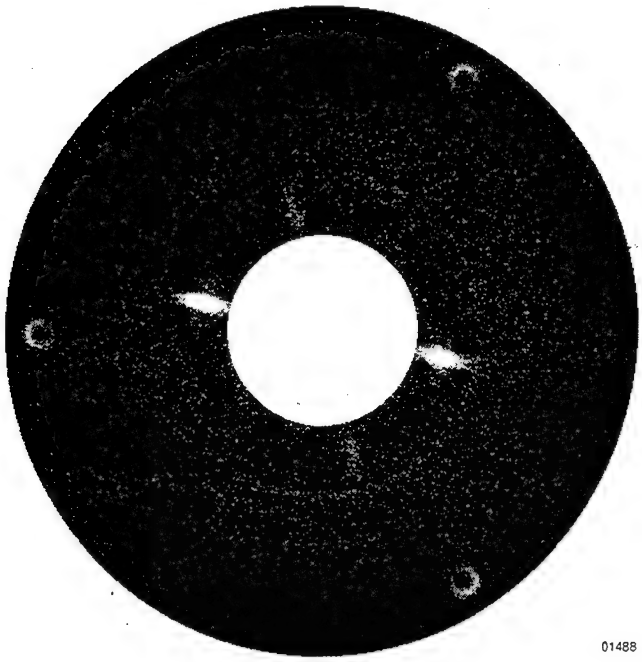

FIGURE 3-4. SELECTIVE FILTERING OF CIRCULAR FEATURES ENABLES OTHER FEATURES TO BE MORE EASILY OBSERVED. TO SEE WHY THE PHANTOM GAPS ARE NOT DETECTABLE IN THIS PROCESSED RECONSTRUCTION, IMAGINE TRANSPLANTING A 60-DEGREE PORTION OF THE NOMINAL BOLT RING SIGNAL INTO THE HIGHER AMBIENT NOISE REGION JUST BEYOND THE OIL-PORT RADIUS.

Among the phantom's radial gaps, the largest is located at about 225 degrees (four o'clock) just outside the inner radius of the phantom. This gap, though similar in width to the bolt gap just discussed, is much shorter (0.13 versus 0.67 in.). To be reliably detectable, such a feature must produce a modulation about three times the image noise level. The noise level (standard deviation) in this reconstruction is about five percent (increasing to 6 percent at the gap radius).

This means that, to be detectable, small features must produce a modulation of about 18 percent or more, depending on the presence of masking reconstruction artifacts. Thus, as suggested by figure 3-4, the 0.010-in. gap hovers on the verge of detectability. A small reduction in signal noise, achievable by substituting the intended 16-bit analog to digital (A/D) converter for the 12-bit converter actually used, would likely render the gap and its smaller siblings detectable. Several other approaches for optimizing detection of small radial gaps are also available. The technique should be able to detect radial cracks of size 0.001 in. width, having an area of 0.01 in.^{2}, (e.g., 0.1 in. by 0.1 in.) or larger.

4. POST DATA ACQUISITION ANALYSIS.

The images in section 3 show that the first feasibility demonstration was successful in accomplishing its main objective: freeze-frame cross-sectional imaging of the interior of a turbine jet engine. It is emphasized that three major concepts were demonstrated in the feasibility program:

1. Synchronized pulsing of an X-ray source to a rapidly rotating member. (Precision of synchronization is discussed in subsection 7.2.)

2. Reconstruction of transaxial planes from data acquired in planes not coincident with the reconstruction.

3. Use of very limited data compared to the requirements of traditional CT.

These images are not perfect; they have problems related to constraints of the only data acquisition subsystem available within the time and budget constraints of the program. However, the diagnostic quality of those images can be easily improved with the use of a different electronic digitization scheme, which was not available to the experiment at the time of the demonstration. A simple substitution of a different A/D converter in that experiment from a 12-bit to a 16-bit output could change the sensitivity by a factor of approximately three, all other things being equal. Thus, the demonstration system would have yielded sensitivity to cracks of 0.003 in. width with the addition of a standard electronic tool. We did not take advantage of the full dynamic range of the signal. (The burden of a fast 16-bit A/D subsystem was not a permissible increment under the extremely tight cost constraints of this Phase II SBIR program. It is a minuscule cost relative to the total cost of a full-up production unit.)

Sufficient X-ray photons will be present to the extent that a 20-bit linear A/D unit will yield excellent signal resolution in the range over which expected absorption measurements will be made. This is a dynamic range of a factor of 1 million. Alternatively, a nonlinear A/D scheme, e.g., a logarithmic or square-rooting A/D, may also be used. In any case, these are standard products that can be procured from a variety of sources. The effect on the final image will be spectacular in that it will increase the sensitivity by a factor of 5 to 10 over what was seen in the demonstration.

4.1 IMAGES AND DETECTABILITY: SPATIAL RESOLUTION, CONTRAST, ENTROPY, AND ARTIFACTS.

Detectability of features in an imaging inspection system depends on the spatial resolution, the contrast, the inherent image complexity (entropy), and the particular artifacts of the imaging system.

Detectability and accuracy of location of features are two concepts that are often confused. Frequently, imaging inspection systems are utilized at the limit of their detection capability; and the two numbers are used interchangeably, but incorrectly. We note the difference between

spatial resolution and detectability. Spatial resolution is the ability to locate a feature to a certain accuracy. Detectability is the ability to detect that feature. In most imaging systems, features whose characteristic sizes are below the spatial resolution limit of the system can be detected with the system, although the feature itself cannot be resolved. Thus, SXS can find cracks of size 0.001 in. and *average* displacements to that accuracy. Clearances can be measured to a very high precision, because the region being checked for clearance has a substantial extent in its other dimensions. In a system with good spatial resolution and poor contrast, features (especially low contrast features) that are larger than the spatial resolution may not be detectable because of the graininess of the intrinsic image.

Contrast is a quantitative measure of the graininess of the image. If the contrast is poor, then the high graininess can overwhelm the system response on the image to a small feature in the test specimen.

The complexity of the test specimen itself has a marked influence on the ability of the system to detect various features: Finding the duck on the surface of a calm pond is much easier than finding it among the reeds of a marsh. This complexity is referred to as the entropy of the image. (One reason that SXS is so good at finding flaws is that the high-entropy scenes of the typical shine-through radiographic projections are eliminated in the reconstruction.)

The last major issue that has a bearing on the identification and severity of features is the artifact level associated with the final image. Artifacts are features that appear in the image, but are not present in the test specimen. Thus, shadows and concentric rings are common types of artifacts in CT and CT-derivative systems like SXS. The important point is minimizing artifacts and understanding the residuals to the point that they do not mask or masquerade as features of concern.

4.2 IMPROVEMENTS IN IMAGING QUALITY.

The reconstructed images of section 3 may be impressive for a first feasibility demonstration; however, the analysis shows that spatial resolution, contrast, and artifact level can be significantly improved. Each of these changes will lead to a much higher quality image and to significantly smaller thresholds for flaw detection.

Spatial resolution was degraded from optimum because of significantly greater scatter signal and detector crosstalk in the system than can be ultimately achieved.

A better alignment scheme would have cut this scatter and crosstalk signal significantly. According to our analysis, collimator constraints on the breadboard system did not permit as tight an alignment as would be possible with a full-up production system.

Contrast can be improved simply by having the signal digitization scheme match the intrinsic signal-to-noise ratio available in the X-rays, as was mentioned earlier in this section.

Artifacts present in the reconstructed image include some circular rings, a false radial gradient in the density, and a "ghost" image of a keyhole slot in the test specimen. The circular rings and the false radial gradient result from an insufficient calibration of the entire system as a whole. Experiment time on the 9 MeV X-ray source at Thiokol was very limited, and we could not get as much data as needed to make a proper calibration. Clearly, these problems are solvable at the production level. The "ghost" image of the oil ports is probably the result of scattering for the particular (and relatively crude) geometry of the demonstration. This will not occur in the full-up SXS system because part of the next phase involves an optimized geometry.

4.3 EXPECTED DIAGNOSTIC IMPROVEMENTS.

On the basis of a strawman turbine engine and reconstruction models, it is calculated that data acquisition slice per slice will vary from approximately 1 minute on smaller engines to 5 minutes on larger engines. The minimum size crack detectable is one that will have an open volume of at least 0.00002 cm^3 (0.000001 cubic in.). This is equivalent to a crack 0.1 in. long, 0.015 in. deep, which opens to a crack width of 0.002 in. under load.

5. UPDATED SXS DESIGN.

Originally, several possible implementations for the SXS full-up production system were considered. These included variations on two general themes:

1. A system for examining the turbine engine on a test stand, detached from the airplane, and

2. on-wing engine inspection.

Modern engines and airplanes are designed so that engines can be removed and attached with a minimum of time and effort. An SXS system designed for on-wing inspections would require significantly more effort than an off-wing inspection: Remote controls, variable heights, and a huge facility that would have to accommodate different airplanes are among the major issues. For these reasons an updated design for the off-wing system has been pursued. Outwardly, the system configuration as shown in figure 5-1 and the system block diagram already shown in figure 1-2 have not changed from the conceptual design. The major changes that have resulted from the Phase II experience are highlighted in the list of features shown below. In addition the principal investigator and his colleagues have conceived and demonstrated an X-ray detection system on another program that can accept data on a number of CT slices simultaneously and thus significantly reduce inspection time. This detection system has the added benefit of reducing SXS system cost by approximately $200 thousand.

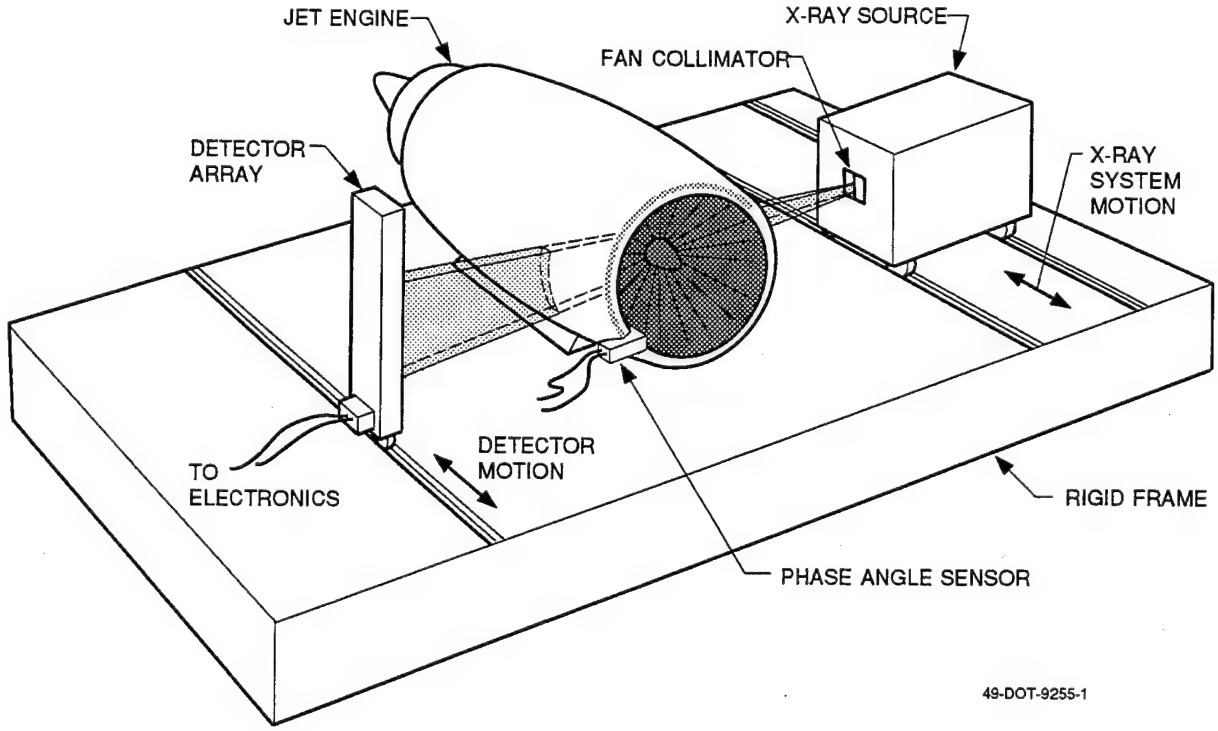

FIGURE 5-1. SXS TEST CELL CONFIGURATION

5.1 SXS SYSTEM FEATURES.

- 16 MeV electron linac as the X-ray source.
- 1000-element array of detectors.
- 20-bit digitization scheme and associated digital electronics.
- Work station that includes operator functions and computationally intensive processor for SXS data reduction, storage, and analysis.
- Mechanical gantry for holding the engine.
- Programmable motion control system for moving/indexing the SXS system's axial position relative to the engine for inspection of preselected regions.
- Phase angle position monitoring system for the various disks that are to be inspected.
- Facility that allows engine to be run at speed and that provides radiation protection for operators.

5.2 THE RADIATION SOURCE.

The radiation source is a Varian 16 MeV electron linac. Initially, a 9 MeV X-ray generator was considered to be the likely radiation source; however, the larger engines on newer turbine aircraft require the extra penetrating power provided by the 16 MeV source. The source is rated at 13,000 rad/min at 1 m from the focal spot. The source is pulsed remotely when the engine phase angle is appropriate for gathering a data sample. The source is pulsed at the rate of 180 times per second. The X-ray pulse length is approximately 3 μsec.

5.3 THE DETECTORS AND ANALOG CHAIN.

The detection system consists of a 1000-element array of individual detectors. The detectors are cadmium tungstate crystals, each of which has an active size of 1/2 by 4 by 6 mm (deep). The crystals themselves are actually larger in the 4 mm (lateral) dimension, because they form their own radiation-resistant light pipes, which are coupled to silicon photodiodes. The photodiodes' outputs are routed to a sample-and-hold circuit and then sequentially directed to charge amplifiers and the signals digitized.

5.4 DIGITIZATION.

Digitization is accomplished by a fast 20-bit A/D system, operating in an average range of 5 μsec per sample. While this is at first glance an extremely fast conversion time for a single A/D

converter, these times are made possible with an assembly of multiplexed A/D units, and a careful calibration scheme.

5.5 DIGITAL ELECTRONICS FOR PROCESSING.

A work station based on the Digital Equipment Corporation's DEC Alpha station is the heart of the processing system. This system is hefty enough to process the data into an image in a time commensurate with the acquisition of the next image. Fortunately, no custom hardware is required. All of the hardware, from the 170 MHz processor to the digital signal processing boards, can be purchased as stock items from commercial sources. This is a large improvement on the production CT systems that were first employed on major aerospace systems a decade ago, where every function required custom engineering. Present work stations are a small fraction of the price of those pioneering aerospace CT nondestructive testing (NDT) digital subsystems.

5.6 OPERATOR'S CONSOLE.

Functionally, the operator's console is separate from that of the data acquisition and processing task of the work station. Physically, however, the work station also functions as the operator's interface. These operator functions include real-time machine functions like motion control, data acquisition, system control and override; and nonreal-time functions, e.g., image processing and display, archiving, file selection.

5.7 FIXTURE FOR HOLDING ENGINE AND GANTRY FOR SLICE POSITION SELECTION.

This mechanical subsystem includes a gantry for holding the engine and a subsystem for moving/indexing the SXS system's axial position relative to the engine for inspection of preselected regions. The engine gantry subsystem must also include an accurate phase angle position monitoring system for the various disks that are to be inspected. (See subsection 7.2.)

5.8 FACILITY.

The facility that houses the engine and the SXS system must fulfill several functions: It must allow the engine to be run at speed; it must shelter the SXS system and provide required utilities (electrical power, water); it must provide radiation protection for operators; the facility must also house the work station and archival storage system. With the exception of the engine's running at speed, these requirements are typical of facilities that contain large X-ray systems.

5.9 RADIATION SAFETY FOR PERSONNEL AND AIRCRAFT HARDWARE DURING INSPECTION.

The use of radiation brings concerns for issues of personnel safety and integrity and reliability of aircraft hardware.

Insofar as personnel are concerned, all operation of the X-ray source occurs while operating personnel are in the control room, which is heavily shielded from the radiation produced by the source. The X-ray source produces significant radiation only when energized. A tiny bit of residual radiation remains for several tens of minutes after the source is shut off, but this phenomenon is well understood; workers in such environments are not exposed to doses that exceed the Bureau of Radiological Health standards. For 9 MeV generators, the only hazard arises from an operator sticking his hands and head very close to the tungsten target located deep inside the generator within half an hour of the system's use, as for example, when the machine is being serviced. For 15 MeV generators, the operator should stay away from the immediate path of the X-ray beam for approximately half an hour after the system is shut down. The hazard is residual radioactivity and above 15 MeV neutrons.

The only parts of the engine that might be susceptible to radiation are on-board electronics, organics, e.g., seals and lubricants, and plastics. Except for the electronics and for Teflon specifically, thresholds for damage to all of these items are very high relative to expected lifetime radiation exposure with SXS. Teflon parts should withstand radiation damage of 100,000 rad (10 inspections) without any complication. While modern electronics tend to be resistant to radiation to the same levels, certain classes of electronics, e.g., analog N-MOS devices, are more radiation sensitive. While analog N-MOS devices are rarely employed in such engine applications, we note that this is a concern that should be addressed before widespread use of SXS begins.

6. DATA REDUCTION AND ANALYSIS.

Once the data are acquired, the entire CT process must be fine-tuned in order not to produce severe artifacts in the image. The algorithms must compensate for the fact that perfect CT data—including all parts of the specimen at all times falling within the field of view of the detectors—will not be available. These compensations are numerous, but they appear to work well.

6.1 OFF-AXIS DATA.

For SXS, data are obtained at various off-axis angles—the closer to the strict transaxial case, the easier is the transformation—and are averaged to provide an image that appears to be transaxial. In general, smaller engines require less off-axis tilt in data acquisition than larger engines. The reason for this off-axis tilt is getting sufficient flux through the test specimen and into the detectors. Typical off-axis angles are 5 to 8 degrees. Our estimate of a typical off-axis amount of metal to be penetrated is 8 to 12 in. On-axis X-ray penetration could be several feet of metal depending on engine size and thus would limit the application of SXS technology only to the smaller engines.

6.2 NOISE: NONROTATING, COROTATING, AND NONSYNCHRONIZED ROTATING CHAFF.

A series of data reductions by use of a proprietary Hough transform* is the key to obtaining images of diagnostic quality. We distinguish between three different kinds of image chaff: stationary clutter, corotating clutter, and nonsynchronized rotating clutter. Each of these is handled in a different manner.

Stationary clutter—the shadowgraph of the fixed parts of the engine on the detectors—is handled in a straightforward manner simply by subtracting the equivalent of a running average of response for each detector element.**

Corotating clutter is clutter which is generally outside the circle of reconstruction of interest. One of the aspects of the SXS is that the closer the region of interest is to the axis of rotation of the engine, the easier the reconstruction becomes. In general, these are exactly the regions that *are* of interest. Regions outside the radius of reconstruction will have a characteristic geometrical pattern in the raw data, which can be filtered by the application of the proper Hough transform.

Nonsynchronized rotating clutter contains frequency components that are not synchronized with the particular disk under study. In modern engines, various elements may have different rotating speeds; some are indexed to each other through gearing, e.g., by a multiple of 2 or 3; others are independent. These are the hardest of all types of clutter to compensate for. In these cases, a Hough transform band-pass filter for the rotation frequency of interest is the method of choice.

---

* The proprietary Hough transform was developed by team member, Perceptics, Inc.

** The actual procedure is significantly more complex than a simple running average, but that is the most important component of the procedure for removing stationary clutter.

The big problem with all of these transform techniques is the introduction of noise and artifacts into the resulting image. Unfortunately, there is no easy way to predict the severity of the noise or the type of artifact without examining each aircraft engine in each configuration. Our only data point is in the reduction of major artifacts made with the demonstration system. Ridding that image of the worst of the artifacts required several man-weeks, and that system was not optimized in any way for the particular engine, nor did we have any experience in doing so. Prior experience of the PI and his team in developing and producing large CT/NDT systems bodes for a successful implementation of a full-up SXS system.

7. FEASIBILITY OF ROUTINE ENGINE INSPECTION WITH SXS; PROCEDURE FOR ENGINE INSPECTION.

SXS should provide routine engine inspection without difficulty. Consistent with our initial choice of the off-wing inspection approach, the sequence proposed here involves an engine that is removed from the airplane and placed in a cradle. The SXS system would provide primary inspection of the engine for these major flaws:

1. Cracks in turbine disks, which may cause catastrophic failure.

2. Cracks in turbine blades, blade roots, and disk regions in close proximity to the blade roots, which are typically not catastrophic.

3. Clearances.

4. Presence of clogged lines, slow flow, etc., which cannot be seen by other methods when the engine is stopped.

The economic return is high, particularly if the use of SXS saves the cost of an engine teardown.

7.1 PROCEDURES FOR ENGINE INSPECTION (OFF-WING INSPECTION SYSTEM) BEFORE/AFTER DATA ACQUISITION.

The procedure begins with the removal of the engine from the wing. The engine is set on a cradle and wheeled into position between the source and the detector in the SXS system. This entire procedure should require between 1 and 4 hours per engine on jet aircraft. For each different engine type there is a template that yields engine position, slice position, and the sequence for obtaining all the data. The engine must be fitted with the phase angle registration device which is used as an input for synchronized strobing of the X-ray source. The engine must also be fitted with remote control electronics.

The time required at the end of the inspection to reattach the engine should be 1 to 4 hours depending on aircraft type.

7.2 SYNCHRONIZATION REQUIREMENTS BETWEEN ENGINE PHASE ANGLE AND STROBING OF X-RAY SOURCE.

From discussions with Rolls-Royce and the other engine manufacturers it was learned that engine speed on stand can be held extremely constant but were unable to obtain these data to the precision required for SXS performance. This leads to the following concern: Because of the precise positioning requirements for reconstructive imaging, a single timing position for every rotation of the disk in question may be an insufficient monitor on which to subdivide the cycle and pulse the X-ray source.

The SXS accuracy requirement of the phase angle is approximately 10 minutes of arc at the time of strobing of the X-ray source. This represents rotational variation of one part in several thousand over a cycle. If the engine speed does vary by more than one part in 3,000 over the course of a single cycle, then sensor(s) that measure the engine phase angle at a series of intermediate phase positions will be required to maintain the spatial resolution. The sensor outputs will be used to trigger the X-ray strobe. If the disk is spinning at 10,000 rpm, the nominal jitter time is 1 to 3 μsec (which is, fortuitously, about the time length of the X-ray pulse). Microsecond accuracies are well within the capabilities of standard electronics. Therefore, it does not appear to be a serious problem to the implementation and operation of the SXS system.

7.3 DATA ACQUISITION.

Data acquisition will vary between one and five minutes of time per slice. The difference is due to the amount of material along the line of sight between the X-ray source and the detector and varies from one position within the engine to another and from one engine to another.

The number of slices taken per engine can vary from about 12 to 50, depending upon which disks are being inspected and which characteristics of disks are being emphasized. Acquiring data on blades and blade roots, particularly on larger disks, may require a slightly different setup for the detector array. Each time that a different setup is required, realignment and recalibration are necessary. After the SXS system has been used to establish a standard procedure, this realignment and recalibration will be accomplished very quickly and automatically.

Total data acquisition time, which includes the time of moving the SXS system to its new positions between slices, is then 16 to 64 minutes for the 12 slice engine (4 disks, 3 positions on each disk; overhead time of 20 seconds between slices). The 50 slice regimen would require between one and five hours. These data acquisition times can be significantly reduced by incorporating the multislice detector system discussed in section 5.

7.4 TOTAL INSPECTION TIME; TOTAL ENGINE CYCLE TIME.

Total engine cycle time includes not only the inspection itself within the SXS facility, but also counts the time required for removing and replacing the engine from or onto the wing. Thus, total engine cycle time includes the time that the engine (and hence the airplane) is out of service. The actual engine inspection time by the SXS system is typically a small fraction of the total engine cycle time. Even within the SXS cell, time must be allocated for moving the SXS gantry into initial position, performing any preliminary calibrations, and moving the gantry out of the cell after the inspection is complete.

The total time for removing the engine, and reattaching the engine will vary from three to nine hours, depending upon the engine and the engine change procedure. The actual inspection time per engine within the SXS system might be as low as one hour per engine. Our preliminary estimate is two hours per engine actually spent within the SXS test cell. This SXS cycle time is the average center-to-center time for engine inspection, i.e., the average engine flow rate within

the cell. The SXS cycle time tells us what the process rate for airplanes through the facility is. In most cases, the tasks that can be performed outside the SXS cell can be performed in parallel with SXS operations inside. Thus, many engines can be removed and reattached while the SXS is being used to inspect other engines. The number of man-hours per engine is probably 20 to 30 for all operations combined.

It is noted that the comparison time for a complete engine teardown is typically five to eight weeks, the cost is $300 thousand to $800 thousand (depending upon engine type) and there is a significant probability that the engine will not be reassembled correctly. The SXS approach is cost-effective because the alternatives are expensive, time-consuming, and prone to error.

8. MARKET FOR SXS.

In this section the market for SXS as a research tool and as a commercial inspection tool is examined. There is significant benefit to using SXS in both contexts.

8.1 RESEARCH TOOL.

As a research tool, the logical customers are commercial turbine engine manufacturers, the U.S. military, the FAA, and other national (U.S. and foreign) agencies. As a research tool, SXS can be used to examine many other interior features of turbine engines besides flaws in disks, blades, etc. Because the range of possible problems and applications is so great, the upside utility of the SXS system in a general diagnostic setting is unlimited. The attraction of the SXS lies in its imaging capability: What other nondestructive testing modalities can only hint at, SXS can show.

An SXS system which is configured as a research tool would be used primarily by aerospace scientists and engineers. Philosophically, the system would be a modified turnkey system that would allow tremendous latitude in test specimen and configuration. The painstaking calibration and validation schemes needed to qualify a system for production usage, as described below, would be absent. (Production and research tools are inherently antithetical in their use: Production systems are used according to an unwavering, previously validated procedure. Significant effort has gone into the interpretation of the system's response to various known conditions. Systems that are utilized as research tools are used to explore unknown or hazily understood conditions. Typically, part of the research effort is to work backward to a feature giving rise to a system output.)

8.1.1 Cost.

The parts cost of such a system is approximately $3 million, plus approximately $2 million for the facility. Nonrecurring engineering costs for the first system are probably on the order of $2 million. Final price of the system is dependent upon flexibility, the interface, how much preprogrammed sequencing would be available, etc.

8.1.2 Cost Benefit.

Given the expected usage of such a system, it might be expected only that one to two research systems be procured for the entire country, one being located at a military facility, the other at a national engine test facility. The cost of an individual engine manufacturer or engine overhauler owning and utilizing such a system for research may be justified in terms of resolving problems, but SXS system usage would probably be minimal; the issue of efficient time utilization of such a machine pushes towards a single shared facility for all producers of turbine engines.

8.2 COMMERCIAL INSPECTION TOOL.

A production unit for routine inspection of engines is much different from the research system from the perspective of use, even though the production system and the research system might appear to be identical. The production system is dominated by procedures and interpretations of the system's output, which have been meticulously correlated with the conditions giving rise to those outputs. This process will require several years before a completely qualified procedure is available.

The likely customers are overhaul centers for engines. Typically, these are run by a number of the largest airlines which do maintenance work for many other airlines as well. We estimate that five or six systems are all that would be required for the entire U.S. Another six to ten should suffice for the rest of the world (depending upon which is considered most critical: system utilization or location).

8.2.1 Cost.

The cost for the first system includes the parts cost, the nonrecurring engineering charges, the facility, as well as the qualification program. The preliminary estimate is $15 million. This does not include the work component that must be provided by the various turbine engine manufacturers in providing expertise in interpreting the data outputs for each type of engine. Follow-on units would cost approximately $7 million, including the facility.

8.2.2 Cost Benefit.

The cost benefit is relatively straightforward to calculate. Currently there are 11,000 turbine engine airplanes in the world inventory. The average turbine engine is torn down two or three times in its lifetime. The tear down costs an average of $500 thousand to $800 thousand, depending upon the engine type. Out-of-service time is typically eight weeks, and the probability of putting the engine back together incorrectly is non-negligible.

If we assume an average of 0.5 teardown per year per airplane (once every 6 to 8 years for each multi-engine airplane), the annual cost of this procedure is about $2 billion to $3 billion. With a projected development cost of $15 million, (including the first unit) and follow-on costs of approximately $7 million per system, the installation of 15 systems worldwide at the depot level would require a capital outlay of about $100 million. An assumption of annual operating costs (not including amortization) of $2 million per system shows that SXS could become cost-effective if it provided confidence levels that would stretch the interval between teardowns by only a few percent. If SXS inspections increased the confidence level so that interval could be lengthened by only 10 percent, the SXS NDT systems capital cost and services up to that point would be paid for in approximately 6 months.

8.3 SENSITIVITY ANALYSIS AND COST BENEFIT.

The NTSB Aircraft Accident Report of the Sioux City DC10 D crash on 19 July 1989 (PB90-910406 NTSB/AAR-90/06) concludes that the crack progressing through the CF6-6 fan disk had been present from its initial installation. It grew at an accelerating rate. It is believed that this crack would have been visible to the SXS by the time it reached the level of the 0.1 in. long by 0.015 in. deep, many thousands of cycles before the catastrophic failure occurred, and well before the last UAL inspection of April 1988 which was 15 months before the accident and which did not find the crack. Had SXS been available and used regularly as an inspection tool, the crack might have been caught in a routine inspection.

While the incidence of such catastrophic cracks is minuscule, other noncatastrophic events not leading to the loss of an aircraft (but perhaps the loss of an engine) could be found before the event occurs. The loss of a single engine is many times more costly than the price of a full-up SXS facility.

SXS can be applied to engines of all sizes, as long as sufficient X-ray flux exists to penetrate the test specimen and provide a statistically significant absorption sample emerging beam. Some of the larger engines require a larger off-axis angle to provide the necessary emerging beam (because too much absorption exists in trying to penetrate the disk directly). The costs of development of an SXS for a smaller engine are actually quite close to those required for normal large engines. The major differences arise in the X-ray source (approximately $500 thousand), in the building and other related shielding issues (approximately $300 thousand), and in the gantry ($200 thousand), for a total of about $1 million in savings by going to an SXS system for a smaller turbine engine.

9. CONCLUSIONS.

The SXS Phase II experiment demonstrated the physics basic to the SXS concept.

Unambiguous, computed tomographic images of a turbine disk spinning at 1800 rpm inside a T 53 turboshaft engine were successfully reconstructed. Specifically this required demonstrating:

- Collecting CT data from only the area of interest in the engine (i.e., the hub area of the second stage turbine disk).

- Collecting CT data at a small oblique angle (two to six degrees) to the orthogonal in order to more rapidly penetrate the high-Z material of the disk.

- Elimination (within the image) of the considerable rotating and stationary structure within the engine that would normally obscure the area of NDT interest (i.e., the dark hub).

Unfortunately, it was not possible to demonstrate the ability of the system to find features smaller than 0.008 in. Funding constraints forced the use of borrowed equipment to conduct the SXS demonstration. It is believed a small reduction in signal to noise achievable by substituting the intended 16-bit A/D converter to the 12-bit converter actually used would have yielded resolution closer to the 0.001 in. feature detection capability that was calculated from the model, which is believed necessary for reliable engine NDT.

In addition to demonstrating the basic science of SXS, it also showed through a model analysis of GE F101 fan disk that cracks do open up under load sufficiently for detection by SXS long before catastrophic failure.

APPENDIX A—ENGINE SURVEY AND SELECTED RESPONSES

A.1 THE SURVEY OF MANUFACTURERS AND USERS AND ITS (IR)RELEVANCE.

A survey was undertaken of 22 turbine engine manufacturers and users through a questionnaire to determine the size of flaws that was required by manufacturers and users of the SXS system. Unfortunately, it was not realized that the answers provided by the respondents were contingent upon bench inspection practices for components, which are predicated upon very rare inspections. By contrast, SXS can be utilized on a much more frequent basis, so that flaws do not have to be caught at such an incipient stage.

The questionnaire is provided on the next page followed by letters from six of the most responsive organizations. Each of these letters defines a minimum crack size based on their experience with direct inspections of disassembled disks. These data were not relevant, as discussed in section 2. However, each of these letters also provides other highly relevant data that were useful in the development of SXS and support future implementation of SXS.

A.2 REFERENCES.

All figures relating to numbers of aircraft, engines, etc., were provided by the Information Management section of the Boeing Commercial Aircraft Group. Costs for engine teardowns, etc., were provided by the Engine Economics subsection.

SXS PERFORMANCE REQUIREMENTS QUESTIONNAIRE

September 28, 1992

Dear :

Under FAA research sponsorship, Foster-Miller is developing a new NDT (non-destructive testing) technique that makes it easier to find and measure anomalies - including very small cracks - in aircraft turbine engines. This approach, Synchronous X-ray Sinography (SXS), is described in the brief accompanying attachment. **The SXS technology is used to image the insides of these engines while they are running.** Small cracks that are closed in a cold, static, unloaded condition are impossible to find; however, when the turbine is operating (hot and under load), the cracks open, then they can be found quite easily.

Foster-Miller has demonstrated the feasibility of the SXS technology. We are now planning a full scale demonstration of SXS on an actual turbine engine disk containing both natural and machined calibrated cracks rotating at a few thousand RPM. The performance capabilities of the full scale SXS system when it is built will be based on this full scale demonstration. Our goal is to design and build an SXS system that will be a useful tool to the turbine engine designer/builder, the turbine engine user and the turbine engine inspector or regulator.

We need your help to reach this goal to build a cost effective SXS system of maximum usefulness to such a broad range of interests. Your opinion, comments and answers to the following questions will be important to achieving this goal.

Please consider that while providing the answers to these questions, that detection of ever-smaller features (like cracks) is possible, but the smaller the detection threshold, the more the system will cost and the bigger it will be. Thus, it's important to give us a flavor of how important it is to you to see features of different sizes.

1. How small a crack would you like to detect in an engine? Please provide width, length, and depth, and why you would like to know this.

2. In what areas of the engine are you most interested in finding such cracks (e.g., turbine disk, blades)?

3. What other engine anomalies, clearances, or dimensions are you interested in imaging and measuring while an engine is running.

4. Would running such an inspection (estimated duration: one hour) on an engine test stand (i.e., off-wing) be acceptable?

5. Could such a system be run concurrently with other normal maintenance procedures? How often is the engine removed from the wing and in connection with which procedures?

6. Is there merit to consider conducting a SXS inspection on wing, considering it could easily double or triple SXS system/facility cost.

In appreciation for your answers and opinions we will be pleased to provide a report on our first full-scale demonstration, scheduled for October 1992. To be considered in our design, **we need your answers by June 30**. I will call to see if you have any questions. Please feel free to call me at (617)290-0992.

Sincerely,

FOSTER-MILLER, INC.

Ted E. Kirchner, Principal Investigator

enc.

ROLLS-ROYCE plc
PO Box 3, Filton, Bristol BS12 7QE
Telephone: 0272 791234, Telex: 44185

T.E Kirchner
Technology Developers
350 Second Avenue
Waltham
Ma 02154-1196
U.S.A.

272 797083

JDR/5129

10th January 1992

Dear Ted,

Firstly, my apologies for not having written to you earlier but, after returning from the conference in Atlantic City, I have been busy on tests away from Bristol and am only now able to catch up on other work. I greatly appreciated being able to meet both Paul Burstein and yourself and to discuss your plans for the next phase of the SXS project. I hope that you have now received the go-ahead for the start of the new contract.

One of the questions raised during our discussions was, in the case of an engine on a test bed, the degree of jitter in rotational speed which might be encountered at a constant operating condition. Due to the complex interactions between the compressors and the fuel control system, there may be speed variations of ~ 1/4% at any (nominally) constant operating condition. Variations may be greater in the LP turbine than in the HP turbine. A once-per-rev timing pulse can normally be obtained on each engine for timing purposes. However, the provision of more pulses per rev requires the special installation of a phonic wheel in the engine gearbox. It might be possible to make use of a fast pyrometer sensor to obtain a pulse for each passing turbine blade. With such pyrometers, however, flare due to incandescent carbon particles or to the combustion flame may result in saturation of the pyrometer signal during the passage of a number of blades. It would, therefore, be necessary to supply other external trigger pulses for strobing during this dead time. In addition, these sensors will only be effective at or above temperatures corresponding to operation at 80 - 85% NH (% of HP turbine maximum speed).

It has been estimated that, over 20 revs, the variation in individual turbine blade timing is ≤ 1/4%. Long running times may, therefore, give larger variations.

Registered office: 65 Buckingham Gate, London SW1E 6AT
Company number: 1003142, Registered in England

I have recently spoken to Malcolm Perry of the NDT Laboratory at Bristol and he has expressed his willingness to arrange for the loan to you of one or two crack specimens for inclusion in the spinning rig tests. As the turbine disc being supplied to you by the FAA will only be spun at a low speed, these specimens could be held in place on the disc, perhaps one on either side. These would be of real interest in that they represent calibrated actual cracks in place of machined-out specimens. The size of each of these crack standards is:

a) 2mm length, 1.5mm depth and b) 0.7mm length, 0.35mm depth
Crack width is of the order of a few µm.

If there are any other questions I can answer at this time, particularly with regard to the effective metal thicknesses for the spinning disc demonstrator, please do not hestitate to contact me. I look forward to seeing the details of your tests at the Hercules facility.

I expect to be visiting the U.S.A. again to attend a conference in San Fransisco (May 10th - May 16th). If convenient,it would be very useful if I could take the opportunity to visit your test site at the Allegheny Ballistic Laboratories.

Best wishes

Dr.J.D.Rogers

(JDR/5129)

ROLLS-ROYCE INC.

ENGINEERING

2849 Paces Ferry Road, Suite 450
Atlanta, Georgia 30339-3769
Telephone: (404) 436-7900
FAX: (404)436-8570, Easylink: 62330720

Our Ref: JTP.92-71

July 10, 1992

Mr. Ted Kirchner
Foster-Miller, Inc.
350 Second Avenue
Waltham, MA 02154-1196

Dear Ted:

This letter is to confirm our telephone conversation of July 2 with respect to the information you requested about crack sizes of interest to us and the parts which we are interested in inspecting to determine the presence or otherwise of cracks.

We have an interest in reliably detecting cracks in blades and disks. However, the critical issue is not to determine the shortest crack which can be detected but the shortest crack which can be detected with a high degree of confidence and a minimum of false positive indications. As such we feel that the most useful information which could come out of this exercise would be to develop probability of detection curves of real, not phantom, cracks of different sizes.

To this end we are interested in reliably detecting ¼" long cracks in turbine blades. A useful objective with respect to disks would be to be able to reliably detect cracks 0.050" long with a width close to zero and a depth in excess of 0.005" with a probability of 95%.

I have discussed the possibility of obtaining calibrated cracked specimens with our NDE specialists in Rolls-Royce plc. They have expressed a willingness to provide material suitable for attaching to the periphery of the T53 disk to be used during the October tests at Hercules on the understanding that, on completion of the test, they are returned to Rolls-Royce. If you are in agreement with this arrangement, please let me know so that I can organize their delivery to you.

With regard to the information you have requested on speed variation, as I said during our conversation, I am sure that such information must exist. However, I doubt that it has

been analyzed in the way which you prefer. I am trying to make contact with that area of Rolls-Royce which would be most likely to have raw data suitable for your needs. My object is to supply these data for you to analyze. I will contact you to keep you informed of my progress in this regard.

Please let me know if you need any further information.

Sincerely,

J.T. Pinder

Copies:

D.W.J. Cason (Csn) - Derby
B.J. Tester (Tsr) - Derby
M. Perry (EW5-8) - Bristol
A.B. Wassall (ABW) - Derby
R.B. Price (RBP) - Derby
J.D. Rogers (GP2-5) - Bristol

DEPARTMENT OF THE AIR FORCE
WRIGHT LABORATORY (AFSC)
WRIGHT-PATTERSON AIR FORCE BASE, OHIO 45433-6563

REPLY TO ATTN OF: WL/POTC 23 Jun 92

SUBJECT: Crack Detection Threshold Survey

TO: Foster-Miller Inc
ATTN: Ted E. Kirchner
350 Second Avenue
Waltham, MA 02154-1196

1. In your letter of 27 May 92 you asked a series of questions on desirable flaw detection capabilities for aircraft engines. The responses below are roughly in the order of your questions.

2. Crack size requirements vary from one engine to another, but as a guideline, typical minimum detectable (maximum acceptable) crack sizes are:

Surface Cracks in Disks:

In specific areas (the bore, dovetails, and bolt holes): .005" long x .010" deep. The ATF engine requirement is tighter, at .005" long x .005" deep. Eddy current inspection would commonly be used.

In other areas (webs, large surfaces): .015" long x .030" deep. Usually fluorescent penetrant inspection.

Sub-surface Cracks in Titanium or Nickel Forgings or Castings:

Current standard is No 1 Flat Bottomed Hole. Used to be No 3, but has tightened to No 1 in recent years.

The usual standard is 90% Probability of Detection with 95% Confidence Interval. The reason for wanting to find these sizes of cracks is that the component design methodology (whether safe-life or damage tolerant) is based on the assumption that no larger cracks exist.

2. The components of greatest interest for crack detection in an engine would be the large rotating components, variously termed fracture-critical or Group A components. They are usually defined as components whose failure would hazard the aircraft or its occupants, and include disks and shafts. Blade failures are not usually critical, but with fan blade sizes increasing significantly, flaw detection in blades will become more of a concern.

3. A lot of work goes into the design of clearances between rotating and static components in engines, and there are a number of methods of active and passive clearance control. The potential of your technology to enable these clearances to be seen clearly in a running engine would be attractive, at least during development testing and possibly on a production basis. Rolls-Royce Bristol has used direct-viewing X-ray techniques to measure clearances in running engines, but your technique may give better resolution.

4. I would see your technology as being most attractive if it could be used on-wing. Then, for example, a suspect batch of engines could be checked for flawed disks relatively quickly and without the penalties of engine removal, transportation, test stand installation, re-installation in aircraft, etc. However, even having to put such a batch of engines through a test stand would be better than the present state of having to strip the engines to remove and inspect the suspect components.

5. Engines are removed from the wing for a number of reasons, including life expiry (eg a disk reaching its fatigue life), defect investigation (eg vibration), removal for access (eg to repair an adjacent fuel tank). Practices vary between engines and operators, but only sometimes will an engine be run in a test stand before being overhauled; nearly always it will be tested after overhaul. I think, at some stage, you need to address the question of when your inspection would be performed, and what extra benefits the operator will get from the inspection. For example, can the inspection be used to determine whether or not an engine needs to be stripped, or to what depth it needs to be disassembled? Would it be used as a routine inspection method, or only as a tool to investigate specific engine or fleet problems?

6. I realize I haven't answered all your questions, but I've tried to cover those where I have an opinion! I've enclosed copies of 2 report abstracts, following on from the "have cracks, will travel" data I gave you recently. If you want to get into this area, the reports can be ordered from the National Technical Information Service (NTIS), phone (703) 487-4650.

7. Please call me at (513) 255-2351 if you have any further questions. Your program is very promising and I wish you luck with the demonstration.

MICHAEL E. McINTYRE, Sqn Ldr, RAF
Project Engineer
Components Branch
Turbine Engine Division
Aero Propulsion & Power Directorate

Allison

June 26, 1992

Mr. Ted E. Kirchner
Foster-Miller, Inc.
350 Second Avenue
Waltham, MA 02154-1198

Dear Mr. Kirchner:

The following replies have been assembled in response to your facsimile letter of June 19, 1992. I solicited inputs from several disciplines within Allison, and result is a composite of their inputs.

You recognize, of course, that your questions entail far reaching technical, economic and regulatory considerations that vary from individual instance to instance. In order to respond in a timely and efficient manner, our responses are a "broad brush" approach that may result in contradiction to actual requirements for some specific cases.

The numbered statements attached refer to the questions of your June 19, 1992 letter. Please call if you need any clarification.

Regards,

Richard D. Zordan

Dr. Richard D. Zordan
Materials & Processes

Enc

Allison Gas Turbine Division General Motors Corporation P.O. Box 420 Indianapolis, Indiana 46206-0420

Response to Foster-Miller Technical Survey
SXS Inspection Technology

1. To be consistent with current crack limits on existing rotating components, cracks as small as 0.030 in. length by 0.015 in. depth need to be detected. Rotating parts with larger cracks are typically rejected, both in new production and at overhaul.

2. Cracks are of concern in all areas, since they can ultimately lead to component failures. Cracks in rotating hardware such as turbine disks, turbine blades, compressor disks and compressor blades are of greatest interest because of the flight safety aspects of failures in these components. Detection of cracks in less safety-critical, non-rotating components such as vanes or combustors would also be valuable for repair and maintenance purposes.

3. Gas path clearances between stationary and rotating components are generally more important to engine operating performance and performance retention than to safety issues. The ability to measure these clearances on running engines could be a real benefit, especially in light of emerging active clearance control technologies. On-wing rather than test stand capability would be a real advantage in this case.

4. Most engines currently being introduced into service are maintained through an "On-Condition" (read as "observation of some operational anomaly") maintenance concept. They are not typically removed from service just for inspection. Therefore, if it can be assumed that some anomaly has resulted in an engine being removed, then the ability to detect the problem on a test cell using SXS technology is of questionable value, since the engine will still require disassembly for problem correction. It would be a combined technical and economic decision whether SXS would facilitate the diagnosis and repair of the exact operational problem.

5. Some major aircraft inspections require engine removal. However, unless operational problems exist with the engine, there would be no need to run the engine in a test cell. The frequency of engine removal varies greatly depending on aircraft and engine requirements.

6. From a maintenance perspective, the ability to do on-wing inspections is very desirable, especially in view of modern "On-Condition" maintenance practices. Facility justification would involve a very detailed cost analysis that would be aircraft and engine specific, operator specific, and dependent upon the actual flaw detection capability of the SXS technique. If SXS performs extremely well, as an on-wing device it might be more justifiable as an enabling technology, rather than just one more of a whole host of off-wing inspection techniques. In either case, justification for SXS technology investment will be closely linked to its detection capability.

Ref. Letter, Ted E. Kirchner, Foster-Miller, Inc., dated June 2, 1992

Provided below and attached for response to subject letter.

Question #1

A difficult question for Army AVSCOM since parts retirement is based on safe - life criteria i.e. design life limit based on crack initiations. Parts retired (in theory at least) at this design life point. If we ever follow Air Force into crack growth/damage tolerance criteria we would probably have similar (to AF) crack size retirement criteria. With our current approach, any defect detectable by MPI in a critical area (e.g. disc bore) is rejected. Standard MPI limit is 0.015 "length, 0.0037" depth.

The combustor could be a candidate part for a large crack limit, since cracks in this part generally must be large before serious engine damage occurs. However, combustor cracks typically do not cause engine failures in Army engines, since engines are typically returned to depot for overhaul due to other causes prior to large combustor cracks developing.

Question #2

All rotating structural parts including shafts & accessories which are safety critical. Also critical static parts such as high pressure vessels (combustors/turbine case, high pressure fuel lines and cartings, compressor discharge pressure control lines & oil supply) and bearing races under high hoop stress.

Question #3

As a development tool, all performance - imparting clearances are of interest e.g. airfoil trip/shroud turbine seals, compressor discharge air seals, combustor interface seals.

SUBJECT: Foster-Miller, Inc. Questionaire on SXS Testing

1. AVSCOM Maintenance does not currently require a system for detecting cracks in operating engines except possibly on an exception basis. Maintenance Engineering is not aware of any information indicating we have a cracking problem on any critical components that has not been addressed at this time. Maintenance Engineering also does not have any information relating cracks on non life limited components to usage or time nor any information on the time to failure once a crack is initiated, both, necessary information for setting an inspection interval in which a reasonable chance of detecting a failure exists. Exceptions could exist when a safety of flight condition arises due to discrepant materials, procedures, etc. which could be related to a known set of conditions enabling us to set criterion and an interval for inspection. The width, length and depth of the potential crack would be dependant on the failure mode determined at the time.

2. Unique to the failure mode as determined on an exception basis.

3. Maintenance Engineering would be interest in cost efficient methods for determining failures which exhibit a relationship to a known cause or usage factor or a long duration failure such as: critical gaps or clearances, or damage due to exceedances. There are also other items where an inspection which does not require disassembly would be useful but, do not require running of the engine such as: inspection of clogged cooling holes in blades and nozzles, inspection for corrosion/erosion to rotating components, inspection of oil wetted components for confirmation of AOAP or chip detector indications.

4. Yes, depending on the failure mode and criticality.

5. Maintenance Engineering would attempt to align such an inspection with scheduled maintenance in order to minimize downtime.

6. There is merit to conducting a SXS inspection on wing as it would have a breader range of application however, this application would be more sensitive to overall cost because a larger number would be procured.

FAA - WHOLE ENGINE CT

The following is a response to the FAA's question:

"IF an x-ray CT slice of an engine were available, what would be a useful volumetric object to be able to image."

1 Assembly configuration - presence or absence of parts, offsets and clearances

2 Foreign object damage detection - FOD extent, foreign body presence and location, determination of tear-down extent

3 Dynamic clearances - engine steady-state condition

4 Defect detection - gross cracks in metals, cracks and/or delaminations in composite materials

QUALIFIERS

General:

Based on experience in whole engine dynamic radiography using an 8MeV, 1mm focal spot size linear accelerator, the proposed CT system would have to be high energy (>8MeV) and very high output(>3000R/min). Long scan times probable. Disk inspections impossible. Rotating the engine core to produce the CT image would be a possibility but difficult to implement.

Specific to above:

1 Most likely application of CT system. Would need resolution around 'O'-ring or spring size.

2 Gross damage assessment feasible. Depends on resolution.

3 Engine must be at steady state condition. Existing high energy dynamic radiography probably good enough for axial and radial clearance measurements.

4 Crack detection in metals would require open cracks of the order of magnitude of the CT image pixel size (0.020"?) This would probably be too coarse to provide useful output in large critical areas (e.g. disks). Crack and delamination detection in composite components is more likely, e.g. carbon-carbon nozzle flaps, composite cases, composite vanes and blades. Sensitivity to low density composites in metallic surroundings would be a problem, however.

APPENDIX B—GE F101 STAGE FAN DISK CRACKING ANALYSIS

Stress Technology Incorporated
1800 Brighton-Henrietta Town Line Road
Rochester, New York 14623

TECHNICAL REPORT PA859

GE F101 STAGE FAN DISK CRACKING ANALYSIS

Submitted to:

Mr. Ted Kirchner
Director, Materials Technology Group
Foster Miller Incorporated
350 Second Avenue
Waltham, MA 02154-1196

Prepared by:

Dr. Hao Yu
Structural Engineer

Reviewed by:

Tony C. T. Lam
Vice President-Engineering

April 28, 1994

EXECUTIVE SUMMARY

As requested by Foster Miller, Inc., the disk cracking analysis for the GE F101 fan was performed. Steady Stresses and displacements in the disk were calculated under the centrifugal load. The results were further used to predict the crack mouth displacements for 10 surface cracks and 10 corner cracks whose locations and sizes were provided by Foster-Miller. In addition, for each crack, the curve of the estimated stress intensity factor versus the normalized distance along the crack front was given.

This report describes the results of the analytical work performed by Stress Technology Incorporated. (STI).

TABLE OF CONTENTS

1.0 COMPUTER MODELING AND STEADY STRESS CALCULATION B-5

2.0 FRACTURE ANALYSIS B-9

3.0 REFERENCES B-18

APPENDIX B-19

1.0 COMPUTER MODELING AND STEADY STRESS CALCULATION

The computer model of a single root-disk segment was created to perform the steady stress analysis. In order to obtain accurate results, a finer mesh was used in the disk bottom area. Moreover, the whole root-disk finite element model with 50 single segments was further generated by BLADE™ for the disk cracking analysis. The single segment model has 89 elements and 205 nodes while the whole root-disk model has 10, 250 elements and 4,450 nodes. These models are shown in figure 1.1. The element used for these models is an 8-noded solid element with 3 degrees of freedom at each node.

The weight density and Poisson's ration of the material were assumed to be 0.16 lb/in^3 and 0.33 respectively. A Young's modulus of 17,000 Ksi was used. The material behavior was assumed linearly elastic and isotropic.

Steady stresses in the finite element model of a single root-disk segment were computed under the effect of the centrifugal forces due to the rotational speed. The effect of these forces on the airfoil of the blades was calculated from the original 3-D model and transmitted to the single segment model. The body force due to the centrifugal force was calculated using the following equation:

$$F_{cf} = \int^{v} \rho\omega^2 R \, dv$$

Figures 1.2 and 1.3 show the distribution of the predicted stress (von Mises stress) in the root-disk single segment from two different views. The calculated maximum stress of 65.8 Ksi was found to be at the bottom area of the disk.

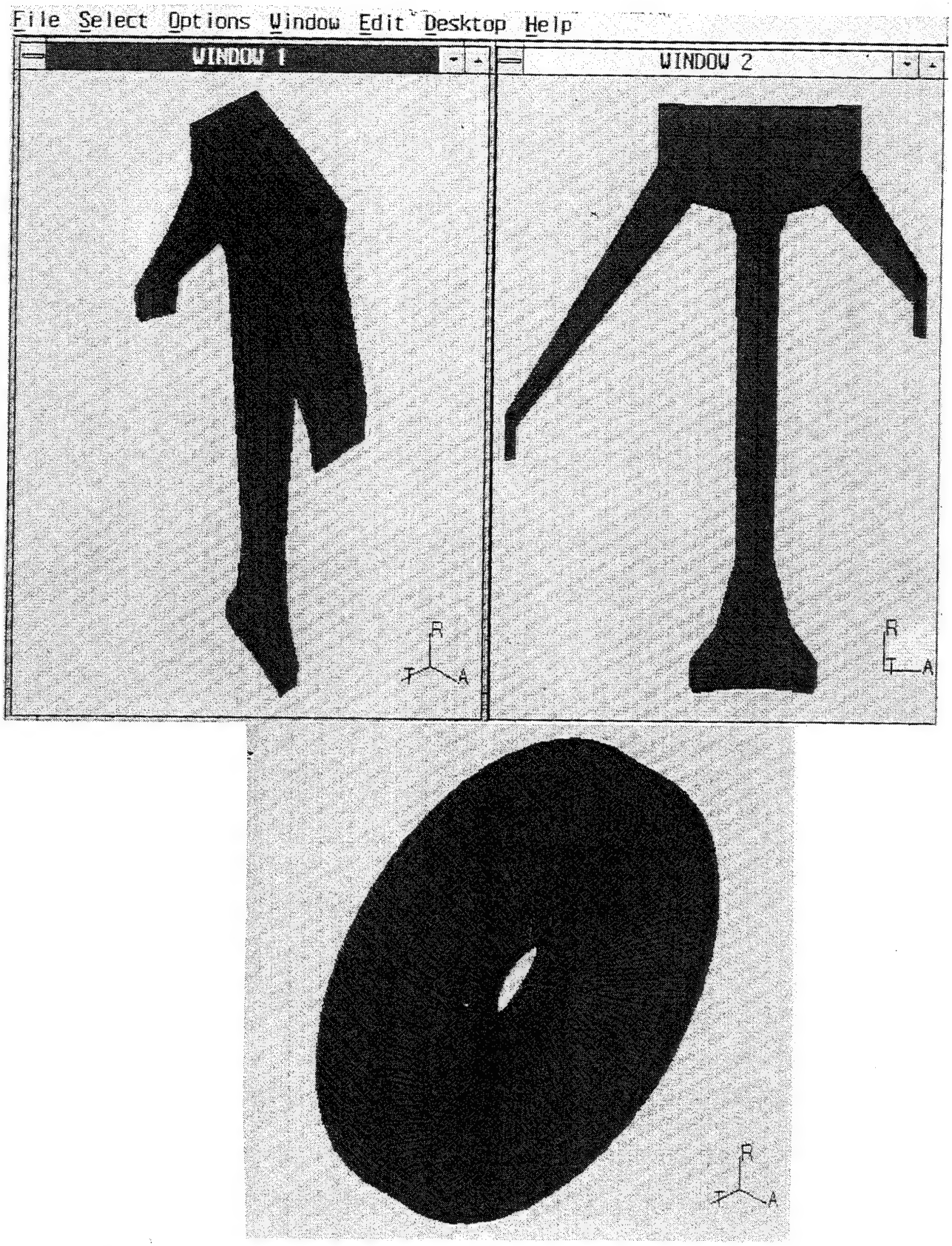

FIGURE 1.1 FINITE ELEMENT MODELS OF ROOT-DISK STRUCTURES

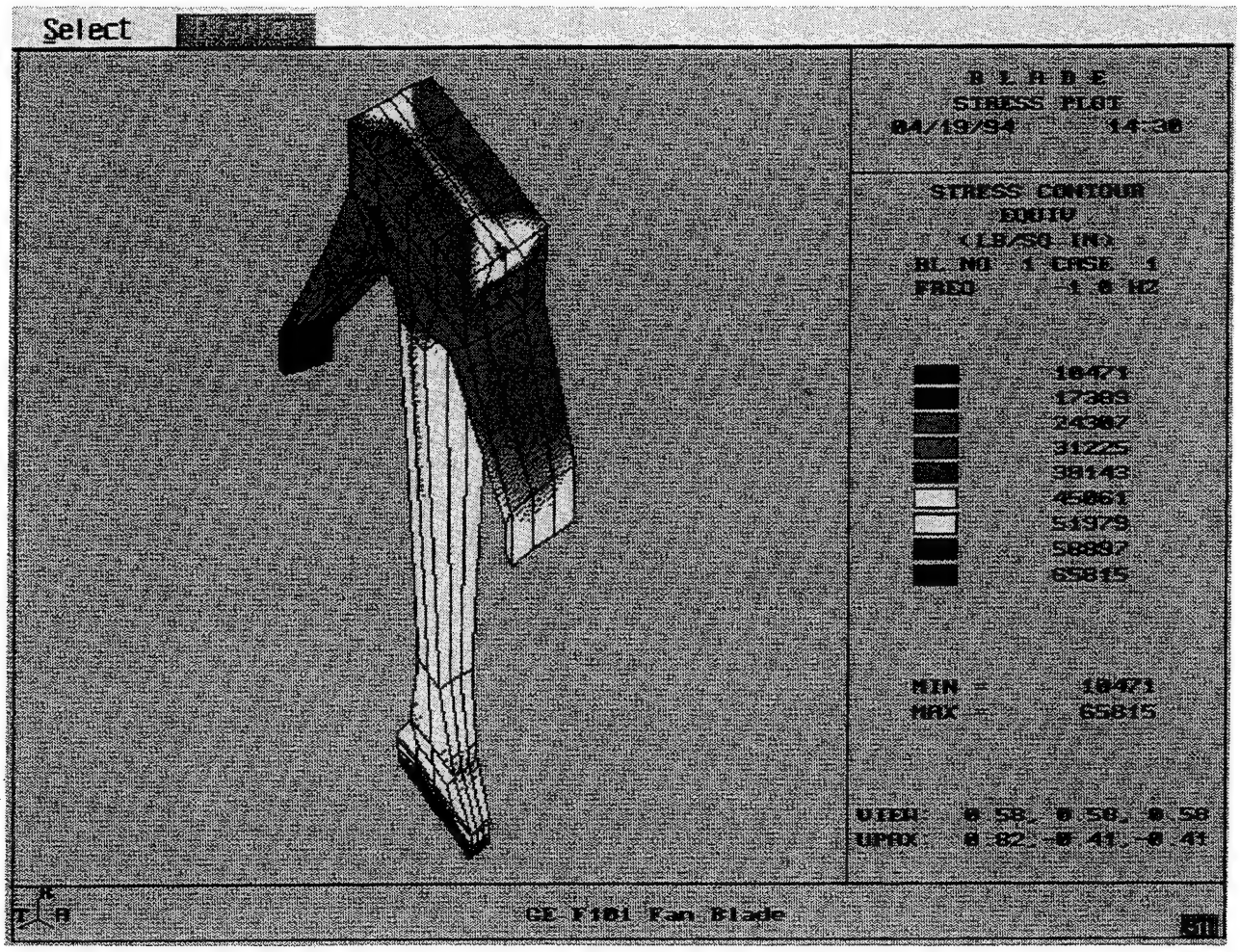

FIGURE 1.2 STRESS IN A ROOT-DISK SINGLE SEGMENT

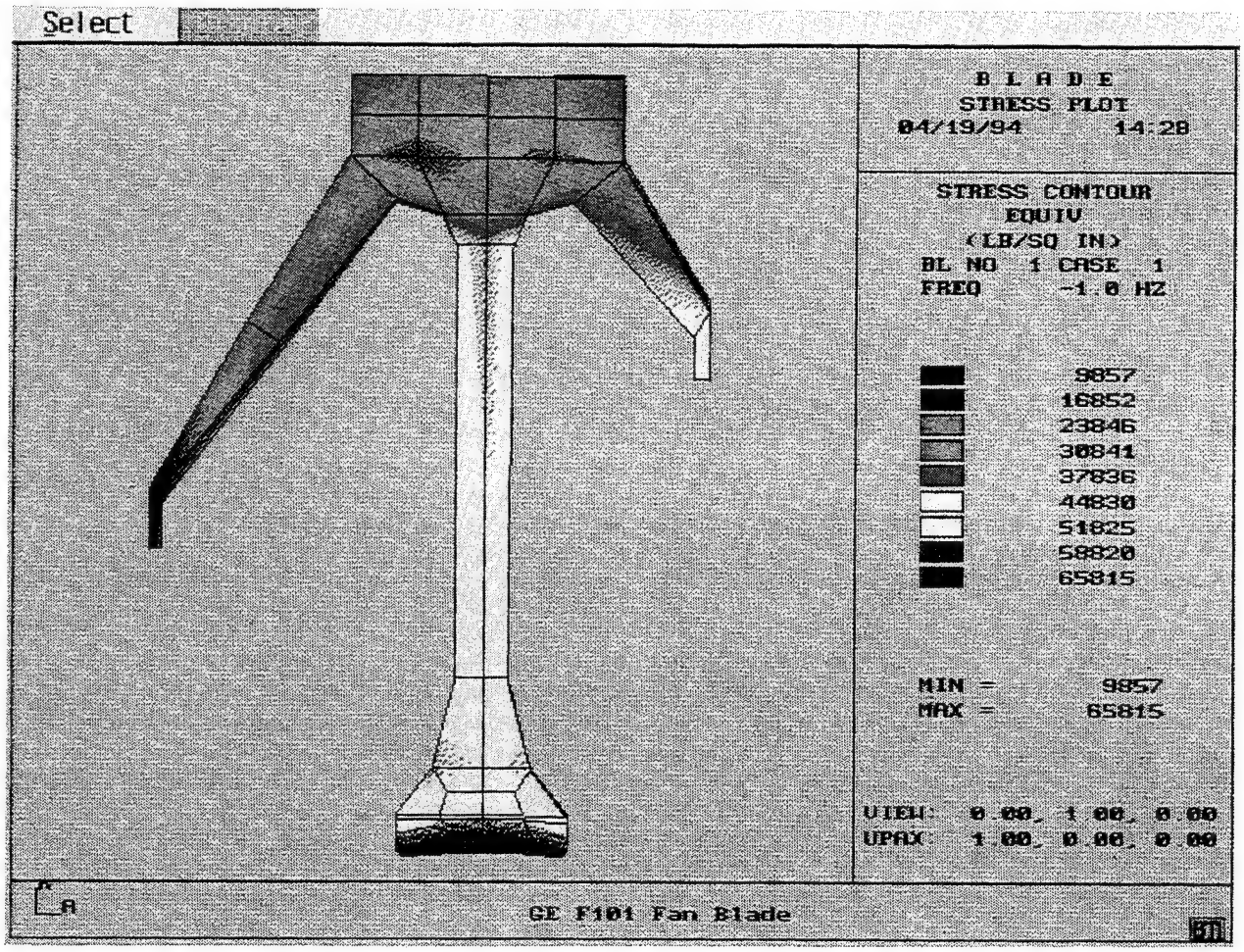

FIGURE 1.3 STRESS IN A ROOT-DISK SINGLE SEGMENT (TANGENTIAL VIEW)

2.0 FRACTURE ANALYSIS

In the disk cracking analysis, as listed in table 2.1, there are 10 surface cracks and 10 corner cracks being analyzed, whose sizes and locations are provided by Foster-Miller.

TABLE 2.1 CRACK TYPE AND SIZE

Crack #	Surface Crack (inch)		Corner Crack (inch)	
	Length l	Depth d	Length l	Depth d
1	0.01	0.005	0.005	0.005
2	0.05	0.25	0.025	0.025
3	0.1	0.05	0.05	0.05
4	0.17	0.085	0.085	0.085
5	0.3	0.15	0.15	0.15
6	0.5	0.25	0.25	0.25
7	0.8	0.4	0.4	0.4
8	1.0	0.5	0.5	0.5
9	1.3	0.65	0.65	0.65
10	1.5	0.75	0.75	0.75

Using the resulting stresses and displacements along with the finite element models provided by STI, the disk fracture analysis was performed with the FRANC-3D crack propagation system by the Fracture Analysis Consultants (FAC), Inc. in Cornell University, Ithaca, New York. This System incorporates capabilities for solid modeling, mesh generation, boundary-element based stress/displacement analysis, and fracture mechanics. Figures 2.1 through 2.6 show the deformations of some typical surface and corner cracks in the disk respectively. For each crack listed in the table, in the appendix there is a corresponding illustration showing the size, location, and mesh of the crack. In addition, the calculated crack mouth displacements in the

X, Y and Z directions at the defined points (i.e., a, b, c ..., etc.) along the crack are given, and the curve of the calculated stress intensity factor versus the normalized distance along the crack front is shown. Note that for each crack in the illustrations, the predicted crack opening at each point is the total displacement in the Y direction (i.e., the rotational direction of the disk) at that point. For each surface or corner crack, tables 2.2 through 2.3 list the value of the crack opening at each point in the crack mouth.

TABLE 2.2 CRACK MOUTH DISPLACEMENT (INCH) IN ROTATIONAL (Y) DIRECTION

Point	Surface Crack Size (inch x inch)			
	0.01x0.005	0.05x0.025	0.10x0.05	0.17x0.085
a	0.000	0.000	0.000	0.000
b	0.00003388	0.00022961	0.00034637	0.00055998
c	0.00004648	0.00017289	0.00045174	0.00076214
d	0.00005247	0.00025981	0.00051358	0.00086045
e	0.00005406	0.00026809	0.00053121	0.00088248
f	0.00005248	0.00025868	0.00051559	0.00085864
g	0.00004650	0.00017200	0.00045659	0.00075387
h	0.00003365	0.00022806	0.00034451	0.00055553
i	0.000	0.000	0.000	0.000

TABLE 2.2 CRACK MOUTH DISPLACEMENT (INCH) IN ROTATIONAL (Y) DIRECTION (CONTINUED)

Point	Surface Crack Size (inch x inch)			
	0.30x0.15	0.50x0.25	0.80x0.40	1.00x0.50
a	0.000	0.000	0.000	0.000
b	0.00096160	0.00161092	0.00257018	0.00304753
c	0.00129964	0.00210861	0.00331830	0.00412237
d	0.00146887	0.00237273	0.00371728	0.00464025
e	0.00150928	0.00245586	0.00383307	0.00479025
f	0.00146804	0.00238266	0.00372033	0.00465854
g	0.00129846	0.00211531	0.00333081	0.00418194
h	0.00096033	0.00160225	0.00256770	0.00322705
i	0.000	0.000	0.000	0.000

TABLE 2.2 CRACK MOUTH DISPLACEMENT (INCH) IN ROTATIONAL (Y) DIRECTION (CONTINUED)

Point	Surface Crack Size (inch x inch)	
	1.30x0.65	1.50x0.75
a	0.000	0.000
b	0.00439791	0.00558889
c	0.00551411	0.00693380
d	0.00622178	0.00762755
e	0.00641519	0.00782914
f	0.00620554	0.00764325
g	0.00547381	0.00692336
h	0.00436598	0.00549981
i	0.000	0.000

TABLE 2.3 CRACK MOUTH DISPLACEMENT (INCH) IN ROTATIONAL (Y) DIRECTION

Point	Corner Crack Size (inch x inch)			
	0.005x0.005	0.025x0.025	0.05x0.05	0.085x0.085
a	0.000	0.000	0.000	0.000
b	0.00003376	0.00017669	0.00033268	0.00058489
c	0.00004342	0.00022868	0.00045429	0.00077676
d	0.00004713	0.00025926	0.00052154	0.00088598
e	0.00004745	0.00027074	0.00055501	0.00094556
f	0.00004712	0.00025988	0.00051952	0.00088332
g	0.00004299	0.00022838	0.00045723	0.00077628
h	0.00002880	0.00017467	0.00033952	0.00056899
i	0.000	0.000	0.000	0.000

TABLE 2.3 CRACK MOUTH DISPLACEMENT (INCH) IN ROTATIONAL (Y) DIRECTION (CONTINUED)

Point	Corner Crack Size (inch x inch)			
	0.15x0.15	0.25x0.25	0.40x0.40	0.50x0.50
a	0.000	0.000	0.000	0.000
b	0.00094680	0.00166713	0.00249322	0.00345108
c	0.00119001	0.00215039	0.00333232	0.00430969
d	0.00137992	0.00250403	0.00390764	0.00496460
e	0.00152947	0.00274556	0.00431292	0.00552503
f	0.00160412	0.00279808	0.00462152	0.00588395
g	0.00166566	0.00283867	0.00462853	0.00621172
h	0.00171061	0.00269347	0.00463642	0.00617861
i	0.00174769	0.00251216	0.00441094	0.00614382
j	0.00165815	0.00228103	0.00417105	0.00578526
k	0.00154737	0.00193464	0.00388151	0.00542374
l	0.00138883	0.00143753	0.00349966	0.00497646
m	0.00115883	0.000	0.00299736	0.00442249
n	0.00080204	-----	0.00234658	0.00365592
o	0.000	-----	0.000	0.00250988
p	-----	-----	-----	0.000

TABLE 2.3 CRACK MOUTH DISPLACEMENT (INCH) IN ROTATIONAL (Y) DIRECTION (CONTINUED)

Point	Corner Crack Size (inch x inch)	
	0.65x0.65	0.75x0.75
a	0.000	0.000
b	0.00442827	0.00508389
c	0.00581643	0.00673918
d	0.00677426	0.00803000
e	0.00749036	0.00893265
f	0.00784421	0.00965252
g	0.00818504	0.01000273
h	0.00844942	0.01031392
i	0.00870848	0.01059207
j	0.00852359	0.01031522
k	0.00794668	0.00955155
l	0.00737162	0.00880305
m	0.00672685	0.00796832
n	0.00592284	0.00697763
o	0.00487855	0.00570955
p	0.00335264	0.00387745
q	0.000	0.000

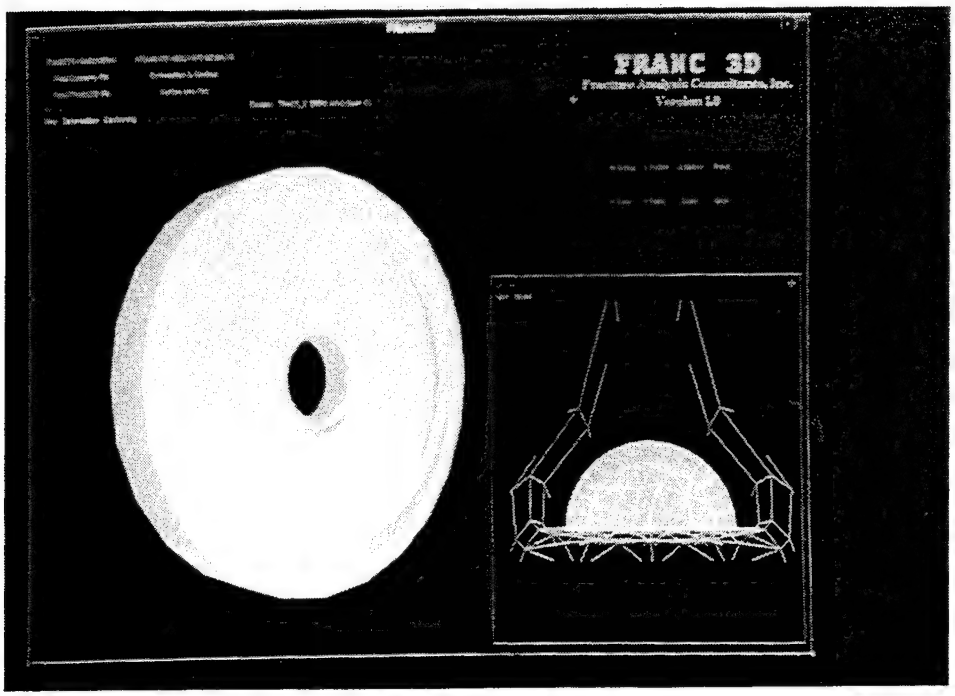

FIGURE 2.1 A SURFACE CRACK IN DISK

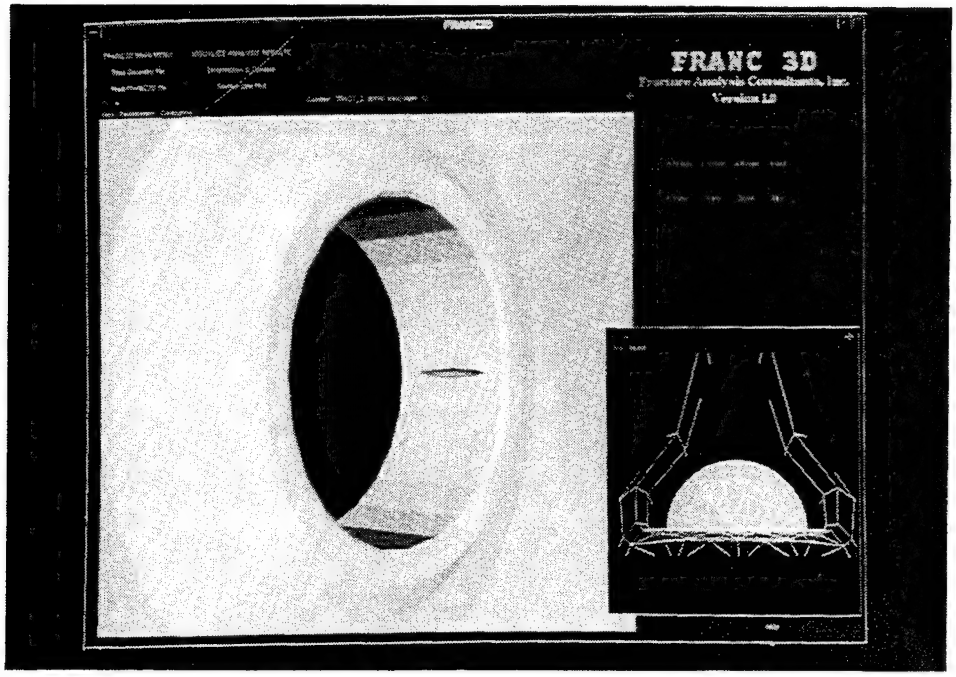

FIGURE 2.2 DETAILS OF A DEFORMED SURFACE CRACK

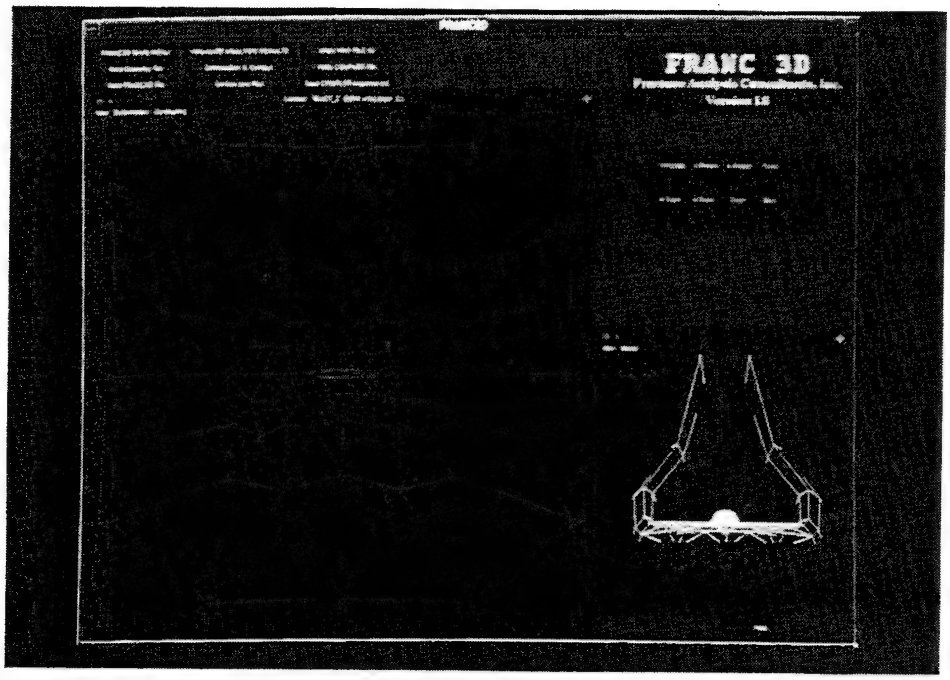

FIGURE 2.3 DEFORMATION OF A SURFACE (CENTER BORE) CRACK (VECTOR PLOT)

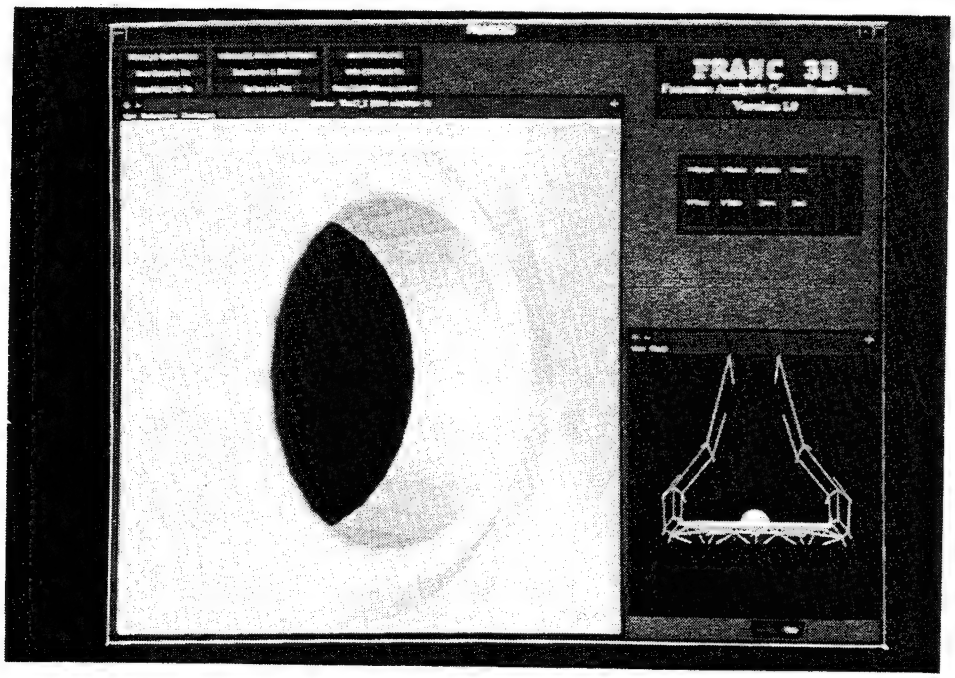

FIGURE 2.4 DEFORMATION OF A SURFACE (CENTER BORE) CRACK (SOLID PLOT)

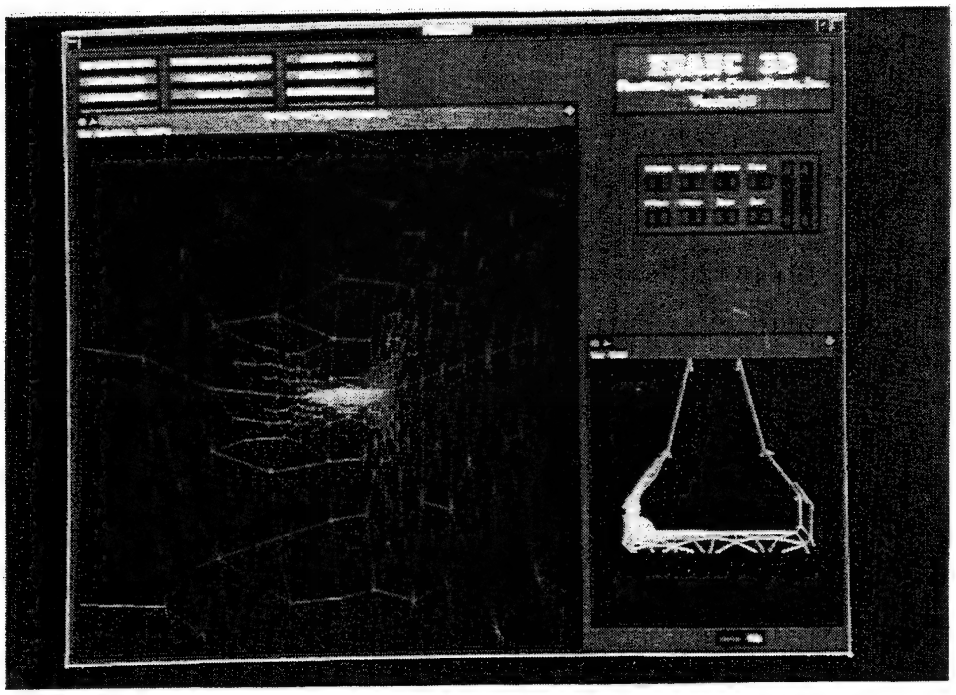

FIGURE 2.5 DEFORMATION OF A SURFACE (CORNER) CRACK (VECTOR PLOT)

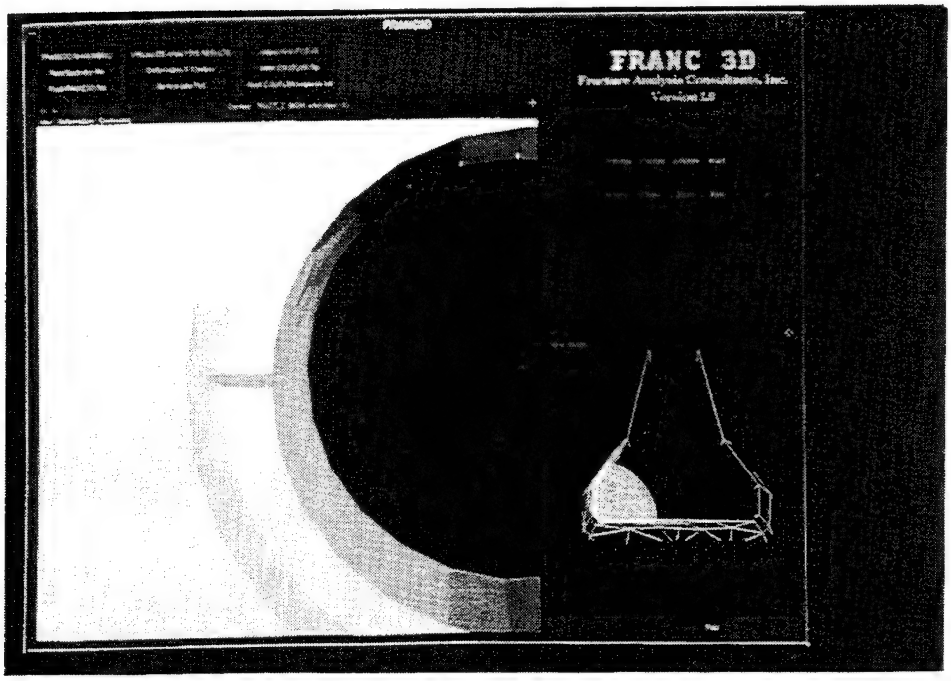

FIGURE 2.6 DEFORMATION OF A SURFACE (CORNER) CRACK (SOLID PLOT)

3.0 REFERENCES

1. BLADE User's Manual, Stress Technology Incorporated, Research version 0.2, January 1989.

2. ANSYS User's Manual, Swanson Analysis Incorporated, Revision 4.2, June 1985.

APPENDIX

Surface Crack: 0.01 by 0.005 inch

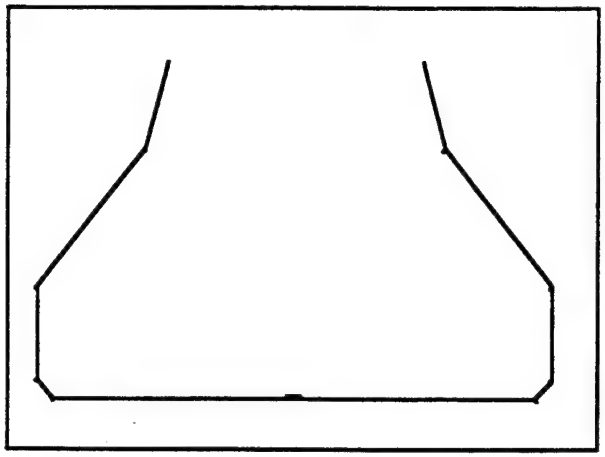

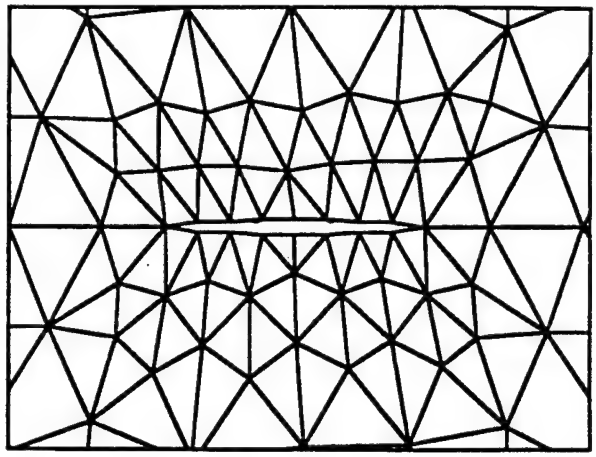

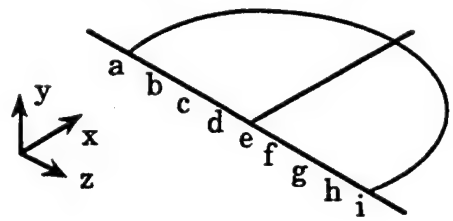

	Undeformed Coordinates x	y	z	Crack Opening	Crack Mouth Displacements dx	dy	dz
a	2.1000	0.0000	0.0050	0.00000000	0.00791578	0.00001105	0.00675513
b	2.1000	0.0000	0.0038	0.00003338	0.00790839	0.00002778	0.00675678
c	2.1000	0.0000	0.0025	0.00004648	0.00790461	0.00003427	0.00676053
d	2.1000	0.0000	0.0013	0.00005247	0.00790315	0.00003725	0.00676321
e	2.1000	0.0000	0.0000	0.00005406	0.00790378	0.00003804	0.00676595
f	2.1000	0.0000	-0.0013	0.00005248	0.00790313	0.00003723	0.00676871
g	2.1000	0.0000	-0.0025	0.00004650	0.00790458	0.00003427	0.00677142
h	2.1000	0.0000	-0.0038	0.00003365	0.00790839	0.00002775	0.00677415
i	2.1000	0.0000	-0.0050	0.00000000	0.00791484	0.00001096	0.00677688

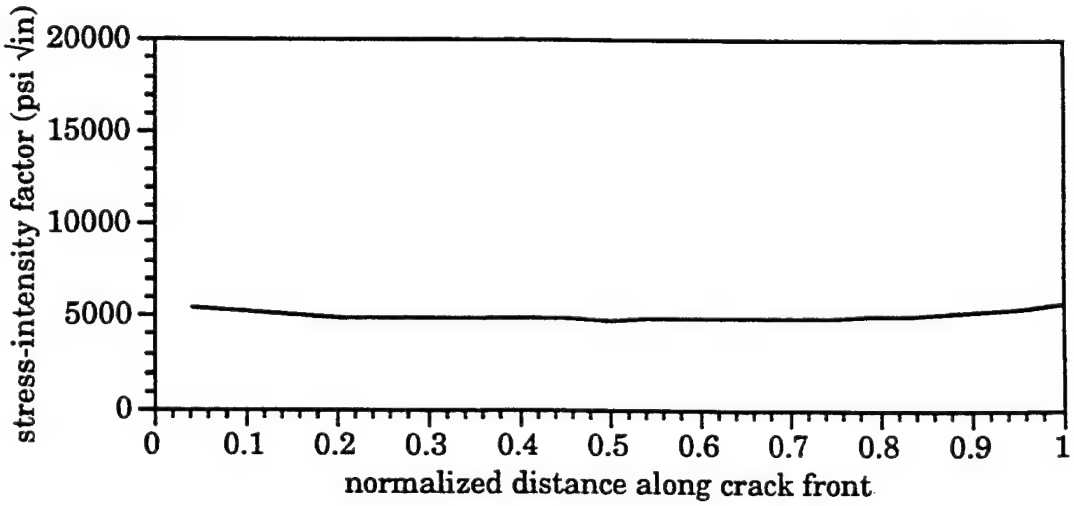

Surface Crack: 0.05 by 0.025 inch

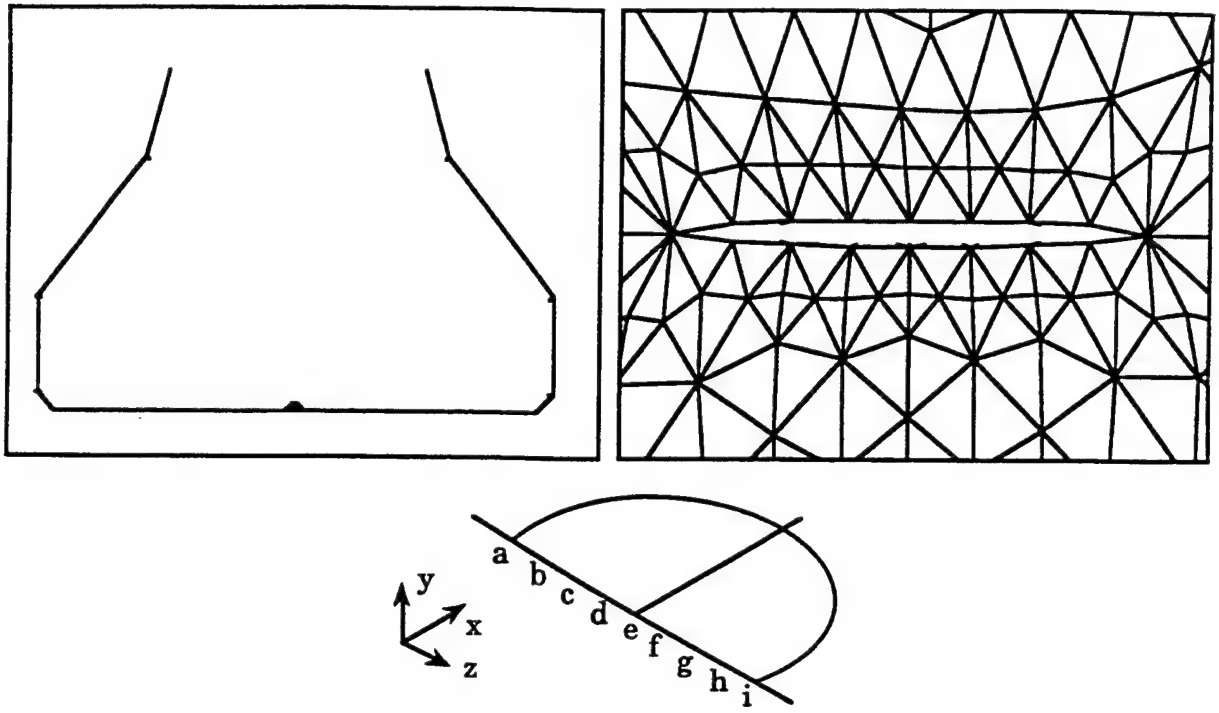

	Undeformed Coordinates x	y	z	Crack Opening	Crack Mouth Displacements dx	dy	dz
a	2.1000	0.0000	0.0250	0.00000000	0.00790963	0.00001111	0.00671375
b	2.1000	0.0000	0.0125	0.00022961	0.00785611	0.00012583	0.00673483
c	2.1000	0.0000	0.0187	0.00017289	0.00786902	0.00009747	0.00671861
d	2.1000	0.0000	0.0063	0.00025981	0.00784865	0.00014093	0.00675070
e	2.1000	0.0000	0.0000	0.00026809	0.00784766	0.00014507	0.00676571
f	2.1000	0.0000	-0.0063	0.00025868	0.00784795	0.00014035	0.00678060
g	2.1000	0.0000	-0.0187	0.00017200	0.00786614	0.00009700	0.00681275
h	2.1000	0.0000	-0.0125	0.00022806	0.00785438	0.00012503	0.00679495
i	2.1000	0.0000	-0.0250	0.00000000	0.00790570	0.00001091	0.00681828

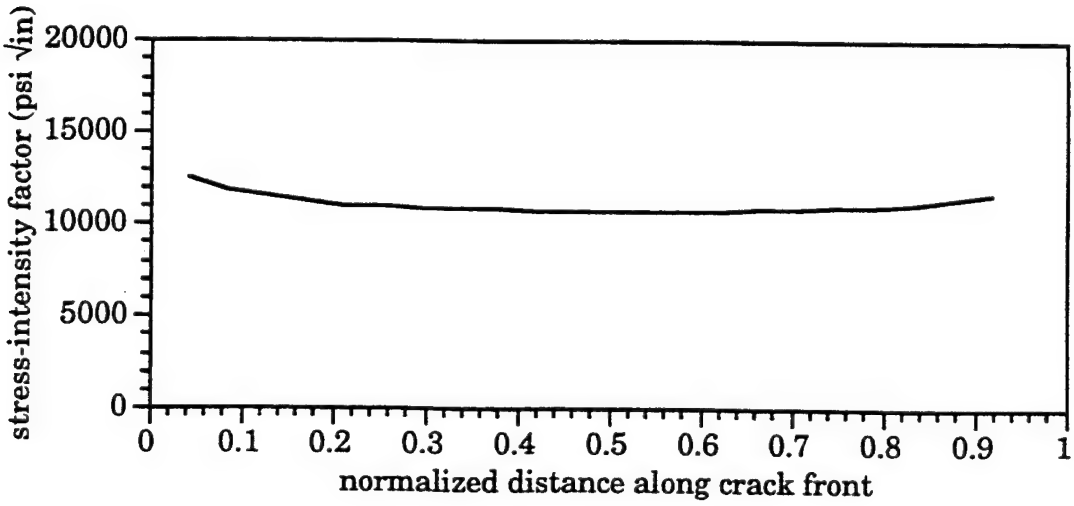

Surface Crack: 0.10 by 0.05 inch

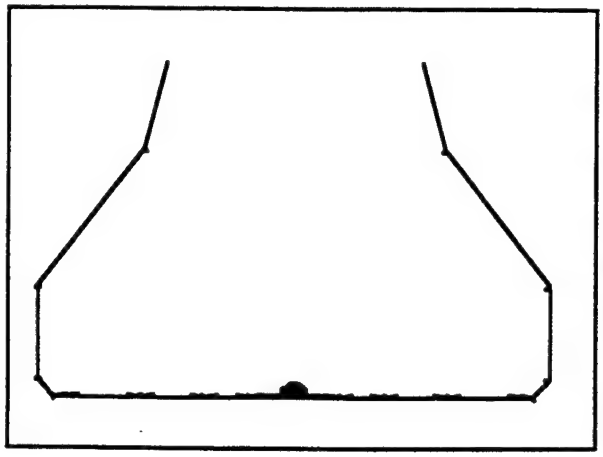

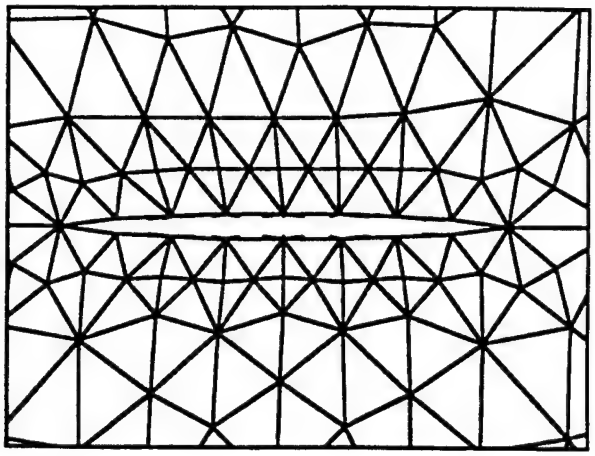

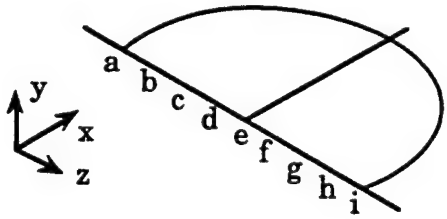

	Undeformed Coordinates x	y	z	Crack Opening	Crack Mouth Displacements dx	dy	dz
a	2.1000	0.0000	0.0500	0.00000000	0.00789963	0.00001123	0.00666133
b	2.1000	0.0000	0.0375	0.00034637	0.00782034	0.00018428	0.00667279
c	2.1000	0.0000	0.0250	0.00045174	0.00779636	0.00023696	0.00670521
d	2.1000	0.0000	0.0125	0.00051358	0.00778208	0.00026789	0.00673560
e	2.1000	0.0000	0.0000	0.00053121	0.00777891	0.00027670	0.00676533
f	2.1000	0.0000	-0.0125	0.00051559	0.00777942	0.00026890	0.00679396
g	2.1000	0.0000	-0.0250	0.00045659	0.00779044	0.00023934	0.00682422
h	2.1000	0.0000	-0.0375	0.00034451	0.00781429	0.00018331	0.00685737
i	2.1000	0.0000	-0.0500	0.00000000	0.00789185	0.00001084	0.00687083

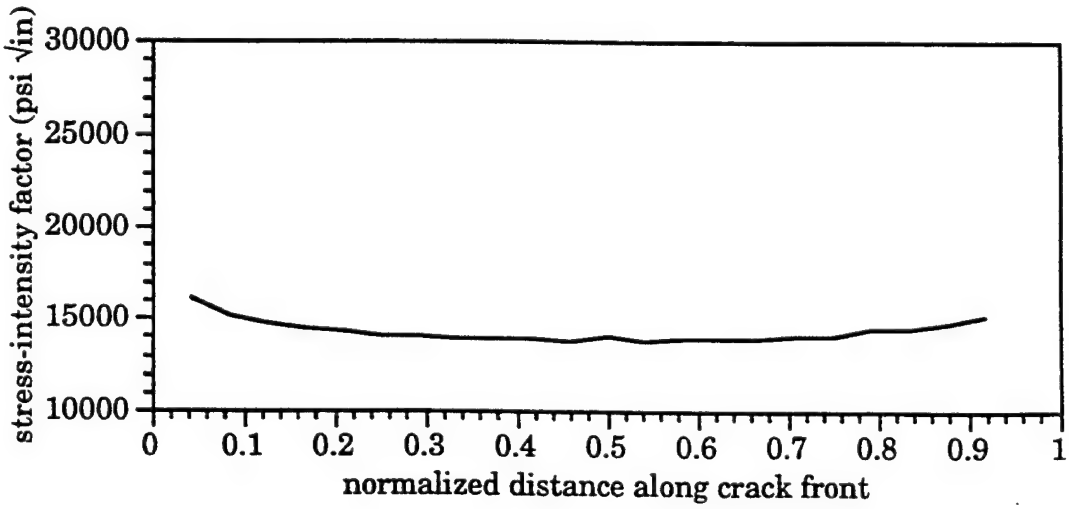

Surface Crack: 0.17 by 0.085 inch

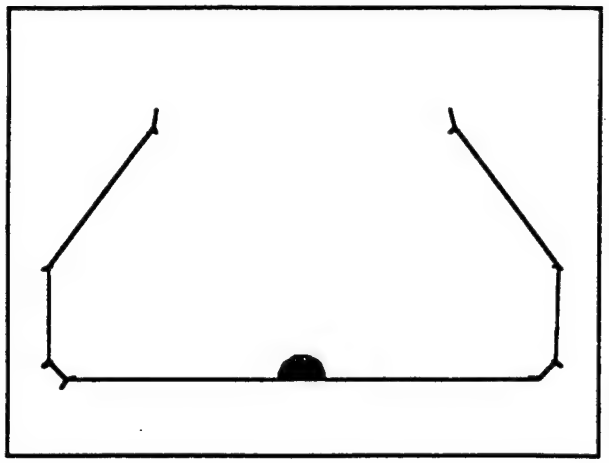

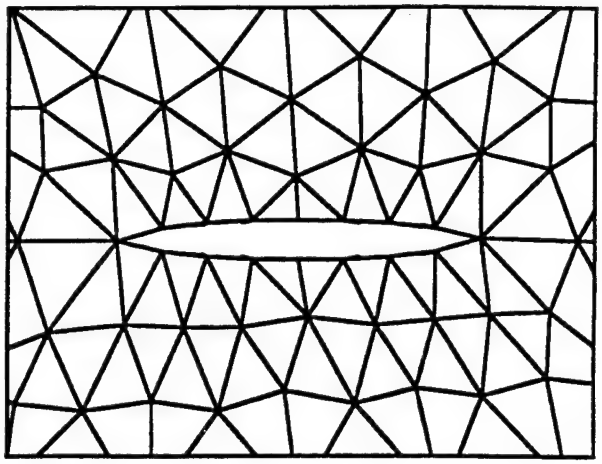

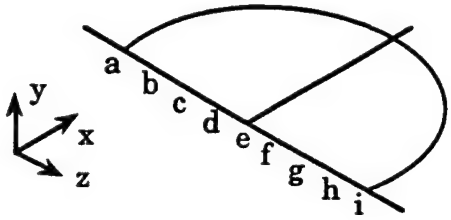

	Undeformed Coordinates x	y	z	Crack Opening	Crack Mouth Displacements dx	dy	dz
a	2.1000	0.0000	0.0850	0.00000000	0.00789094	0.00001176	0.00658810
b	2.1000	0.0000	0.0638	0.00055998	0.00776693	0.00029146	0.00661399
c	2.1000	0.0000	0.0425	0.00076214	0.00771307	0.00039245	0.00666838
d	2.1000	0.0000	0.0213	0.00086045	0.00769072	0.00044130	0.00671703
e	2.1000	0.0000	0.0000	0.00088248	0.00768801	0.00045238	0.00676525
f	2.1000	0.0000	-0.0213	0.00085864	0.00768821	0.00044026	0.00681371
g	2.1000	0.0000	-0.0425	0.00075387	0.00770919	0.00038794	0.00686594
h	2.1000	0.0000	-0.0638	0.00055553	0.00776063	0.00028777	0.00691417
i	2.1000	0.0000	-0.0850	0.00000000	0.00787859	0.00001022	0.00694417

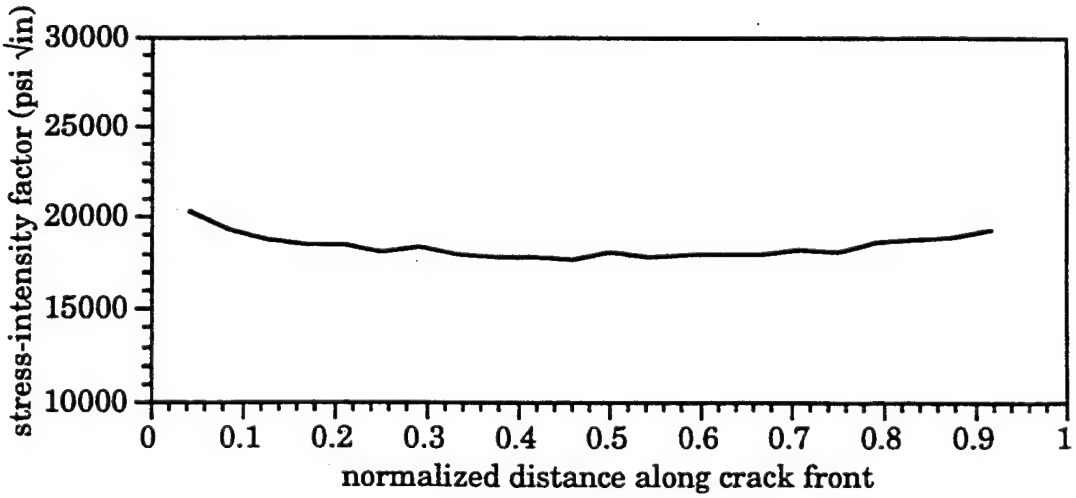

Surface Crack: 0.30 by 0.15 inch

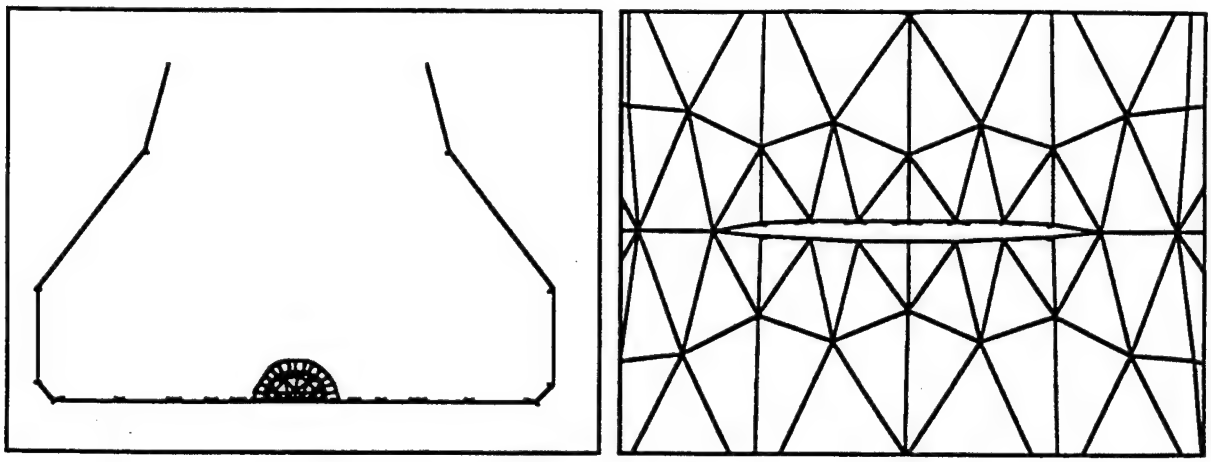

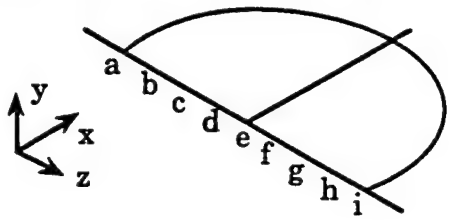

	Undeformed Coordinates x	y	z	Crack Opening	Crack Mouth Displacements dx	dy	dz
a	2.1000	0.0000	0.1500	0.00000000	0.00787366	0.00001153	0.00645240
b	2.1000	0.0000	0.1125	0.00096160	0.00765707	0.00049196	0.00650637
c	2.1000	0.0000	0.0750	0.00129964	0.00757260	0.00066095	0.00659797
d	2.1000	0.0000	0.0375	0.00146887	0.00753122	0.00074555	0.00668235
e	2.1000	0.0000	0.0000	0.00150928	0.00752487	0.00076570	0.00676464
f	2.1000	0.0000	-0.0375	0.00146804	0.00752536	0.00074496	0.00684610
g	2.1000	0.0000	-0.0750	0.00129846	0.00756061	0.00066003	0.00693074
h	2.1000	0.0000	-0.1125	0.00096033	0.00763793	0.00049084	0.00702323
i	2.1000	0.0000	-0.1500	0.00000000	0.00784948	0.00001064	0.00707878

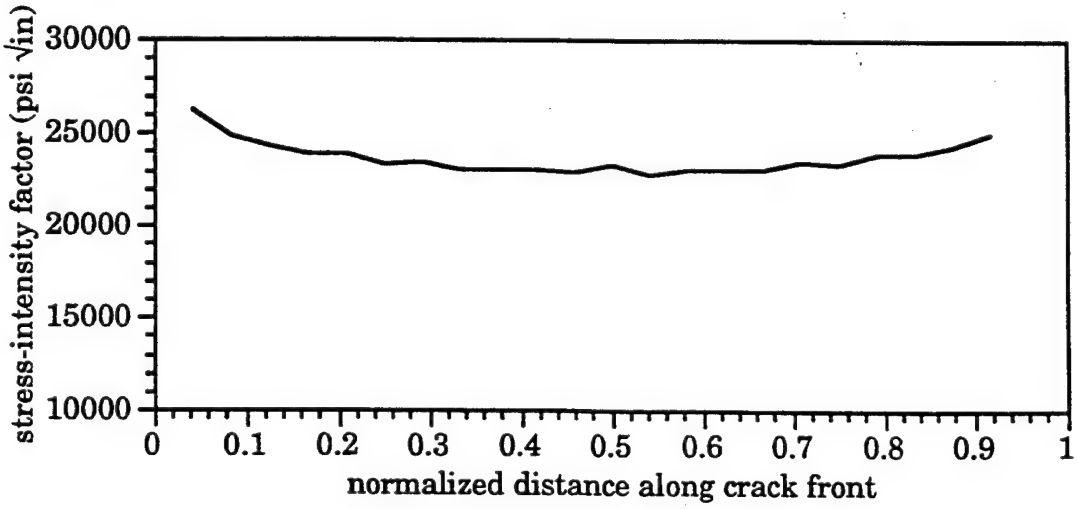

Surface Crack: 0.50 by 0.25 inch

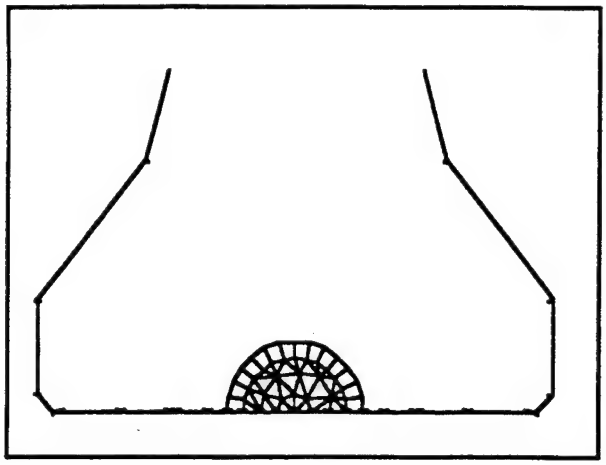

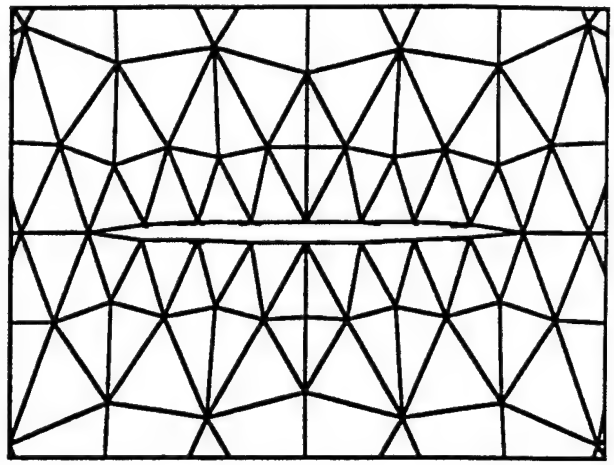

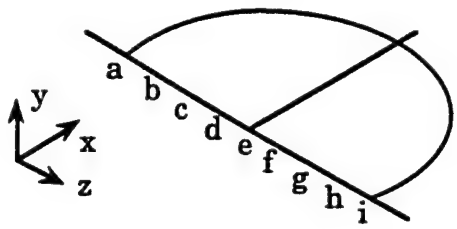

	Undeformed Coordinates x	y	z	Crack Opening	Crack Mouth Displacements dx	dy	dz
a	2.1000	0.0000	0.2500	0.00000000	0.00782274	0.00001179	0.00624602
b	2.1000	0.0000	0.1875	0.00161092	0.00746643	0.00081834	0.00632801
c	2.1000	0.0000	0.1250	0.00210861	0.00734561	0.00106667	0.00647828
d	2.1000	0.0000	0.0625	0.00237273	0.00728890	0.00119797	0.00662182
e	2.1000	0.0000	0.0000	0.00245586	0.00727372	0.00123899	0.00676378
f	2.1000	0.0000	-0.0625	0.00238266	0.00727607	0.00120180	0.00690452
g	2.1000	0.0000	-0.1250	0.00211531	0.00732490	0.00106734	0.00704703
h	2.1000	0.0000	-0.1875	0.00160225	0.00744183	0.00081002	0.00720706
i	2.1000	0.0000	-0.2500	0.00000000	0.00778159	0.00001035	0.00728408

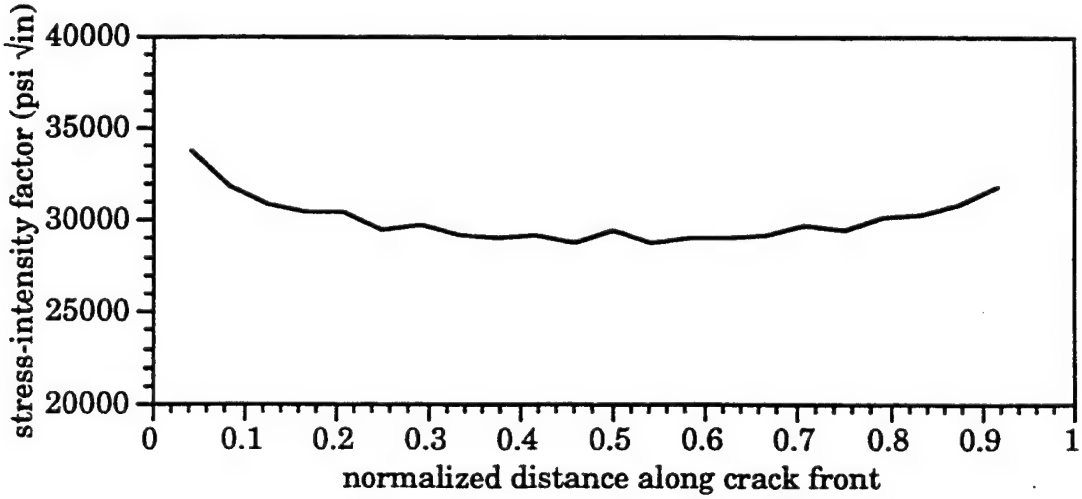

Surface Crack: 0.80 by 0.40 inch

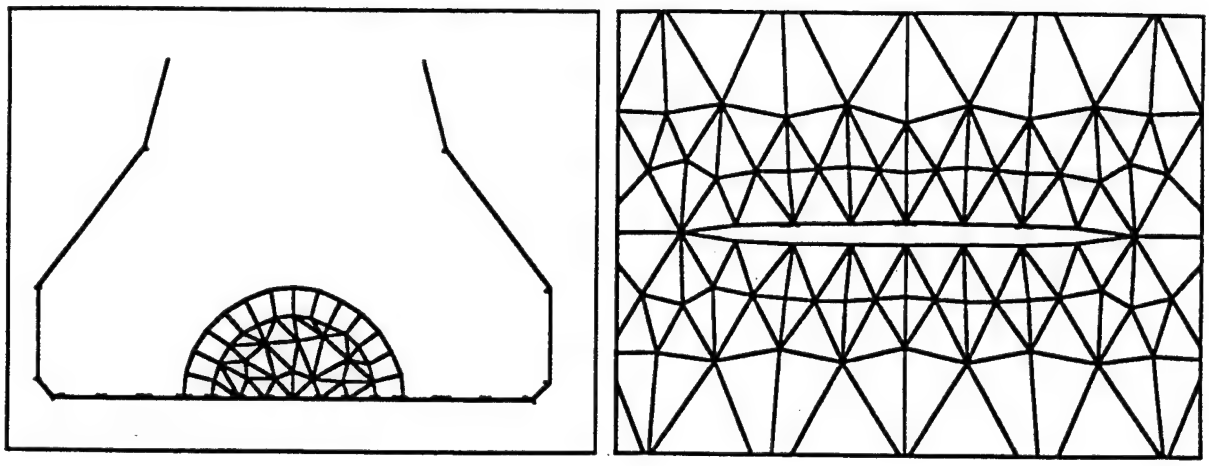

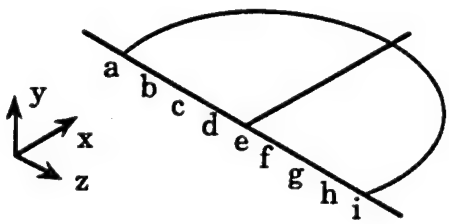

	Undeformed Coordinates x	y	z	Crack Opening	Crack Mouth Displacements dx	dy	dz
a	2.1000	0.0000	0.4000	0.00000000	0.00763551	-0.00097526	0.00593727
b	2.1000	0.0000	0.3000	0.00257018	0.00713474	0.00130227	0.00604786
c	2.1000	0.0000	0.2000	0.00331830	0.00698830	0.00167661	0.00630337
d	2.1000	0.0000	0.1000	0.00371728	0.00691124	0.00187250	0.00653514
e	2.1000	0.0000	0.0000	0.00383307	0.00689828	0.00192760	0.00676405
f	2.1000	0.0000	-0.1000	0.00372033	0.00690252	0.00186834	0.00699265
g	2.1000	0.0000	-0.2000	0.00333081	0.00697293	0.00166954	0.00722174
h	2.1000	0.0000	-0.3000	0.00256770	0.00711074	0.00128810	0.00748458
i	2.1000	0.0000	-0.4000	0.00000000	0.00756852	0.00098854	0.00759461

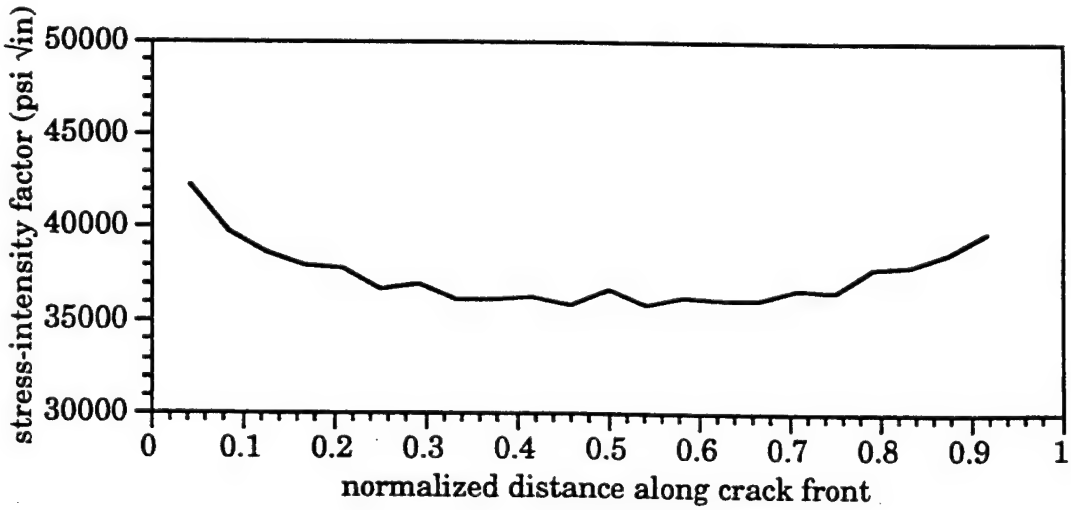

Surface Crack: 1.00 by 0.50 inch

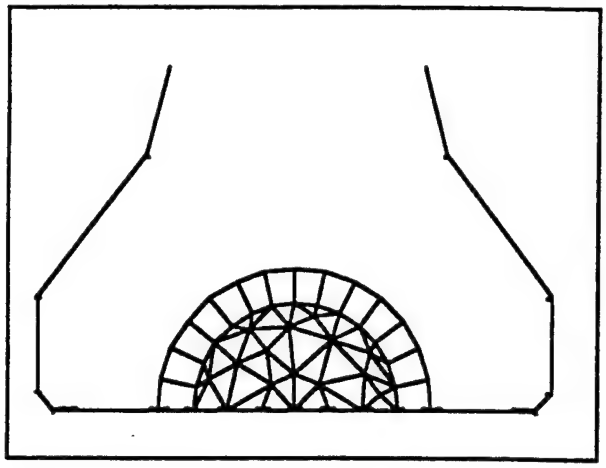

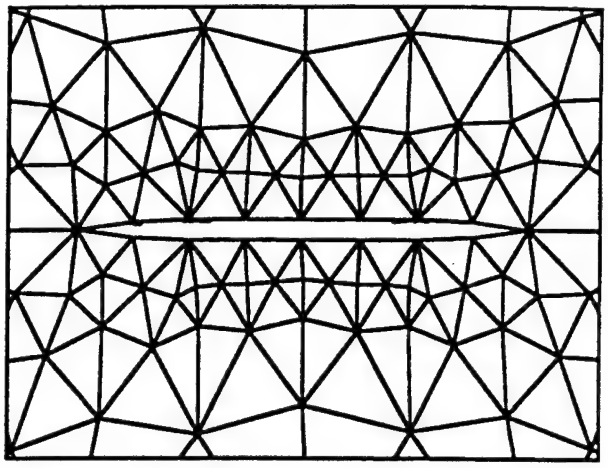

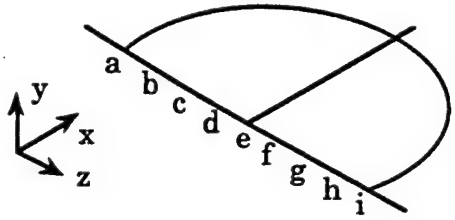

	Undeformed Coordinates x	y	z	Crack Opening	Crack Mouth Displacements dx	dy	dz
a	2.1000	0.0000	0.5000	0.00000000	0.00752227	-0.00097231	0.00572929
b	2.1000	0.0000	0.3750	0.00304753	0.00690515	0.00053907	0.00584073
c	2.1000	0.0000	0.2500	0.00412237	0.00674152	0.00207851	0.00615992
d	2.1000	0.0000	0.1250	0.00464025	0.00664503	0.00233527	0.00646571
e	2.1000	0.0000	0.0000	0.00479025	0.00662958	0.00240640	0.00675982
f	2.1000	0.0000	-0.1250	0.00465854	0.00663253	0.00233675	0.00705314
g	2.1000	0.0000	-0.2500	0.00418194	0.00670985	0.00209536	0.00735086
h	2.1000	0.0000	-0.3750	0.00322705	0.00676960	0.00260802	0.00766998
i	2.1000	0.0000	-0.5000	0.00000000	0.00744176	0.00097976	0.00780786

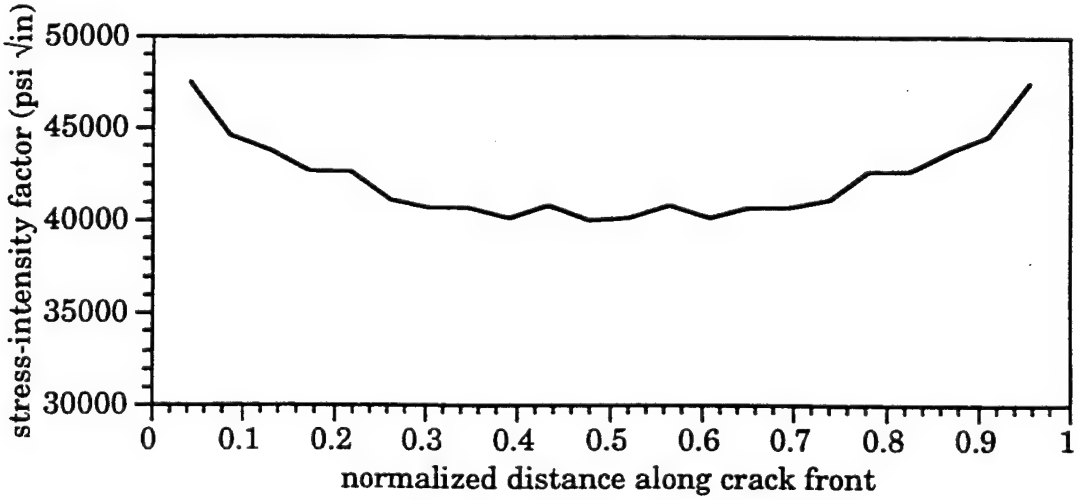

Surface Crack: 1.30 by 0.65 inch

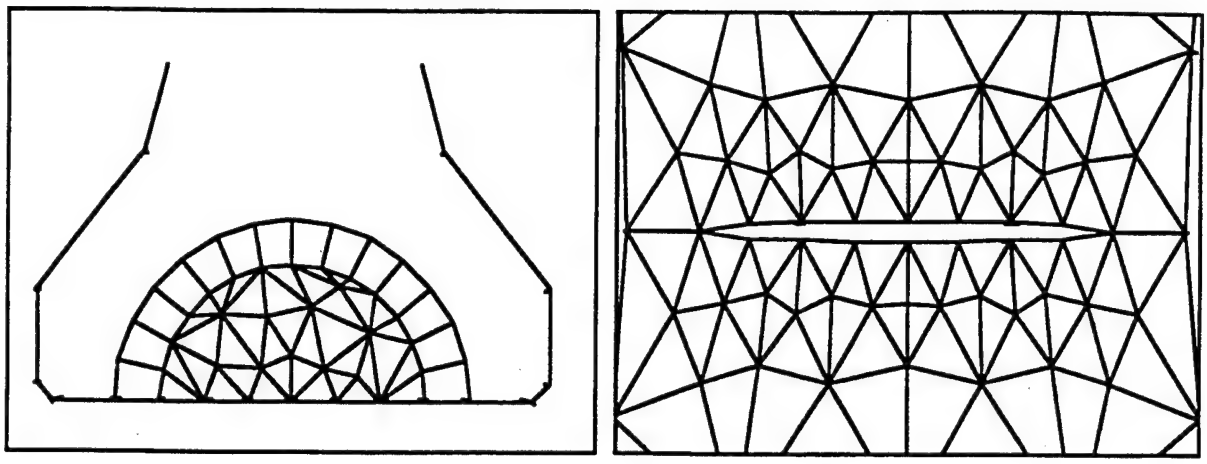

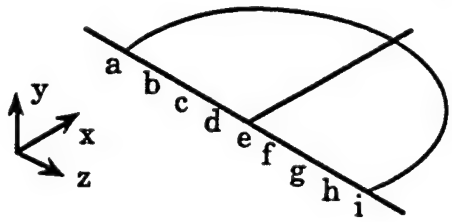

	Undeformed Coordinates x	y	z	Crack Opening	Crack Mouth Displacements dx	dy	dz
a	2.1000	0.0000	0.6500	0.00000000	0.00727112	-0.00096253	0.00537412
b	2.1000	0.0000	0.4875	0.00439791	0.00642778	0.00122265	0.00557068
c	2.1000	0.0000	0.3250	0.00551411	0.00624599	0.00278250	0.00599989
d	2.1000	0.0000	0.1625	0.00622178	0.00616665	0.00313215	0.00639143
e	2.1000	0.0000	0.0000	0.00641519	0.00615276	0.00322028	0.00678487
f	2.1000	0.0000	-0.1625	0.00620454	0.00616916	0.00310675	0.00717869
g	2.1000	0.0000	-0.3250	0.00547381	0.00628524	0.00273796	0.00757991
h	2.1000	0.0000	-0.4875	0.00436598	0.00634392	0.00316310	0.00800553
i	2.1000	0.0000	-0.6500	0.00000000	0.00716309	0.00096644	0.00819913

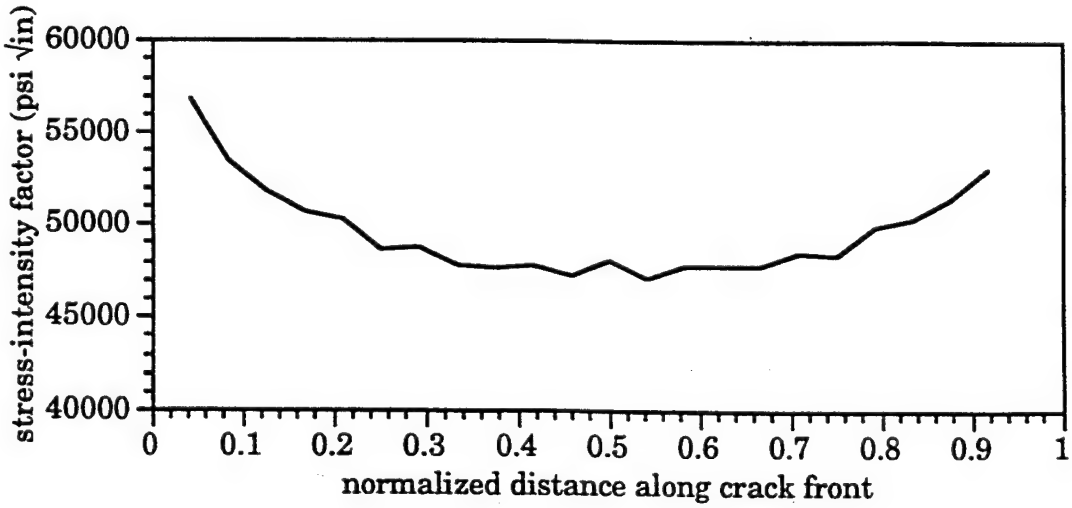

Surface Crack: 1.50 by 0.75 inch

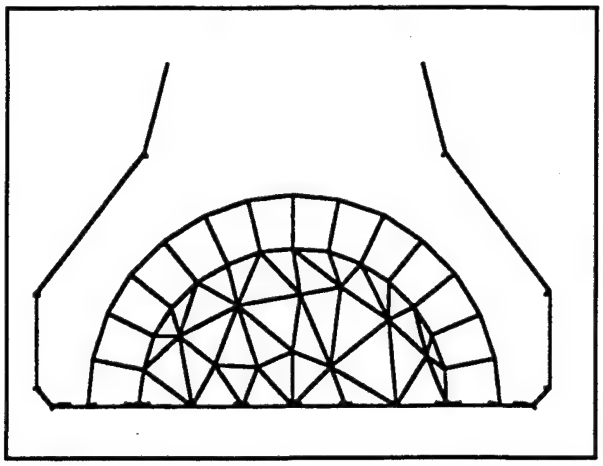

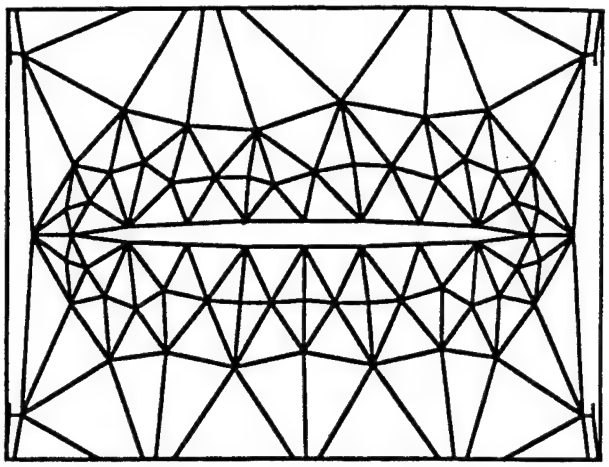

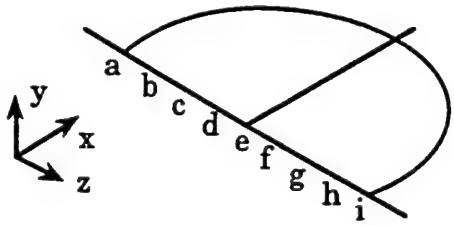

	Undeformed Coordinates x	y	z	Crack Opening	Crack Mouth Displacements dx	dy	dz
a	2.1000	0.0000	0.7500	0.00000000	0.00695621	-0.00095656	0.00506018
b	2.1000	0.0000	0.5625	0.00558889	0.00595358	0.00180718	0.00529458
c	2.1000	0.0000	0.3750	0.00693380	0.00577429	0.00248658	0.00584643
d	2.1000	0.0000	0.1875	0.00762755	0.00572670	0.00383424	0.00633331
e	2.1000	0.0000	0.0000	0.00782914	0.00571505	0.00393264	0.00680878
f	2.1000	0.0000	-0.1875	0.00764325	0.00569644	0.00383769	0.00729186
g	2.1000	0.0000	-0.3750	0.00692336	0.00567186	0.00446275	0.00778894
h	2.1000	0.0000	-0.5625	0.00549981	0.00585290	0.00372444	0.00833027
i	2.1000	0.0000	-0.7500	0.00000000	0.00682849	0.00095410	0.00856029

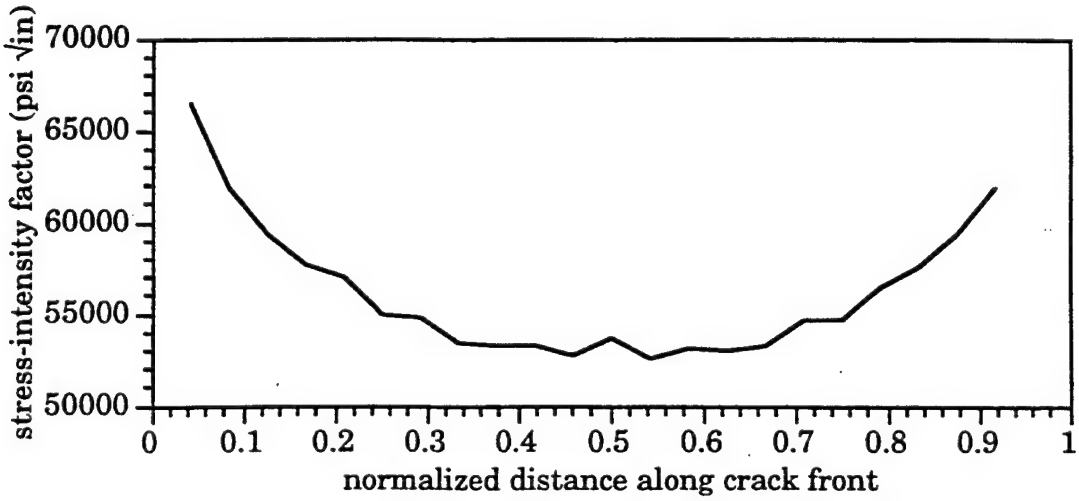

Corner Crack: 0.005 by 0.005 inch

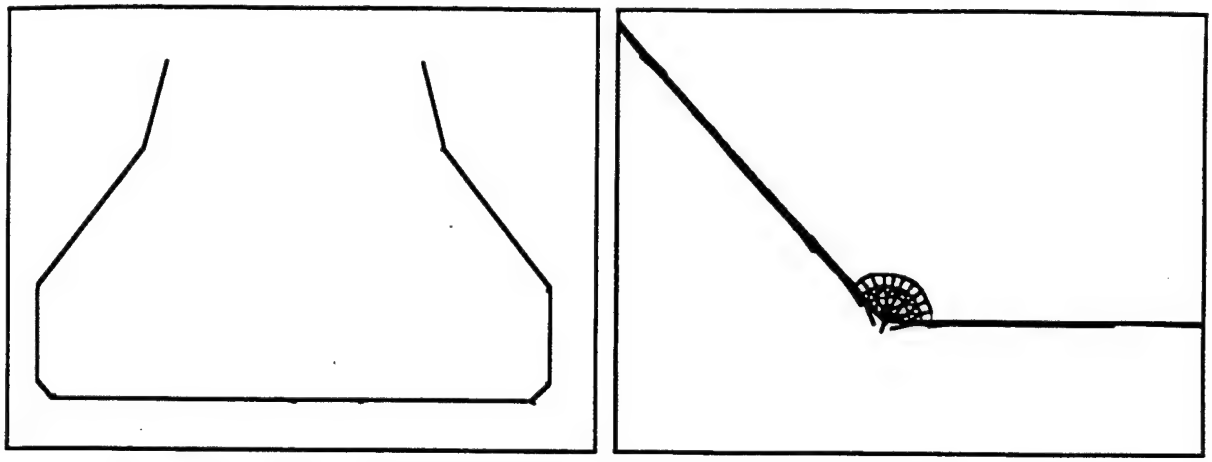

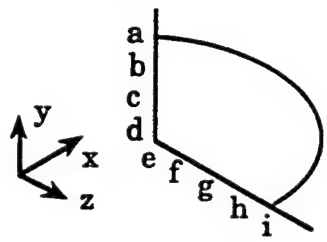

	Undeformed Coordinates x	y	z	Crack Opening	Crack Mouth Displacements dx	dy	dz
a	2.1037	0.0000	0.8764	0.00000000	0.00749579	-0.00093902	0.00540178
b	2.1027	0.0000	0.8755	0.00003376	0.00749186	-0.00092239	0.00540747
c	2.1018	0.0000	0.8747	0.00004342	0.00749180	-0.00091774	0.00540957
d	2.1009	0.0000	0.8738	0.00004713	0.00749368	-0.00091618	0.00541097
e	2.1000	0.0000	0.8730	0.00004745	0.00749751	-0.00092270	0.00540859
f	2.1000	0.0000	0.8718	0.00004712	0.00749448	-0.00091637	0.00541044
g	2.1000	0.0000	0.8705	0.00004299	0.00749609	-0.00091854	0.00541222
h	2.1000	0.0000	0.8692	0.00002880	0.00750170	-0.00092600	0.00541329
i	2.1000	0.0000	0.8680	0.00000000	0.00750846	-0.00094039	0.00541526

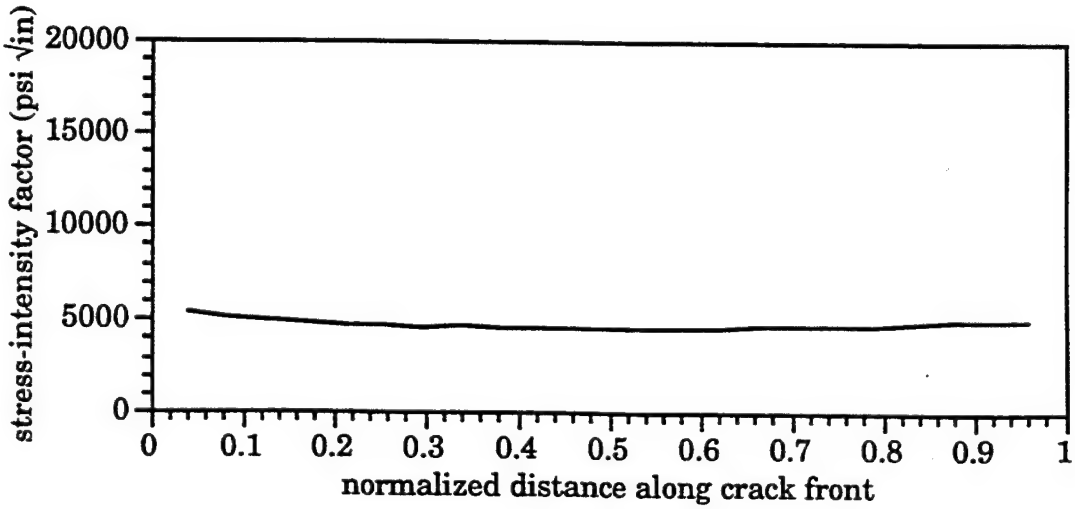

Corner Crack: 0.025 by 0.025 inch

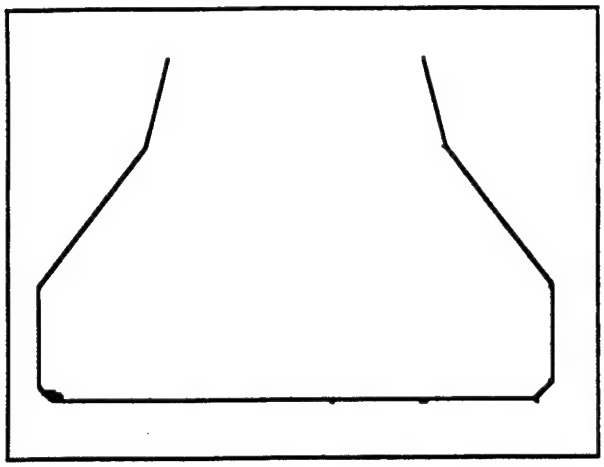

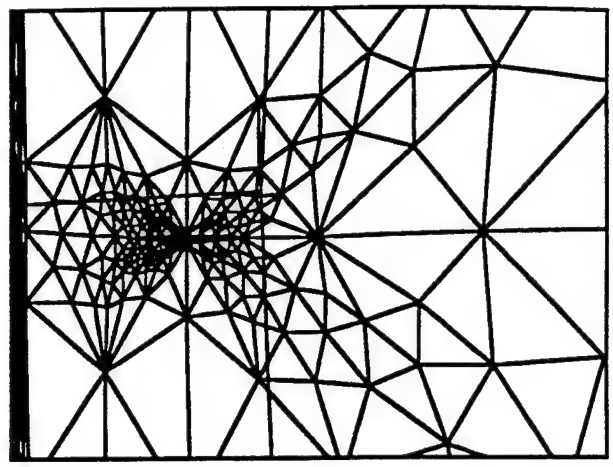

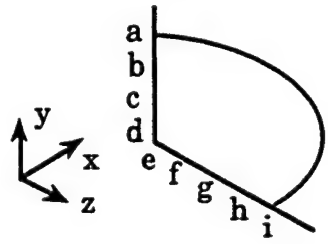

	Undeformed Coordinates x	y	z	Crack Opening	Crack Mouth Displacements dx	dy	dz
a	2.1184	0.0000	0.8899	0.00000000	0.00745515	-0.00093521	0.00538929
b	2.1135	0.0000	0.8854	0.00017669	0.00743112	-0.00084821	0.00541623
c	2.1091	0.0000	0.8813	0.00022868	0.00743203	-0.00082354	0.00542892
d	2.1046	0.0000	0.8772	0.00025926	0.00743513	-0.00080925	0.00543440
e	2.1000	0.0000	0.8730	0.00027074	0.00744068	-0.00080448	0.00543231
f	2.1000	0.0000	0.8668	0.00025988	0.00744274	-0.00081024	0.00543668
g	2.1000	0.0000	0.8606	0.00022838	0.00745301	-0.00082646	0.00544351
h	2.1000	0.0000	0.8544	0.00017467	0.00747010	-0.00085406	0.00545384
i	2.1000	0.0000	0.8480	0.00000000	0.00751593	-0.00094208	0.00545590

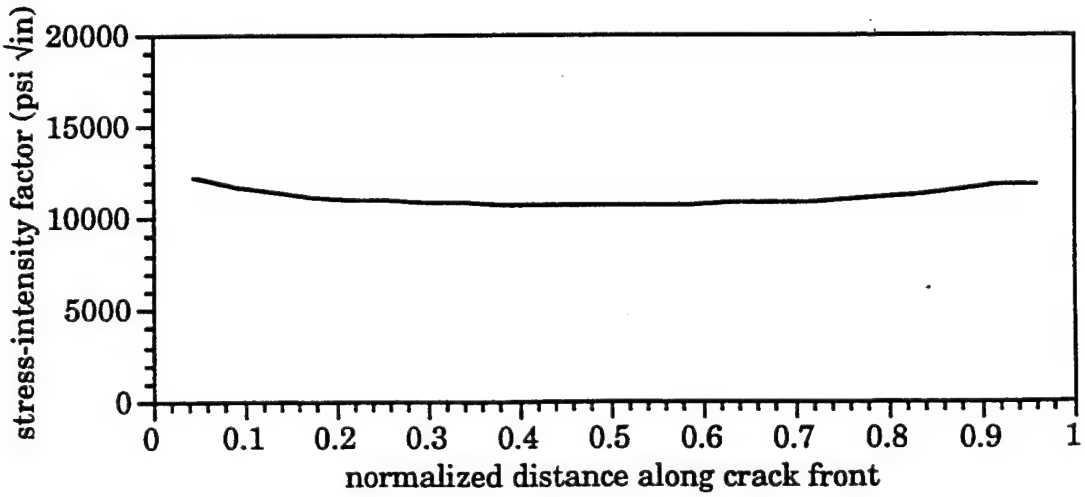

Corner Crack: 0.05 by 0.05 inch

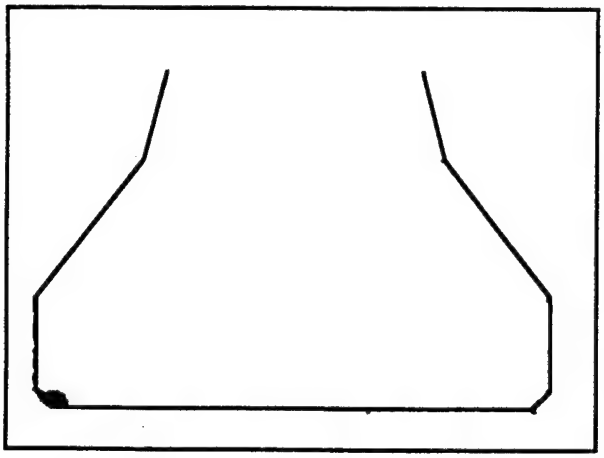

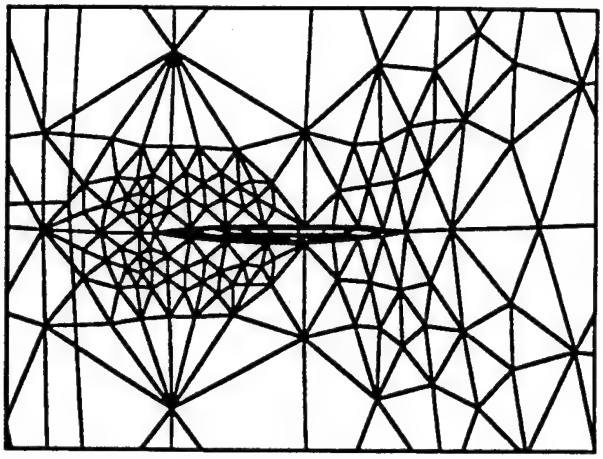

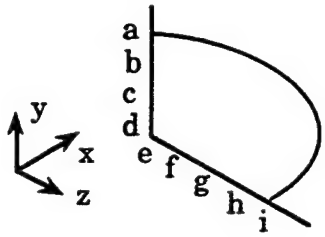

	Undeformed Coordinates x	y	z	Crack Opening	Crack Mouth Displacements dx	dy	dz
a	2.1369	0.0000	0.9067	0.00000000	0.00740215	-0.00093062	0.00537394
b	2.1282	0.0000	0.8987	0.00033268	0.00735565	-0.00076717	0.00542163
c	2.1187	0.0000	0.8901	0.00045429	0.00735708	-0.00070873	0.00545161
d	2.1092	0.0000	0.8814	0.00052154	0.00736194	-0.00067733	0.00546446
e	2.1000	0.0000	0.8730	0.00055501	0.00736871	-0.00066247	0.00546252
f	2.1000	0.0000	0.8605	0.00051952	0.00737900	-0.00068096	0.00546811
g	2.1000	0.0000	0.8480	0.00045723	0.00740019	-0.00071309	0.00548036
h	2.1000	0.0000	0.8355	0.00033952	0.00744072	-0.00077396	0.00549867
i	2.1000	0.0000	0.8230	0.00000000	0.00752625	-0.00094440	0.00550807

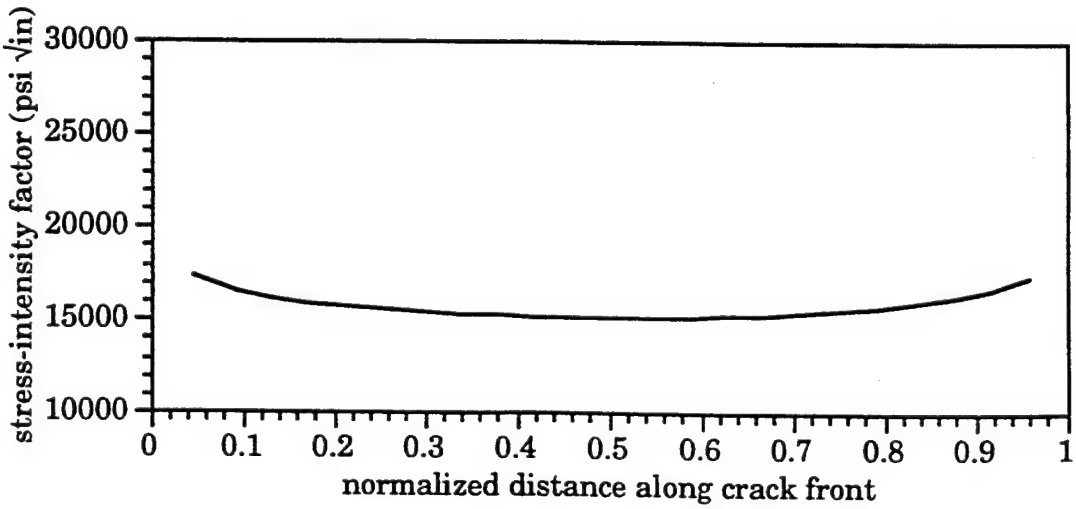

Corner Crack: 0.085 by 0.085 inch

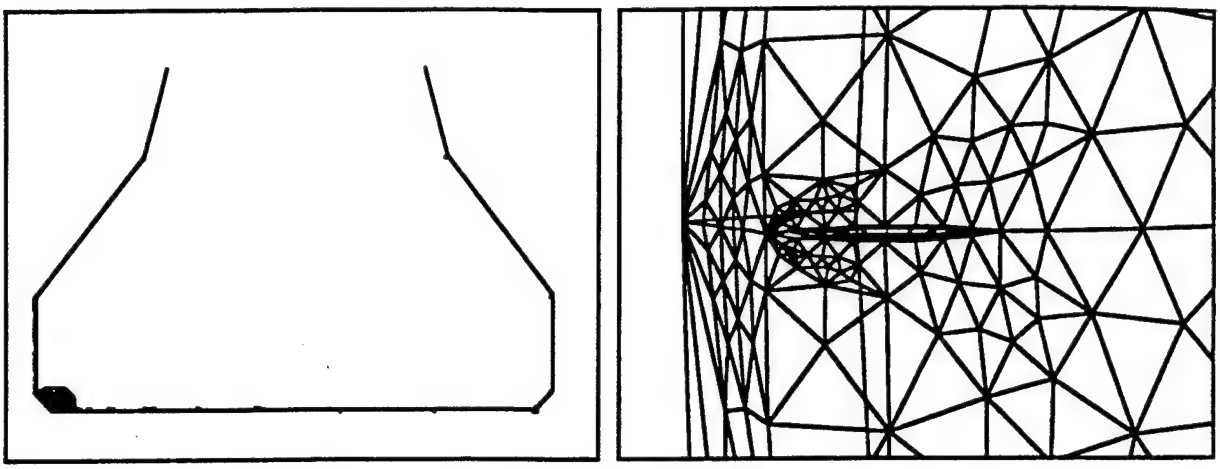

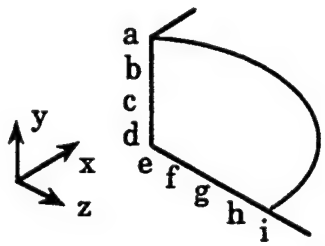

	Undeformed Coordinates x	y	z	Crack Opening	Crack Mouth Displacements dx	dy	dz
a	2.1627	0.0000	0.9303	0.00000000	0.00731284	-0.00092402	0.00535186
b	2.1470	0.0000	0.9160	0.00058489	0.00724539	-0.00063730	0.00544098
c	2.1313	0.0000	0.9017	0.00077676	0.00725281	-0.00054531	0.00549139
d	2.1157	0.0000	0.8873	0.00088598	0.00726279	-0.00049445	0.00551196
e	2.1000	0.0000	0.8730	0.00094556	0.00727301	-0.00046775	0.00551081
f	2.1000	0.0000	0.8518	0.00088332	0.00729191	-0.00050004	0.00551921
g	2.1000	0.0000	0.8305	0.00077628	0.00732782	-0.00055538	0.00554014
h	2.1000	0.0000	0.8093	0.00056899	0.00740200	-0.00066308	0.00556886
i	2.1000	0.0000	0.7880	0.00000000	0.00754105	-0.00094778	0.00558739

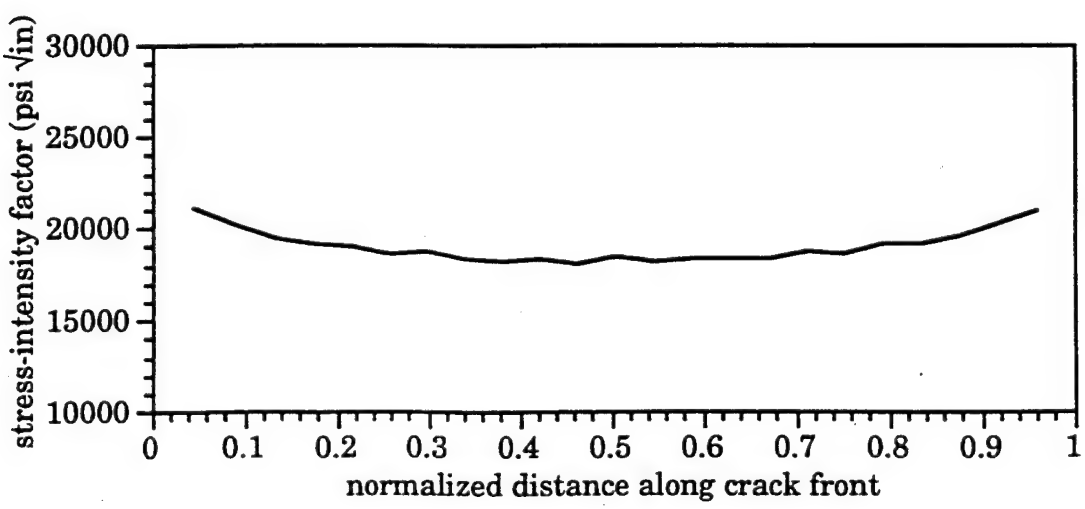

Corner Crack: 0.15 by 0.15 inch

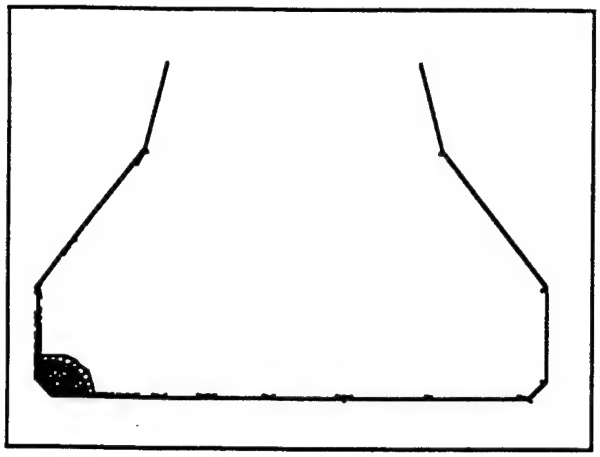

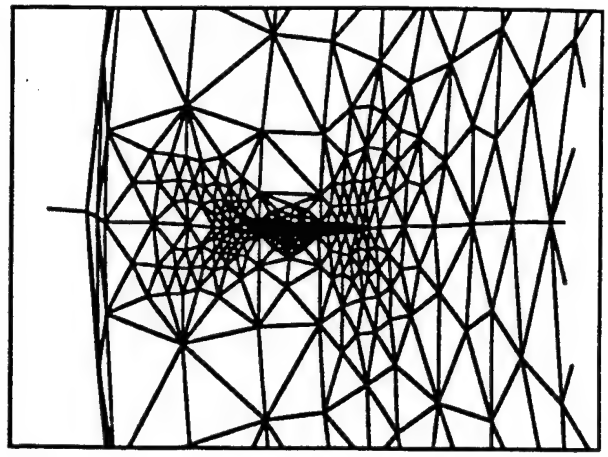

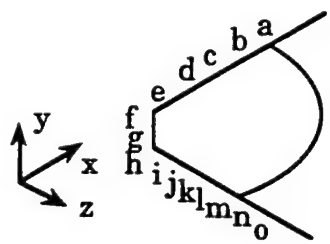

	Undeformed Coordinates x	y	z	Crack Opening	Crack Mouth Displacements dx	dy	dz
a	2.2374	0.0000	0.9330	0.00000000	0.00708231	-0.00091766	0.00544650
b	2.2181	0.0000	0.9330	0.00094680	0.00707643	-0.00045232	0.00562501
c	2.2006	0.0000	0.9330	0.00119001	0.00709767	-0.00033310	0.00566996
d	2.1831	0.0000	0.9330	0.00137992	0.00710756	-0.00023985	0.00569234
e	2.1656	0.0000	0.9330	0.00152947	0.00711054	-0.00016565	0.00570669
f	2.1492	0.0000	0.9180	0.00160412	0.00710651	-0.00012993	0.00571426
g	2.1328	0.0000	0.9030	0.00166566	0.00711138	-0.00010145	0.00571836
h	2.1164	0.0000	0.8880	0.00171061	0.00712073	-0.00008234	0.00571590
i	2.1000	0.0000	0.8730	0.00174769	0.00712983	-0.00006685	0.00570674
j	2.1000	0.0000	0.8475	0.00165815	0.00714736	-0.00011337	0.00571312
k	2.1000	0.0000	0.8220	0.00154737	0.00717635	-0.00017118	0.00572845
l	2.1000	0.0000	0.7964	0.00138883	0.00722040	-0.00025268	0.00575009
m	2.1000	0.0000	0.7709	0.00115883	0.00728545	-0.00036971	0.00577993
n	2.1000	0.0000	0.7454	0.00080204	0.00738886	-0.00055020	0.00582619
o	2.1000	0.0000	0.7230	0.00000000	0.00758101	-0.00095397	0.00581842

Corner Crack: 0.15 by 0.15 inch (Continued)

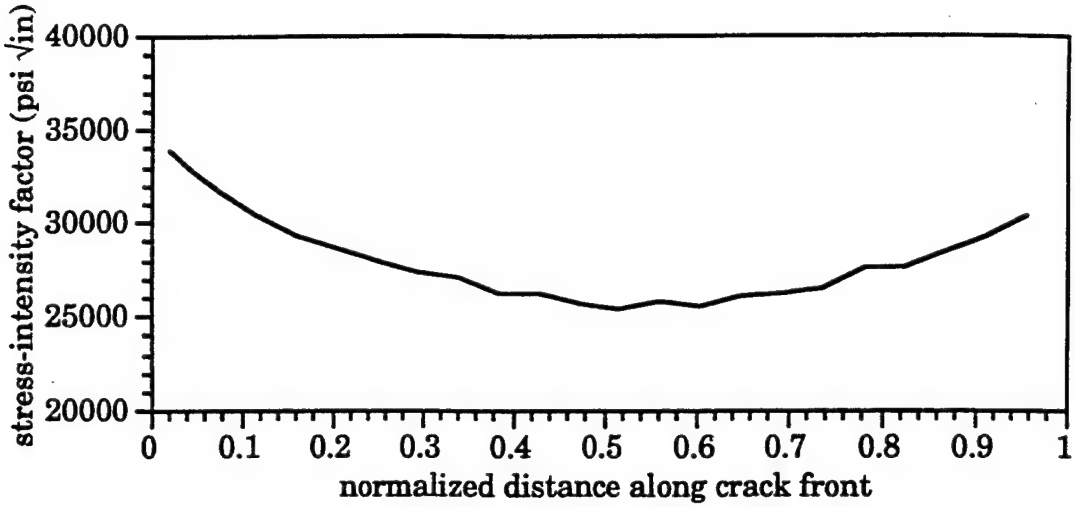

Corner Crack: 0.25 by 0.25 inch

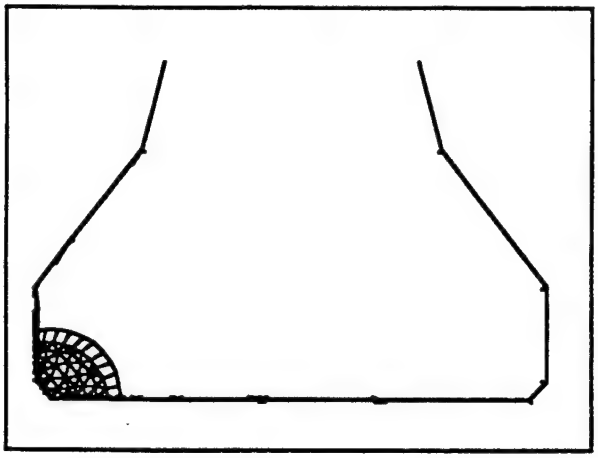

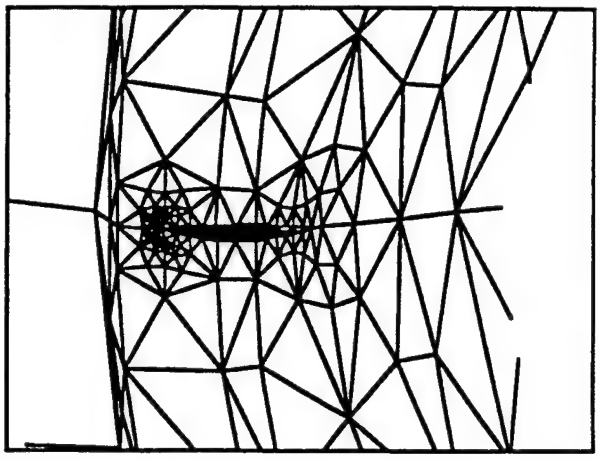

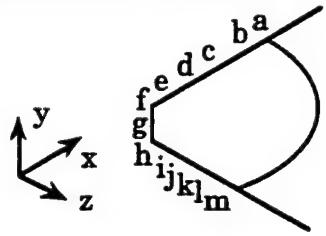

	Undeformed Coordinates			Crack	Crack Mouth Displacements		
	x	y	z	Opening	dx	dy	dz
a	2.3420	0.0000	0.9330	0.00000000	0.00689974	-0.00090720	0.00569911
b	2.2943	0.0000	0.9330	0.00166713	0.00687265	-0.00009727	0.00599965
c	2.2514	0.0000	0.9330	0.00215039	0.00692517	0.00013922	0.00607264
d	2.2085	0.0000	0.9330	0.00250403	0.00694908	0.00031363	0.00610772
e	2.1656	0.0000	0.9330	0.00274556	0.00695699	0.00043219	0.00610954
f	2.1328	0.0000	0.9030	0.00279808	0.00695881	0.00045529	0.00610544
g	2.1000	0.0000	0.8730	0.00283867	0.00697319	0.00047135	0.00608889
h	2.1000	0.0000	0.8320	0.00269347	0.00698890	0.00039854	0.00609671
i	2.1000	0.0000	0.7910	0.00251216	0.00702406	0.00030586	0.00611636
j	2.1000	0.0000	0.7499	0.00228103	0.00707740	0.00018816	0.00614592
k	2.1000	0.0000	0.7089	0.00193464	0.00716484	0.00001277	0.00618388
l	2.1000	0.0000	0.6679	0.00143753	0.00729521	-0.00023739	0.00625452
m	2.1000	0.0000	0.6230	0.00000000	0.00716237	-0.00089763	0.00604527

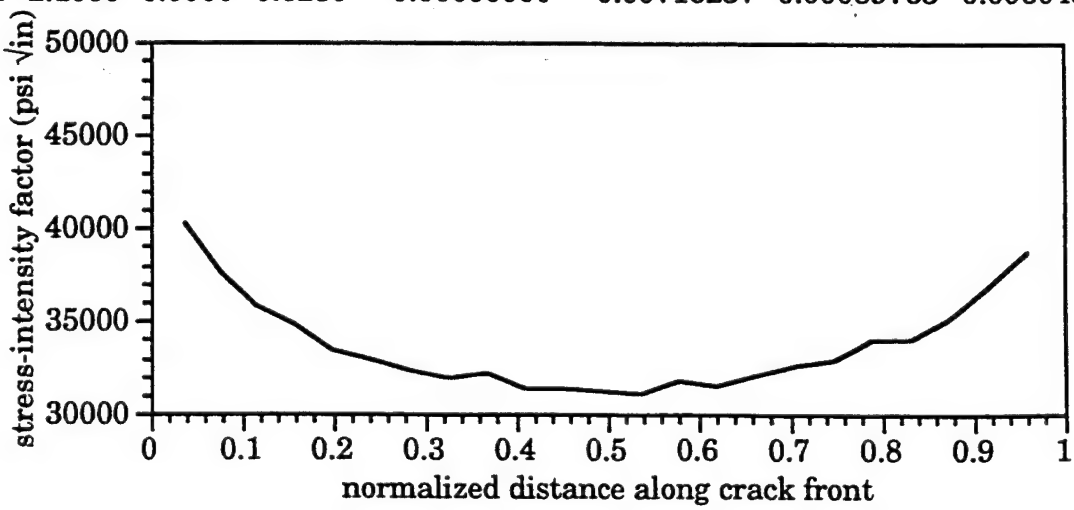

Corner Crack: 0.40 by 0.40 inch

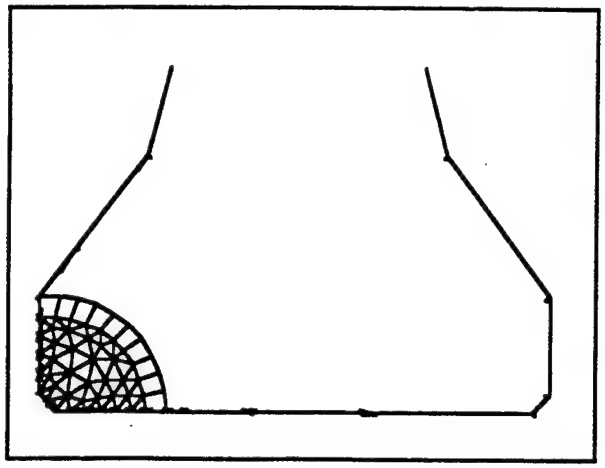

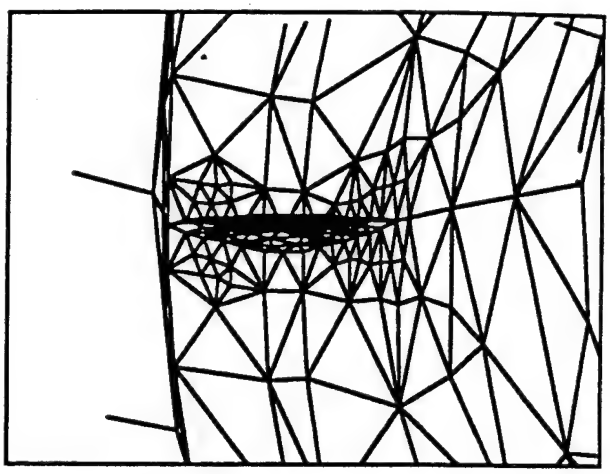

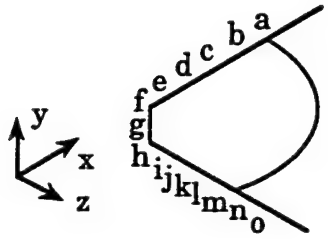

	Undeformed Coordinates			Crack	Crack Mouth Displacements		
	x	y	z	Opening	dx	dy	dz
a	2.5000	0.0000	0.9330	0.00000000	0.00659215	-0.00088749	0.00642549
b	2.4287	0.0000	0.9330	0.00249322	0.00668951	0.00031341	0.00679062
c	2.3629	0.0000	0.9330	0.00333232	0.00678105	0.00071395	0.00695422
d	2.2971	0.0000	0.9330	0.00390764	0.00682951	0.00099262	0.00703646
e	2.2314	0.0000	0.9330	0.00431292	0.00685932	0.00119465	0.00707014
f	2.1656	0.0000	0.9330	0.00462152	0.00686677	0.00134789	0.00707164
g	2.1328	0.0000	0.9030	0.00462853	0.00686813	0.00135202	0.00706968
h	2.1000	0.0000	0.8730	0.00463642	0.00687449	0.00135520	0.00706142
i	2.1000	0.0000	0.8187	0.00441094	0.00687843	0.00124567	0.00707023
j	2.1000	0.0000	0.7644	0.00417105	0.00689697	0.00112564	0.00708645
k	2.1000	0.0000	0.7100	0.00388151	0.00693369	0.00098078	0.00711422
l	2.1000	0.0000	0.6557	0.00349966	0.00699666	0.00079127	0.00715902
m	2.1000	0.0000	0.6014	0.00299736	0.00708920	0.00054145	0.00720946
n	2.1000	0.0000	0.5471	0.00234658	0.00725836	0.00021283	0.00730147
o	2.1000	0.0000	0.4730	0.00000000	0.00779690	-0.00097252	0.00732815

Corner Crack: 0.40 by 0.40 inch (Continued)

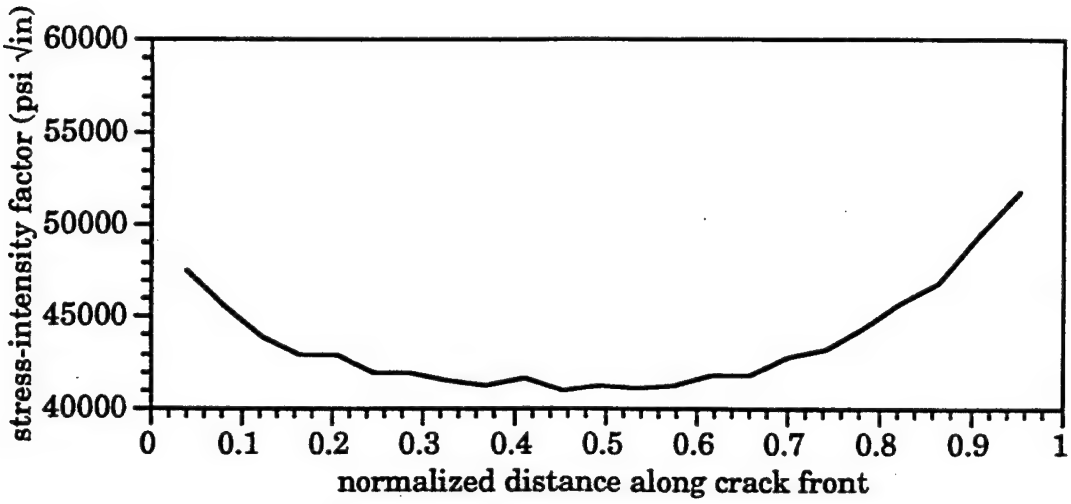

Corner Crack: 0.50 by 0.50 inch

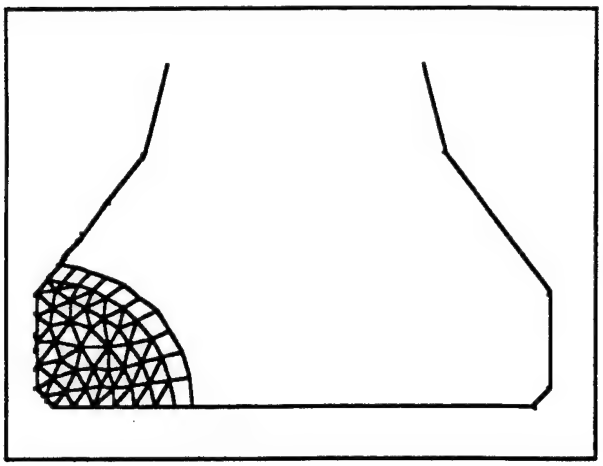

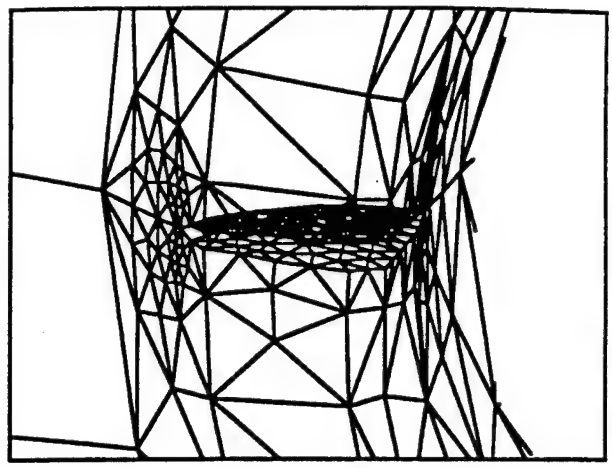

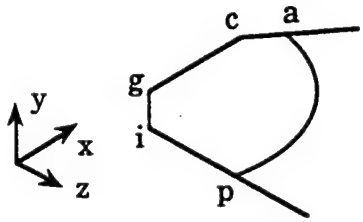

	Undeformed Coordinates x	y	z	Crack Opening	Crack Mouth Displacements dx	dy	dz
a	2.6067	0.0000	0.8504	0.00000000	0.00632738	-0.00088576	0.00748758
b	2.5523	0.0000	0.8927	0.00345108	0.00671806	0.00077838	0.00791234
c	2.5000	0.0000	0.9330	0.00430969	0.00686242	0.00118318	0.00795450
d	2.4164	0.0000	0.9330	0.00496460	0.00687250	0.00150789	0.00805415
e	2.3328	0.0000	0.9330	0.00552503	0.00690043	0.00176817	0.00812276
f	2.2492	0.0000	0.9330	0.00588395	0.00692349	0.00196437	0.00816214
g	2.1656	0.0000	0.9330	0.00621172	0.00692658	0.00212708	0.00817026
h	2.1328	0.0000	0.9030	0.00617861	0.00692249	0.00211350	0.00817708
i	2.1000	0.0000	0.8730	0.00614382	0.00692001	0.00209759	0.00817972
j	2.1000	0.0000	0.8001	0.00578526	0.00690534	0.00192460	0.00818909
k	2.1000	0.0000	0.7272	0.00542374	0.00689229	0.00174627	0.00820773
l	2.1000	0.0000	0.6543	0.00497646	0.00691492	0.00152351	0.00823871
m	2.1000	0.0000	0.5813	0.00442249	0.00697704	0.00124650	0.00829061
n	2.1000	0.0000	0.5084	0.00365592	0.00711464	0.00086055	0.00836695
o	2.1000	0.0000	0.4355	0.00250988	0.00735833	0.00028473	0.00852602
p	2.1000	0.0000	0.3730	0.00000000	0.00788129	-0.00097617	0.00849129

Corner Crack: 0.50 by 0.50 inch (Continued)

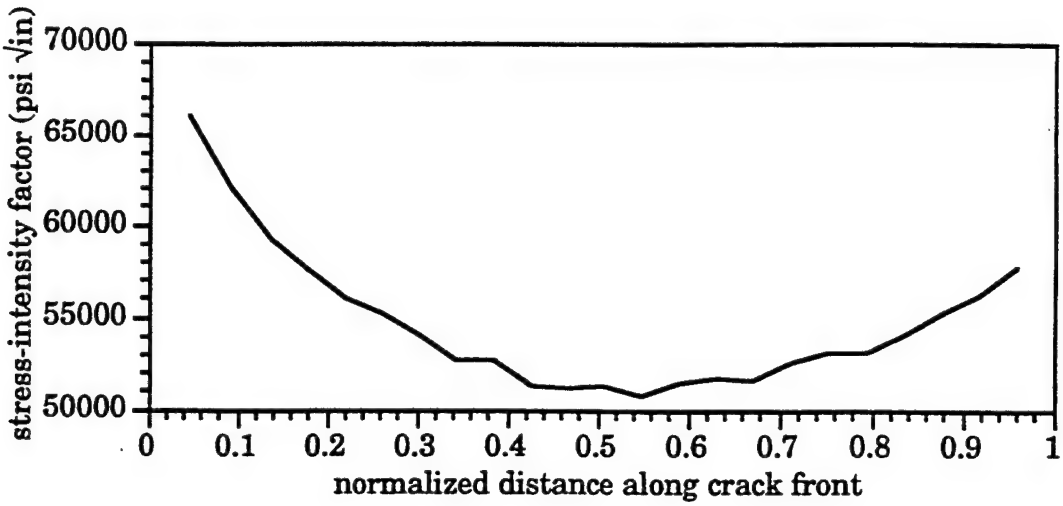

Corner Crack: 0.65 by 0.65 inch

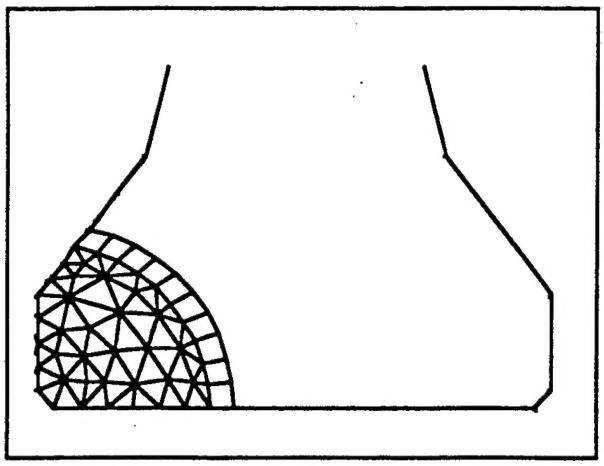

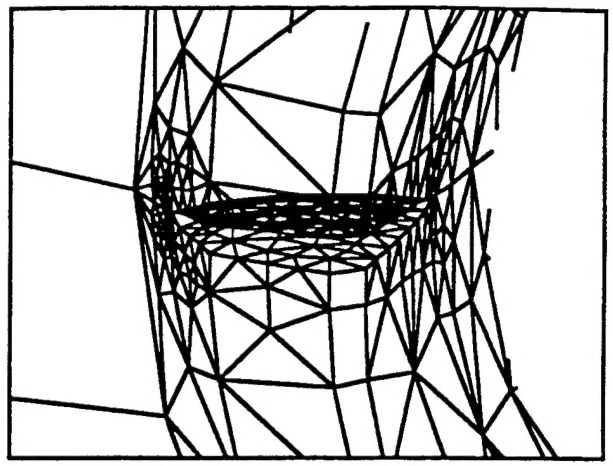

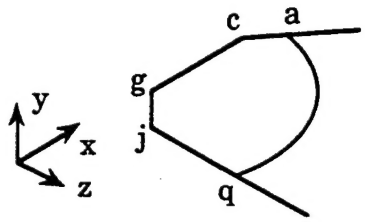

	Undeformed Coordinates x	y	z	Crack Opening	Crack Mouth Displacements dx	dy	dz
a	2.7380	0.0000	0.7488	0.00000000	0.00638385	-0.00090222	0.00906374
b	2.6748	0.0000	0.7977	0.00442827	0.00681461	0.00123941	0.00970477
c	2.6165	0.0000	0.8428	0.00581643	0.00698994	0.00191391	0.00993406
d	2.5583	0.0000	0.8879	0.00677426	0.00711416	0.00237258	0.01000305
e	2.5000	0.0000	0.9330	0.00749036	0.00718522	0.00270833	0.01004447
f	2.4164	0.0000	0.9330	0.00784421	0.00718433	0.00289593	0.01012875
g	2.3328	0.0000	0.9330	0.00818504	0.00718639	0.00306556	0.01020987
h	2.2492	0.0000	0.9330	0.00844942	0.00719556	0.00321177	0.01027453
i	2.1656	0.0000	0.9330	0.00870848	0.00719517	0.00334483	0.01032399
j	2.1000	0.0000	0.8730	0.00852359	0.00715959	0.00326316	0.01036886
k	2.1000	0.0000	0.7782	0.00794668	0.00708444	0.00298917	0.01038118
l	2.1000	0.0000	0.6834	0.00737162	0.00701251	0.00270867	0.01040108
m	2.1000	0.0000	0.5886	0.00672685	0.00696740	0.00239094	0.01044743
n	2.1000	0.0000	0.4938	0.00592284	0.00699170	0.00198881	0.01050610
o	2.1000	0.0000	0.3990	0.00487855	0.00707759	0.00146866	0.01058763
p	2.1000	0.0000	0.3043	0.00335264	0.00738177	0.00170005	0.01074207
q	2.1000	0.0000	0.2230	0.00000000	0.00799547	0.00000941	0.01073773

Corner Crack: 0.65 by 0.65 inch (Continued)

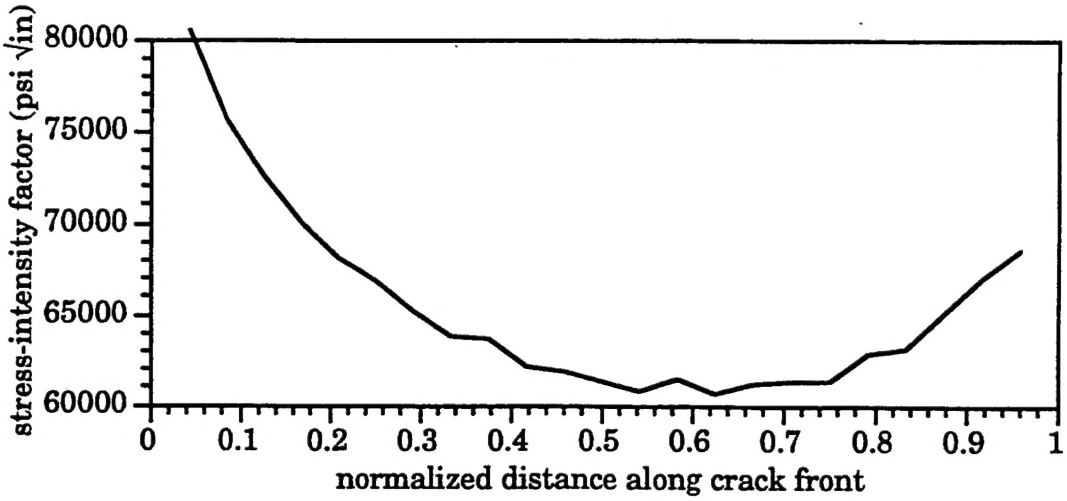

Corner Crack: 0.75 by 0.75 inch

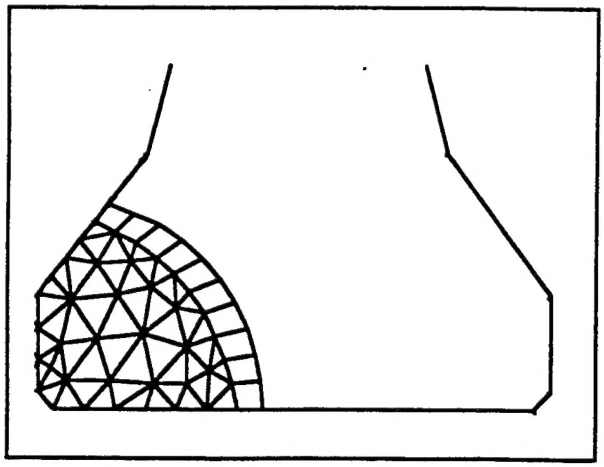

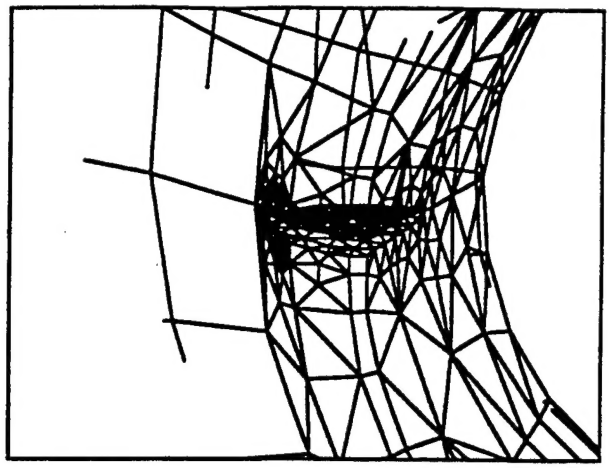

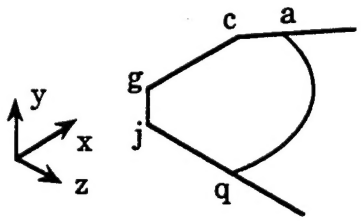

	Undeformed Coordinates x	y	z	Crack Opening	Crack Mouth Displacements dx	dy	dz
a	2.8251	0.0000	0.6814	0.00000000	0.00639528	-0.00090364	0.01043018
b	2.7596	0.0000	0.7320	0.00508389	0.00685716	0.00155713	0.01118586
c	2.6947	0.0000	0.7823	0.00673918	0.00715709	0.00235138	0.01136673
d	2.6298	0.0000	0.8325	0.00803000	0.00723669	0.00298336	0.01159868
e	2.5649	0.0000	0.8828	0.00893265	0.00735134	0.00341226	0.01167683
f	2.5000	0.0000	0.9330	0.00965252	0.00742516	0.00374924	0.01172900
g	2.3885	0.0000	0.9330	0.01000273	0.00742097	0.00394241	0.01186113
h	2.2771	0.0000	0.9330	0.01031392	0.00742229	0.00411229	0.01198973
i	2.1656	0.0000	0.9330	0.01059207	0.00742389	0.00426353	0.01209668
j	2.1000	0.0000	0.8730	0.01031522	0.00736724	0.00414072	0.01216659
k	2.1000	0.0000	0.7636	0.00955155	0.00724138	0.00378004	0.01218150
l	2.1000	0.0000	0.6542	0.00880305	0.00710492	0.00341785	0.01220774
m	2.1000	0.0000	0.5449	0.00796832	0.00700936	0.00300724	0.01225571
n	2.1000	0.0000	0.4355	0.00697763	0.00697213	0.00251741	0.01231885
o	2.1000	0.0000	0.3261	0.00570955	0.00705987	0.00288272	0.01242074
p	2.1000	0.0000	0.2167	0.00387745	0.00728183	0.00196821	0.01260039
q	2.1000	0.0000	0.1230	0.00000000	0.00800217	0.00001077	0.01256324
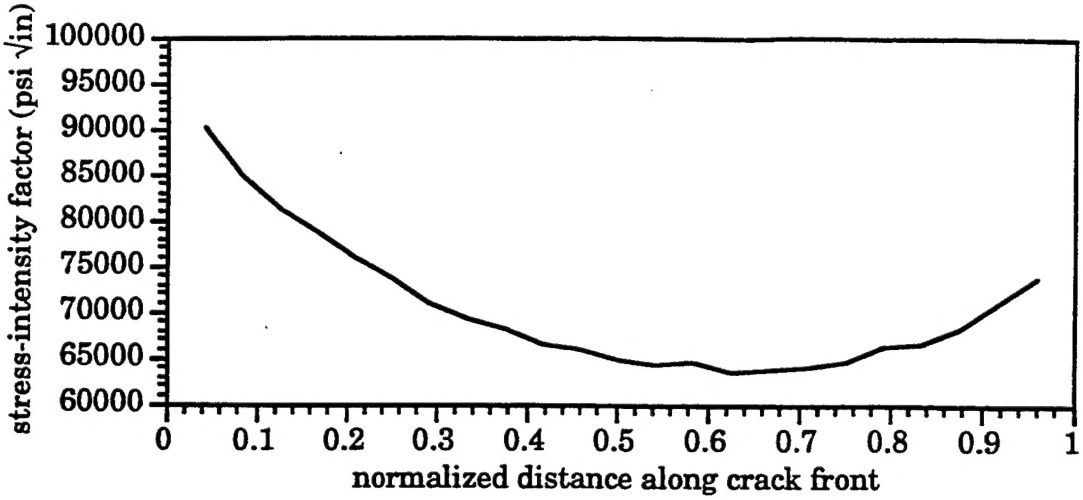
Corner Crack: 0.75 by 0.75 inch (Continued)